Master's thesis

NTNU
Norwegian University of Science and Technology
Faculty of Natural Sciences
Department of Chemical Engineering

Ingvild Emilie Solnes

# Machine Learning Modelling of the Oxidative and Thermal Degradation of Monoethanolamine (MEA)

Master's thesis in Chemical Engineering and Biotechnology
Supervisor: Hanna Knuutila & Andrés Carranza-Abaid
Co-supervisor: Lucas Braakhuis & Vanja Buvik
June 2021

NTNU
Kunnskap for en bedre verden

Ingvild Emilie Solnes

# Machine Learning Modelling of the Oxidative and Thermal Degradation of Monoethanolamine (MEA)

Master's thesis in Chemical Engineering and Biotechnology
Supervisor: Hanna Knuutila & Andrés Carranza-Abaid
Co-supervisor: Lucas Braakhuis & Vanja Buvik
June 2021

Norwegian University of Science and Technology
Faculty of Natural Sciences
Department of Chemical Engineering

NTNU
Norwegian University of
Science and Technology

# Abstract

The human population is growing, leading to increased consumption of resources and emission of greenhouse gases. As a result, the concentration of greenhouse gases in the atmosphere is rising to dangerous levels, and the need for measures to reduce emissions is growing.[1] One measure is $CO_2$-capture and storage, which opens up the possibility of removing $CO_2$ from flue gas, compressing and storing it instead of emitting it to the atmosphere.

One example of a $CO_2$-capture technology is chemical absorption with an amine-based solvent. With this technology, there are also difficulties, mainly degradation of the solvent. Therefore, further understanding of degradation is important for reducing operational costs, solvent management and emission control.

In this thesis, the main focus has been on oxidative and thermal degradation of monoethanolamine (MEA), one of the most researched solvents for chemical absorption. Mathematical machine learning modelling has been used to make a predictive model that can describe the degradation and trends in experimental data. The objective of the work has been to see if machine learning modelling has the potential to give good model predictions, describe the degradation of MEA and the formation of selected degradation compounds.

For the oxidative degradation models, two models were developed. The first model had 3 inputs (MEA-concentration, oxygen concentration, temperature), and the second model had 10 or 11 inputs that included experimental data from the other measured degradation products. This was done to see if the modelled results would improve with more inputs to the model. The output was the calculated experimental reaction rate. For the thermal degradation models, two models were also developed. Here, there was one model with 3 inputs (MEA-concentration, $CO_2$-loading, temperature) and one with 6 inputs that included the other measured degradation products.

From the results, the models seem to be able to capture the trend of the experimental data. The models are data-driven, hence requiring a lot of experimental data. However, the model seems to be sensitive to outliers in the datasets so that the models can identify outliers in experimental data. The results are promising for further modelling, and with more research and more experimental data, the model predictions should quickly improve.

# Sammendrag

Folketallet i verden vokser, noe som fører til en økning i forbruket av ressurser og utslipp av klimagasser. Som et resultat av dette øker konsentrasjonene av klimagasser i atmosfæren til farlige nivåer, og behovet for tiltak for å redusere utslippene øker.[1] Ett tiltak som kan redusere utslipp er $CO_2$-fangst og lagring, som åpner mulighetene for å fjerne $CO_2$ fra røykgass, komprimere og lagre det i stedet for å slippe den ut i atmosfæren.

Et eksempel på en $CO_2$-fangstteknologi er kjemisk absorbsjon med aminbasert solvent. Med denne teknologien er det også utfordringer, hovedsakelig degradering av solventen. Ytterligere forståelse av degradering er viktig for å redusere driftskostnader, kontroll av solventen og utslippskontroll.

I denne oppgaven har hovedfokuset vært på oksidativ og termisk degradering av monoetanolamin (MEA), som er et det absorbsjonskjemikaliet som er forsket mest på innen kjemisk absorbsjon. Matematisk maskinlæringsmodellering har blitt brukt til å lage en prediktiv modell som kan beskrive degradering og trender i eksperimentelle data. Målet med arbeidet har vært å se om maskinlæringsmodellering har potensial til å gi gode modellforutsigelser, beskrive degradering av MEA og dannelsen av utvalgte degraderingsforbindelser.

For de oksidative degraderingsmodellene ble det utviklet to modeller. Den første modellen hadde 3 inputs (MEA-konsentrasjon, oksygenkonsentrasjon, temperatur) og den andre modellen hadde 10 eller 11 inputs, og inkluderte eksperimentelle data fra de andre målte degraderingsproduktene. Dette ble gjort for å se om de modellerte resultatene ville forbedres med flere inputs til modellen. Output fra modellene var den beregnede eksperimentelle reaksjonshastigheten. For modellene for termisk degradering ble det også utviklet to modeller. Her var det en modell med 3 inputs (MEA-konsentrasjon, $CO_2$-loading, temperatur) og en med 6 inputs, som inkluderte de andre målte degraderingsproduktene.

Fra resultatene ser modellene ut til å være i stand til å fange trenden til den eksperimentelle dataen. Modellene er datadrevne, og krever derfor eksperimentell data. Modellen ser ut til å være følsom for avvikende verdier i datasettene, og kan anvendes til å identifisere avvikere i eksperimentelle data. Resultatene er lovende for videre modellering, og med mer forskning og eksperimentelle data, bør modellprediksjonene lett forbedres.

# Preface

This master thesis has been carried out at the Department of Chemical Engineering at the Norwegian University of Science and Technology (NTNU) during the spring of 2021. The thesis has been written for TKP4900 - Chemical Process Technology, Master's Thesis in the Environmental- and Reactor Technology group.

I want to thank Hanna Knuutila, Andrés Carranza-Abaid, Lucas Braakhuis and Vanja Buvik for their guidance and help throughout the fall and spring semester, for teaching me a lot and for the opportunity to work with them on the interesting subject of amine degradation.

I would also like to thank my parents, Sofie and Daniel, for always supporting me and helping me when I needed it. Also, I would like to thank my plants for growing alongside my thesis and always being there after a long, hard day.

Lastly, I would like to thank the friends I have made during these five years for the amazing memories and for making the past five years at NTNU unforgettable!

Trondheim 14/6-2021

# Contents

# List of Figures

# List of Tables

# Table of symbols

| Symbol | Dimension | Description |
|---|---|---|
| $\underline{a}$ | - | Vector of linear transformed variables |
| $\alpha$ | [mol $CO_2$/mol MEA] | $CO_2$-loading |
| $\underline{b_1}$ | - | Biases of the hidden layer |
| $\underline{b_2}$ | - | Biases of the output layer |
| $C$ | - | Chemical component |
| $c^e$ | [kmol/m$^3$] | Experimental concentration |
| $c^{mod}$ | [kmol/m$^3$] | Modelled concentration |
| $C_{MEA,0}$ | [kmol/m$^3$] | Initial concentration of MEA in experimental dataset |
| $\underline{I}$ | - | Hidden layer weight matrix |
| $N$ | - | Number of datapoints in the dataset |
| $n$ | - | Measurement number |
| $\underline{n}$ | - | Simplified variable |
| $\underline{O}$ | - | Output layer weight matrix |
| $O_2$ | [%] | Concentration of oxygen |
| $\Omega$ | - | Vector of nonlinear functions |
| $r^e$ | [kmol/m$^3$*t] | Experimental reaction rate |
| $r^{mod}$ | [kmol/m$^3$*t] | Modelled reaction rate |
| $T$ | [K/°C] | Temperature in Kelvin or Celsius |
| $t$ | [days] | Time in days |
| $\underline{\omega}$ | - | Weight parameter |
| $\underline{X}$ | - | Vector of input variables |
| $\underline{x_A}$ | - | Constant of the hidden layer |
| $\underline{x_B}$ | - | Constant of the hidden layer |
| $\underline{x_C}$ | - | Constant of the hidden layer |
| $\underline{x_n}$ | - | Normalized input vector |
| $\underline{\hat{Y}}$ | [kmol/m$^3$*t] | Vector of predicted output variables |
| $\underline{Y^e}$ | [kmol/m$^3$*t] | Vector of experimental values |
| $\underline{y_A}$ | - | Constant of the output layer |
| $\underline{y_B}$ | - | Constant of the output layer |
| $\underline{y_C}$ | - | Constant of the output layer |
| $\underline{Z}$ | - | Vector of the sigmoid transformed normalized input variables |

# 1 Introduction

The Holocene is the name of the current geological epoch and has been one of the most stable periods in the history of our planet, with relatively small-scale climate shifts. During this period, the average temperature has not wavered more than ± 1 °C.[8] This period has also been called Anthropocene, meaning "The Age of Man", because of the impact humans have had on the planet.[9;10] No other species has changed its habitat more and faster than humans, with agriculture and urbanization of the wilderness. The human species have grown exponentially with the help of improved sanitation and medical care, which has led to increased pressure on the biodiversity of the planet. With an increasing human population, there is also an increase in resource consumption, and the need to meet demands has pushed technological progress forward.[8;9;10]

With increased production, there is also an increase of waste and emissions of greenhouse gases, such as $CO_2$, methane and nitrous oxide. As a result, greenhouse gas concentrations in the atmosphere are growing, affecting human health and global temperatures. In light of these effects, measures are needed to stop the anthropogenic, human-made emissions and possibly slow down global warming. Today, most anthropogenic emissions are from combustion. One measure that is very relevant and widely researched lately is $CO_2$-capture and storage technology, and one of the most promising $CO_2$-capture technologies is chemical absorption with amine-based solvents. Instead of emitting $CO_2$ from flue gas to the atmosphere, it can be removed for compression and storage.

## 1.1 Chemical absorption with amine-based solvents

Amines are well suited for separating $CO_2$ from flue gas because of their temperature dependant reversible reactions with $CO_2$.[11] A schematic of a typical amine-based $CO_2$-capture unit is shown in Figure 1.1. Flue gas is passed through the absorber, where an aqueous amine-based solvent absorbs the $CO_2$.[2] The rich amine is then sent to the top of the desorber to be separated from the solvent. The aqueous solution is heated with steam from a steam cycle, which will trigger the reversible reaction and thus separating the $CO_2$ from the amine. The lean amine is sent through a reboiler and back to the absorber again, and the cycle is repeated. The separated stream of $CO_2$ is taken out at the top of the desorber, compressed and transported through a pipeline for storage.[2]

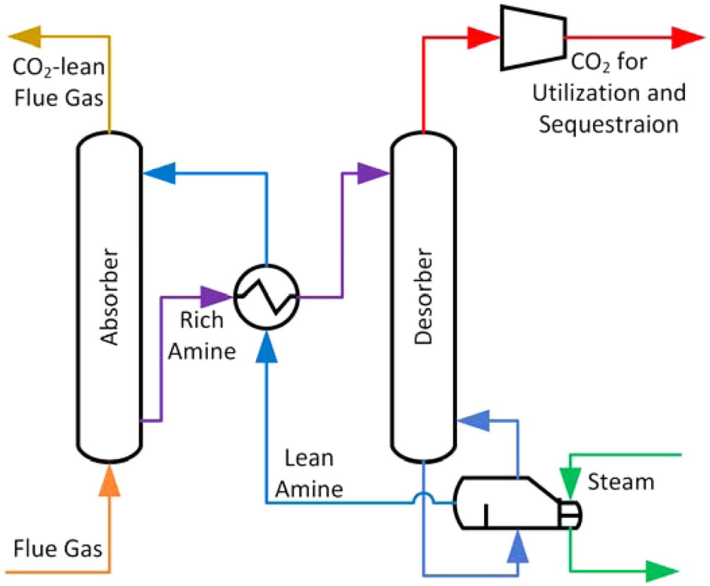


**Figure 1.1:** Schematic of an absorption based $CO_2$-capture unit.[2]

The ideal amine for amine-based $CO_2$ capture combines a high absorption rate and cyclic capacity with a low energy requirement for stripping, in addition to low degradation and corrosion.[5] One of the most researched amines for $CO_2$-absorption is monoethanolamine (MEA). MEA has a high affinity for $CO_2$ at low temperatures and a low affinity at high temperatures. It is also a cheap solvent that is not volatile, and it is therefore well suited for application in chemical absorption of $CO_2$.[12]

There are, however, challenges with chemical absorption, such as corrosion in the system and degradation of the solvent. These problems often have a significant impact on the costs and efficiency of the plant. Degradation can occur oxidatively or thermally and is when a chemical compound is broken down into smaller compounds. Oxidative degradation happens mainly in the absorber, where there is oxygen present in the gas stream. 80-90 % of degradation of amine solvents used in an amine-based $CO_2$-capture plant comes from oxidative degradation. Thermal degradation occurs mainly in the stripper and reboiler and is impacted by, for example, temperature and $CO_2$-loading. Other factors can have an impact on the degradation rate, such as the presence of $NO_x$, $SO_x$, iron and particles in the system.[5;11;12] Understanding the degradation process is vital for emission control and solvent management.

It is estimated that 10 % of the operational cost of a chemical absorption $CO_2$-capture unit can be related to degradation of the solvent.[6;13] It has therefore been essential to review issues related to degradation at an earlier stage of the process before installing a unit.

Oxidative degradation is not well understood today compared to thermal degradation. How fast oxidative degradation occurs, what products are formed, and in how large quantities are questions that are raised. One method that can help to understand further the degradation of solvents in absorption-based $CO_2$-capture plants is mathematical modelling and machine learning. By making a predictive model that can anticipate how fast and in what quantities the most known degradation products are formed, the plant may save money on operational costs. In addition, it is important to research at which conditions, such as temperature, oxygen levels and $CO_2$-loading, the degradation process is affected the most.

## 1.2 Mathematical modelling and machine learning

Mathematical modelling is a helpful tool to increase the understanding of complex problems that are not easily solved by hand and helps us describe the world around us according to our understanding. With a mathematical model, it is easier to see the effects of changes in the system and to get a deeper scientific understanding of a problem.[14]

One category of modelling is a mechanistic model. A mechanistic model uses mechanisms and theoretical information, such as equations of state or reaction equations, together with empirically fitted parameters to describe changes in a system. A mechanistic model often gives accurate predictions, but they are also computationally complex.[4] Therefore, empirical models have also been developed. There is no consideration of mechanisms in empirical models. Instead, the models try to account for changes in a system with different conditions quantitatively. One drawback of an empirical model is that its validity range is often limited.[4;14]

Machine learning (ML) has become increasingly popular because of its simplicity and computational speed. Machine learning technology is used to classify, find patterns and develop data predictions from a dataset.[4] There are three paradigms of machine learning; supervised learning, unsupervised learning and reinforcement learning.[15]

## 1.3 Scope of work and objective

In this thesis, the focus is on oxidative and thermal degradation of MEA. Based on experimental data from degradation experiments, a predictive model will be developed using mathematical machine learning.

This thesis aims to see if the developed machine learning models have good prediction abilities, capture trends in the datasets, and describe the degradation of MEA. The ultimate goal is to develop an ML model that can be applied in different chemical absorption plants to indicate how the solvent will degrade over time and how fast the degradation happens at the given conditions used in that specific plant. However, before this is possible, there is a need to see if machine learning has potential and can be used as a start in the research and development of predictive models for oxidative and thermal degradation.

Furthermore, the impact of the number of inputs have on the results is investigated. For oxidative degradation, two models are developed, one with three inputs and one with ten or eleven inputs. Two models are also developed for thermal degradation, one with three inputs and one with six inputs. The second models use all the available experimental data as inputs to see if there is a possible correlation between MEA and the measured degradation products. Developing these models can help in the further understanding of degradation. Compared to thermal degradation, oxidative degradation is not well understood today. A better understanding of what affects the degradation rate in a capture plant can help reduce operational costs, increase the understanding of the system and the efficiency of the plant.

First, the theoretical background of oxidative and thermal degradation and machine learning is presented in Chapter 2. Then, the methodology of the thesis is given in chapter 3 before the results are presented and discussed in Chapter 4. Finally, the conclusion and recommendations for future work are given in Chapter 5 and 6.

# 2 Theoretical background

In this chapter, the main principles for oxidative and thermal degradation are presented. In this thesis, two publications were used as the primary sources, one publication from Vevelstad et al. (2016) and one publication from Davis (2009). The experimental data that has been used in the machine learning models were retrieved from these two papers. In this chapter, the experimental setup, the methodology, and the main findings from these publications are presented. Furthermore, the suggested reaction mechanisms for the formation of the degradation compounds from MEA are shown. Also, the main principles of machine learning and the theory behind artificial neural networks is explained.

**Table 2.1:** Table of abbreviations, compound names and CAS-numbers for the compounds used for further modelling of oxidative and thermal degradation.[5;6;7]

| Abbreviation | Compound | CAS |
|---|---|---|
| BHEOX | N,N-bis(2-hydroxyethyl)oxalamide | 1871-89-2 |
| | Formate | N/A |
| HEA | N-(2-hydroxyethyl)-acetamide | 142-26-7 |
| HEEDA | N-(2-hydroxyethyl)ethylenediamine | 111-41-1 |
| HEF | N-(2-hydroxyethyl)formamide | 693-06-1 |
| HEGly | N-(2-hydroxyethyl)glycine | 5835-28-9 |
| HEI | N-(2-hydroxyethyl)imidazole | 1615-14-1 |
| HEIA | N-(2-hydroxyethyl)imidazolidin-2-one | 3699-54-5 |
| HEPO | 4-(2-hydroxyethyl)-2-piperazinone | 23936-04-1 |
| MEA | 2-Monoethanolamine | 141-43-5 |
| | Oxalic acid | 144-62-7 |
| TriHEIA | 1-(2-((2-hydroxyethyl)amino)ethyl)-2-imidazolidone | N/A |

## 2.1 Oxidative degradation

Oxidative degradation occurs when oxygen is present in the gas stream. Several factors can affect the degradation rate, such as temperature and oxygen concentration. There are still some gaps in the understanding of oxidative degradation. The experimental data for oxidative degradation is from a systematic study of the degradation of MEA under simulated absorber conditions in lab-scale experiments. The study was conducted by Vevelstad et al. (2016).[5]

Many degradation products have been identified in oxidative degradation studies, and these products are divided into primary and secondary degradation compounds. Primary degradation compounds are those that are first formed through oxidation reactions or radical reactions.[5] Many compounds are considered as primary degradation compounds, but in this study, the focus will be on two of them, formate and oxalic acid, because of available experimental data. Ammonia is also considered a primary degradation compound. However, due to high ammonia volatility, there were uncertainties in the analyses, and the data was not included in the modelling. The primary degradation compounds are reactive, chemical species and may react further with MEA or other degradation compounds to become secondary degradation compounds.[5] There are also many secondary degradation compounds, but in this study, the compounds that will be focused on are HEF, HEI, BHEOX, HEPO, HEA and HEGly. The compound names, abbreviations and CAS-numbers are given in Table 2.1.

When comparing lab-scale experiments to pilot-scale, it is seen that similar degradation products are formed. However, there is a larger variety of degradation products formed in a pilot plant. This is expected, though, because the conditions are more varied in a pilot plant than in the lab-scale experiments, where the conditions are often constant. When comparing lab-scale and pilot-scale experiments, the degraded solvent from the pilot was more similar to the solvent from the oxidative degradation experiments than the solvent from the thermal degradation experiments, suggesting that oxidative degradation dominates in pilot plants.[16]

As mentioned, oxidative degradation is still not well understood. This applies to, for example, under given conditions, what products are formed, their reaction paths, how fast they are formed, and in what quantities. A further understanding of these problems could help optimize the efficiency and possibly decrease the operational costs of a capture plant.

### 2.1.1 Reaction equations describing the degradation of MEA

Suggested reaction equations for the formation of the degradation compounds are presented in this subsection. They are simplified reaction equations collected from previous research where oxidatively degraded solutions from lab-scale experiments and pilot plants have been analyzed. Many components have been found in solvent analyses, and likely reaction paths have been suggested based

on these findings. There are still many uncertainties in the formation reactions, there are several different reaction paths presented in different papers, and they are often very complicated. When the reactions that occur are not entirely understood, this has made it challenging to develop a model that accurately describes oxidative degradation. Complex reaction mechanisms are often simplified in degradation modelling. This is also the case in this thesis. Only the most relevant reaction equations have been included in this thesis.

$$2\mathrm{MEA} + \mathrm{CO_2} \leftrightarrows \mathrm{MEACOO^-} + \mathrm{MEAH^+}\,[2] \tag{2.1}$$

$$\mathrm{MEA} + 3\mathrm{H_2O} \rightarrow 2\mathrm{CH_2O} + \mathrm{NH_3} + 2\mathrm{H_3O^+}\,[17] \tag{2.2}$$

$$\mathrm{CH_2O} + \frac{1}{2}\mathrm{O_2} \rightarrow \mathrm{HCOOH}\,[18] \tag{2.3}$$

$$\mathrm{MEAH^+} + \mathrm{HCOO^-} \leftrightarrows \mathrm{HEF} + \mathrm{H_2O}\,[18] \tag{2.4}$$

$$\mathrm{MEA} + \mathrm{O_2} \rightarrow \mathrm{C_2H_2O_2} + \mathrm{H_2O} + \mathrm{NH_3}\,[17] \tag{2.5}$$

$$\mathrm{MEA} + \mathrm{CH_2O} + \mathrm{C_2H_2O_2} + \mathrm{NH_3} \leftrightarrows \mathrm{HEI} + 3\mathrm{H_2O}\,[19] \tag{2.6}$$

$$\mathrm{C_2H_2O_2} + \mathrm{O_2} \rightarrow \mathrm{C_2H_2O_4}\,[17] \tag{2.7}$$

$$2\mathrm{MEA} + \mathrm{C_2H_2O_4} \leftrightarrows \mathrm{BHEOX} + 2\mathrm{H_2O}\,[18] \tag{2.8}$$

$$\mathrm{MEA} + \mathrm{C_2H_2O_4} \rightarrow \mathrm{HEGly} + \mathrm{H_2O} + \mathrm{CO_2}\,[18] \tag{2.9}$$

$$\mathrm{MEAH^+} + \mathrm{CH_3COOH} \leftrightarrows \mathrm{HEA} + \mathrm{H_2O}\,[18] \tag{2.10}$$

$$\mathrm{MEA} + \mathrm{HEGly} \rightarrow \mathrm{HEPO} + 2\,\mathrm{H_2O}\,[18] \tag{2.11}$$

### 2.1.2 Extensive dataset for oxidative degradation of MEA

The experiments were conducted in an open batch reactor. The experimental setup is shown in Figure 2.1. First, a feed gas, a mixture of $CO_2$ (7.5 mL/min) and air (0.35 L/min), was bubbled through a water vapour saturation tank. Then, the feed gas and a recycle gas stream (50 L/min) were pumped to the glass reactor filled with a preloaded solution of MEA (30 wt% MEA and 0.4 mol $CO_2$ per mol of MEA).[3;5]

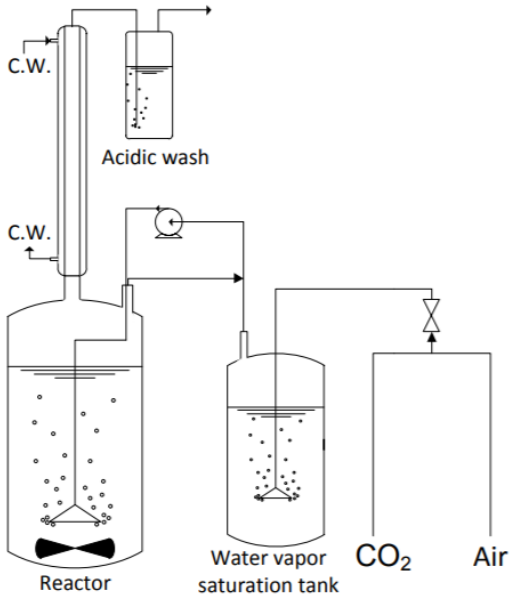


**Figure 2.1:** Overview of the experimental setup for the oxidative degradation experiments.[3]

After the gas was bubbled through the glass reactor, it was led through two condensers. Here, the water vapour was condensed and returned to the reactor, and the gas was passed through an acidic wash and a water wash to absorb volatile and basic degradation products. The length of the experiments varied from 21 - 42 days, depending on temperature and oxygen concentration, and samples were taken out from the glass reactor and analyzed with intervals between 3 - 6 days. The components that were measured and used for the models developed in this study are MEA, formate, HEF, HEI, oxalic acid, BHEOX, HEPO, HEA, and HEGly. The compound names, abbreviations and CAS-numbers for these chemical compounds are given in Table 2.1.[5;7]

The experiments were performed with four different $O_2$-concentrations (6%, 21%, 49% and 98%) at three different temperatures (55 °C, 65 °C, 75 °C). An overview of the experiments and their respective labels is given in Table 2.2. [5]

**Table 2.2:** Overview of the oxidative degradation experiments used in the models, the conditions they were conducted at and their respective labels. [5]

| T [°C] / $O_2$[%] | 6 | 21 | 49 | 98 |
|---|---|---|---|---|
| 55 | A1 | A2-I, A2-II | A3 | A4 |
| 65 | B1 | B2-II | B3 | B4 |
| 75 | C1 | C2 | C3 | C4 |

Because of experimental difficulties, some of the experimental data was not included further in the modelling and data fitting. This applies to experiment B2-I and experiment A2-III. In experiment B2-I, there was a significant water loss resulting in deviations in the mass balance. A water loss will result in higher concentrations of the measured components. This also applies to experiment C2. A correction for water loss was done, and it was decided that experiment C2 would be included in the modelling. Experiment A2-I, A2-II and A2-III were performed at the same conditions, but the results measured from experiment A2-III did not coincide with experiments A2-I and A2-II. It was therefore decided to exclude the results from experiment A2-III in the optimization.

From the experimental results of the study performed by Vevelstad et al. (2016), there was a trend of increased degradation rate with higher temperatures and oxygen concentrations. There is a more significant increase in the degradation rate with increasing temperature than increasing oxygen concentration in the gas phase. This also applies to MEA, where an increased degradation rate was observed with increasing temperature for all oxygen concentrations.

For all oxygen levels, the concentration and the rate of formation of the primary degradation products, formate and oxalic acid, was increasing with increasing temperatures. The concentration levels of oxalic acid are much smaller than for formate, and according to Rooney et al. (1998), this is believed to be because oxalic acid is formed in more steps than formate and the path of formation for oxalic acid is less favorable. [20]

HEGly and HEPO are major degradation compounds found in pilot plants. [12] A trend was seen where the highest concentration levels of HEGly occurred

when the oxygen content was lowest, and it decreases with increasing oxygen concentrations. Therefore, it is believed that HEGly is consumed as the reactant in another reaction dependent on oxygen.[5] The suggested simplified mechanism describing the formation of HEPO from MEA and HEGly is shown in Equation 2.11.[18] The formation rate of HEPO was not affected by the oxygen levels. As mentioned, HEPO is a major degradation compound, but in the experiments performed by Vevelstad et al. (2016), the formation of HEPO observed was low compared to what is generally found in pilot plant samples, indicating that the experiments were not able to capture the typical behaviour of HEPO.[5]

HEF, HEA and BHEOX are believed to be formed from the reaction between MEA and different acids. The suggested reaction mechanism for HEF is shown in Equation 2.4, where MEA and formate ($HCOO^-$) react and HEF and water is formed. HEF formation is believed to be rapid, and the formation rate increases with increasing oxygen levels.[5] The reaction for the formation of HEA is shown in Equation 2.10, where HEA is formed from MEA reacting with acetic acid. HEA was produced in much lower amounts than HEF, about 10 % of the amount. HEA had similar behaviour as the other degradation compounds, where the concentrations increased with increasing temperatures and oxygen levels.[5;18] The reaction for the formation of BHEOX is shown in Equation 2.8, where MEA reacts with oxalic acid. The measured amounts of BHEOX and oxalic acid are low, and this is because these components are formed after several reaction steps. The concentration of BHEOX also increased with increasing oxygen levels, but it seems to go through a maximum after 3-15 days. This might be because BHEOX decomposes at higher temperatures. BHEOX is therefore not a major degradation compound as it will decompose in stripper conditions.[5;18]

The suggested formation reaction for HEI is shown in Equation 2.6. HEI is formed from MEA and primary degradation compounds. The measured concentration levels are around the same as the concentration of HEGly. Therefore, it is an important degradation compound. The formation rate of HEI was similar to many of the other degradation products, favoured by high temperatures and oxygen levels.[5]

The study observed that the accelerated degradation experiments performed at 98 % oxygen could not easily be extrapolated to what happens at 6 % oxygen. The experiments performed at higher oxygen levels will not easily represent the situation in an industrial amine absorption plant, where the oxygen levels are

around 3-11 % regarding products formed and the reaction rates.[5] However, to optimize a model as much as possible, it is favourable to have as much data as possible. When developing a machine learning model, a large amount of data retrieved under various conditions is good for parameter optimization.

## 2.2 Thermal degradation

Thermal degradation occurs in the stripper and reboiler of an absorption-based $CO_2$-capture plant. Thermal degradation mechanisms describe the irreversible reactions between MEA and $CO_2$ without any oxygen present, and degradation rates are affected by parameters such as temperature, $T$, and $CO_2$-loading, $\alpha$.[21] Thermal degradation of MEA in the presence of $CO_2$ has been studied since the 1950s.[16] Several degradation products have been identified, and the main products are 2-oxazolidone (OZD), HEEDA and HEIA. More research has been done on thermal degradation of MEA, and it is more understood than oxidative degradation. Several models on thermal degradation have also been developed in earlier work. The methodology, relevant results, and reaction equations from a study performed by Davis (2009) are presented in the following section.

### 2.2.1 Thermal Degradation of Aqueous Amines Used for $CO_2$-Capture

Davis (2009) conducted the thermal degradation experiments at the University of Texas, and the experimental data used in this study is retrieved from this thesis. The experiments were run for 56 days at two different temperatures, 120 ℃and 135 ℃, 3 different $CO_2$-loadings, 0.2, 0.4 and 0.5 moles of $CO_2$ per mole of MEA, and three different initial MEA concentrations 6.58, 4.9 and 2.88 kmol/m$^3$.[6] An overview of the experiments conducted, their respective labels and the conditions they were conducted in is given in Table 2.3.

The experiments were performed in stainless steel tubes with endcaps. The tubes were loaded with MEA solution and closed. There must be no leaks from the tubes because then the experiment has to be discarded. The tubes were then placed in an oven and heated to the correct temperatures. Samples were taken and analyzed every seven to fourteen days for the eight weeks the experiment was run. The components that were measured during the experiments were MEA, HEEDA, HEIA, and TriHEIA. The compound names, abbreviations and CAS-numbers of the chemical compounds are given in Table 2.1.[6;7;22]

**Table 2.3:** Overview of thermal degradation experiments, the conditions they were conducted at and their respective labels.[6]

| | $C_{MEA,0}$[kmol/m$^3$] / $\alpha$ [mol $CO_2$/mol MEA] | 0.2 | 0.4 | 0.5 |
|---|---|---|---|---|
| | 6.58 | E1 | E2 | E3 |
| 120 °C | 4.9 | E4 | E5 | E6 |
| | 2.88 | E7 | E8 | E9 |
| | 6.58 | F1 | F2 | F3 |
| 135 °C | 4.9 | F4 | F5 | F6 |
| | 2.88 | F7 | F8 | F9 |

Since the experimental data used in this thesis is from Davis (2009), the suggested mechanisms from his publications were also the focus. The suggested reaction equations for the formation of HEEDA, HEIA and TriHEIA from MEA is shown in Equation 2.12 - 2.17. Here, OZD and MEA trimer are known intermediate products, as it is found in small amounts in thermal degradation experiments.[6;22]

$$2\text{MEA} + \text{CO}_2 \leftrightarrows \text{MEACOO}^- + \text{MEAH}^+ \tag{2.12}$$

$$\text{MEACOO}^- + \text{MEAH}^+ \leftrightarrows \text{OZD} + \text{MEA} + \text{H}_2\text{O} \tag{2.13}$$

$$\text{MEA} + \text{OZD} \leftrightarrows \text{HEEDA} + \text{CO}_2 \tag{2.14}$$

$$\text{HEEDA} + \text{CO}_2 \leftrightarrows \text{HEIA} + \text{H}_2\text{O} \tag{2.15}$$

$$\text{HEEDA} + \text{OZD} \leftrightarrows \text{MEAtrimer} + \text{CO}_2 \tag{2.16}$$

$$\text{MEAtrimer} + \text{CO}_2 \leftrightarrows \text{TriHEIA} + \text{H}_2\text{O} \tag{2.17}$$

In the reaction equations, HEIA is formed from HEEDA and not the other way around, which is suggested in other publications on thermal degradation, such as Polderman et al. (1955).[23] In a publication done by Gary and Rochelle (2009),

this was researched further. Two reactors were filled with $CO_2$-loaded HEEDA, one with a solution of HEEDA and MEA, and one with HEIA and MEA was placed in ovens at 135°C. When analyzing the solutions later, it was found that in the reactors containing $CO_2$-loaded HEEDA and MEA, HEEDA converted rapidly to HEIA. On the other hand, in the reactor containing HEIA and MEA, the conversion to HEEDA was not seen until very long hold times.[16;24] This leads us to believe that the reaction presented in Equation 2.15 where HEIA is formed from HEEDA, is reasonable.

In the analysis of the solvent, it was found that the rates of formation of the thermal degradation compounds had a direct correlation with temperature, increasing amine concentration, and increasing concentration of $CO_2$. The most substantial dependency was on the temperature, and the results showed that the rate would double for every 7 °C increase in temperature.[6]

## 2.3 Machine learning

Machine learning is a subset of artificial intelligence. The objective of machine learning is to emulate how a biological brain processes information. This enables a system to be able to learn from data by analyzing it and eventually improving itself.

Today, ML is a part of a human's daily life. Possible applications of ML are inventory predictions, recruitment, or marketing. An example of a common interaction between humans and machine learning from day to day is targeted ads. When one searches for something on the Internet or is in a specific target group, relevant ads appear on social media and other web pages. This is because the company making the ad has an ML algorithm designed to target specific audiences. Another example of machine learning in marketing is contextual relevance. For example, the algorithm identified that ads for chocolate had more impact on consumers in the afternoon than in the morning, so the ads for a specific chocolate product was run more in the afternoon. This saves the company money used for marketing and increases the popularity of the product. Machine learning has improved many fields and has allowed companies to become more strategic and effective than before.[25]

Rather than doing complicated programming, a machine learning model enables a system to learn from data and often simplifies a complex program code. However, ML is not a simple process, but because of the fast-developing capabilities of today's computers, its popularity has increased more and more.

### 2.3.1 Paradigms of machine learning

Machine learning has three different paradigms; supervised learning, unsupervised learning and reinforcement learning.

Supervised learning is based on training with a labelled and established set of data. In that way, supervised learning can find patterns in a dataset and apply them to the intended process. With the understanding of how a dataset is classified, a machine learning model can distinguish between millions of animals based on images and descriptions of the given animals. Machine learning in supervised systems often uses a mapping method, such as a decision tree and logistic regression where an input, $x$, produces an output, $y$.[15;26]

In unsupervised learning, the data is not labelled. The intention is to understand the meaning of the data by using algorithms that find patterns or clusters and classify the data based on them. Examples are in social media, where large amounts of unlabeled data are generally hard to classify. Unsupervised learning is built upon assumptions about the data, such as structural, combinatorial and probabilistic properties.[15;26]

In reinforcement learning, there is no correct output for a given input. Instead, the system learns through trial and error. The training data in reinforcement learning gives only an indication of what is the correct output. If the system gives an incorrect output, it will try again to find a correct output, and when a series of correct outputs has been given, the understanding of the system of the data will be reinforced.[15;26]

In this project, the machine learning models that have been developed are based on supervised learning with a single hidden layer and is called a supervised shallow neural network. In the following section, artificial neural networks and the theory behind supervised shallow neural networks is presented.

### 2.3.2 Artificial neural networks

An artificial neural network (ANN) is the part of a computing system that we would want to analyze and process information similarly to the human brain. Learning in this method happens through iteration. Deep learning uses neural networks in several hidden layers, while shallow neural networks only have one hidden layer. Artificial neural networks are explained in more detail in this section. The procedure for making a supervised shallow neural network model with the Deep Learning Toolbox from MATLAB R2019a is presented in Subsection 3.4. Artificial neural networks were first proposed by Warren McCullough and Walter Pitts in 1944.[27] An ANN is a nonlinear vector of functions that takes in a vector of inputs and weight parameters and provides a vector of outputs. An ANN has the general form shown in the equation below.[4]

$$\underline{\hat{Y}} = \Omega(\underline{X}; \underline{\omega}) \tag{2.18}$$

Where $\Omega$ is a vector of nonlinear functions, $\underline{X}$ is a vector of input variables, and $\underline{\omega}$ is a set of weight variables. This gives the predicted vector of output variables, $\underline{\hat{Y}}$.[4]

In Figure 2.2 the $\Omega$-function is illustrated and shows the training process of a single layer feed-forward neural network (FFNN). The system in the figure has three input variables, four neurons in a single hidden layer, and two output variables. Because the information only flows in one direction, forward, it is called a forward propagation model. A single layer FFNN is the same as a supervised shallow neural network. The loss function compares the predicted output variables, $\underline{\hat{Y}}$, with the experimental or modelled values, $\underline{Y^e}$ and calculates the error. If the system does not meet a predetermined tolerance or the performance is not satisfactory, a backpropagation signal is sent, and the process is repeated until the predictions of the output variables stop improving or the tolerance is met.[4]

The Equations 2.19 - 2.23 describe the operations that occur in pre-processing of the input data before the hidden layer, what happens in the hidden layer and the post-processing of the predicted output data. The variables $\underline{x_n}$, $\underline{x_A}$, $\underline{x_B}$, $x_C$, $y_A$, $y_B$, $y_C$, $\underline{b_1}$, $\underline{b_2}$, $\underline{I}$ and $\underline{O}^T$ together form the weight parameter $\underline{\omega}$ from Equation 2.18. The five equations together form the vectors of nonlinear functions, $\Omega$, from Equation 2.18. $\underline{Z}$ is the result of a sigmoid transformation of the normalized input variables and $\underline{a}$ is the result of a linear transformation of

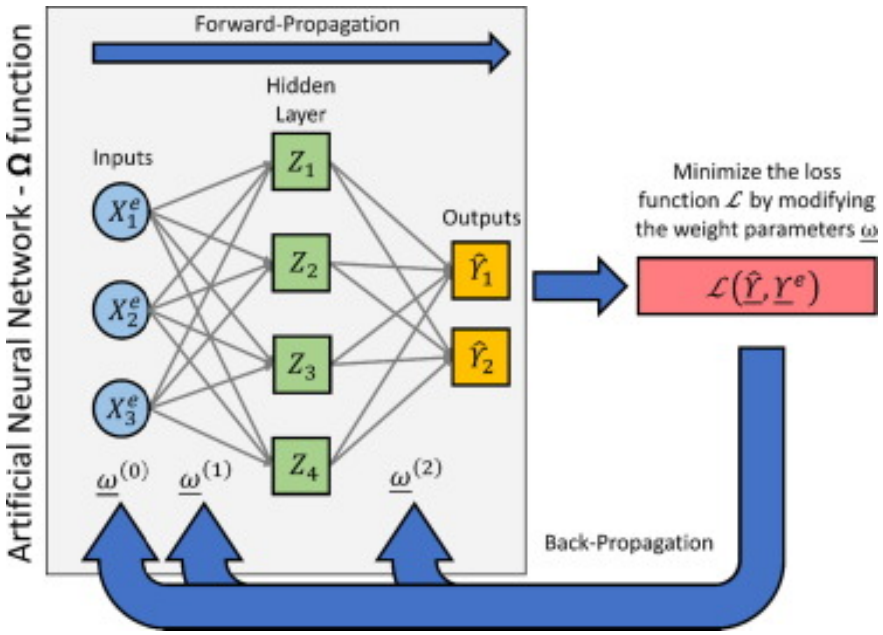


**Figure 2.2:** Schematic of a feed-forward neural network trained by a back propagation algorithm.[4]

the vector $\underline{Z}$. All the equations and a more detailed explanation of them is given below. Example code is given in the appendix in Section C.

The hidden layer is a transformation of the input vector, $\underline{X}$, to a vector $\underline{Z}$, as seen in Figure 2.2. Before the transformation, the vector of input variables is normalized with the following equation.

$$\underline{x_n} = (\underline{X} - \underline{x_A}). * \underline{x_B} + x_C \tag{2.19}$$

Where $\underline{x_n}$ is the vector of normalized input variables, $\underline{X}$ is the vector of input variables and $\underline{x_A}$, $\underline{x_B}$ and $x_C$ are constants or matrices of constants generated by MATLAB. $.*$ is used to do an element-wise multiplication. The sigmoid transformation usually happens through a sigmoid symmetric transfer function, which is a hyperbolic tangent function. This function is shown in Equation 2.20. The matrix $\underline{Z}$ represents the result of the sigmoid transformation of the normalized variables.

$$\underline{Z} = tansig(\underline{n}) = 2./(1 + e^{-2\underline{n}}) - 1 \tag{2.20}$$

where $\underline{n}$ is a simplification of the expression below,

$$\underline{n} = \underline{b_1} * \underline{Q} + \underline{I} * \underline{x_n} \tag{2.21}$$

Here *tansig* is mathematically equivalent to *tanh* with small numerical differences between the two, but the *tansig* function runs faster with MATLAB. In neural networks, the shape of the transfer function is not emphasized. However, speed is important for effective models.[28] $\underline{b_1}$ is the bias of the hidden layer, and $\underline{I}$ is the hidden layer weight matrix. $\underline{Q}$ is the number of samples in the dataset. ./ is used to do an element-wise right division.

Afterwards, the vector $\underline{Z}$ together with the weight parameters $\underline{b_2}$ and $\underline{O}^T$ are transformed with a linear transformation function.[4] The linear transformation function is shown below.

$$\underline{a} = \underline{b_2} * \underline{Q} + \underline{O}^T * \underline{Z} \tag{2.22}$$

Where $\underline{b_2}$ is the bias of the output layer, and $\underline{O}^T$ is the output layer weight matrix. Finally, to get the vector of predicted output variables, $\underline{\hat{Y}}$, the data is un-normalized with the following equation.

$$\underline{\hat{Y}} = \left(\frac{\underline{a} - y_C}{y_B}\right) + y_A, \tag{2.23}$$

where $y_A$, $y_B$, and $y_C$ are constants that MATLAB generates.

# 3 Methodology

All the models presented in this report have a basis in experimental data. The data for oxidative degradation is from work done by Vevelstad et al. (2016), and the data for thermal degradation is from work done by Davis (2009). In this chapter, the methodology of the thesis is described. The method used for developing machine learning models and the different ways of presenting the results, the simplifications and assumptions are presented.

The models that were made in this report are based on the rate of reaction for each component. When using reaction rates, the problem is transformed from requiring a neural network with feedback to a feedforward neural network. Therefore, the data had to be treated and transformed from experimental concentration measurements to the experimental reaction rate for each component. This was done with the following equation.

$$r^e_{C,n} = \frac{\Delta c^e}{\Delta t} = \frac{c^e_{C,n+1} - c^e_{C,n}}{t_{C,n+1} - t_{C,n}} \tag{3.1}$$

$\Delta c^e$ is the change in experimental concentration of the component over the time interval, $\Delta t$. $r^e_{C,n}$ is the experimental reaction rate for each of the components, $C$, and $n$ is the measurement number. $c^e_{C,n}$ is the experimental concentration of the component, and $t_{C,n}$ is the time the measurement was made. This equation measures the change in the concentration of the compounds over time and is a commonly used equation for calculating reaction rates.[29] The rate of reaction was used as an output in the machine learning models.

After developing the machine learning models, a modelled rate is obtained by running the experimental input data through the ML model. This modelled rate was used to find the modelled concentrations of the components at the different measurement points. The modelled concentration, $c^{mod}_{C,n+1}$ was calculated by reversing Equation 3.1. The equation is shown below.

$$c^{mod}_{C,n+1} = r^{mod}_{C,n}(t_{C,n+1} - t_{C,n}) + c^{mod}_{C,n} \tag{3.2}$$

$r^{mod}_{C,n}$ is the modelled reaction rate for each of the components, $C$, at measurement $n$.

Several methods were tried to find the optimal fit, the best way to recreate the experimental data, and optimizing the parameters. This included varying the number of inputs of the machine learning models and how the concentrations were calculated from the modelled rates.

## 3.1 Oxidative degradation models

An evaluation of the raw data from the oxidative degradation experiments has been done. The results showed a significant difference in the measured values between the different analytical methods that analyzed the data. As mentioned in Section 2.1.2, this was because of some experimental difficulties. The results from experiment A2-III did not coincide with experiment A2-I and A2-II, even though the three experiments were performed under the same conditions. The data from experiment A2-III was therefore not included further. Experiment B2-I had a significant water loss, which resulted in a higher measured concentration of MEA, and this data was also not used in any further research or development of a model.[5]

The first modelling method that was tried out was a machine learning model with 3 inputs and one output. The inputs of the model were the experimental MEA-concentration, oxygen concentration, and temperature. The output was the calculated rate of reaction for one of the nine different components. Thus, nine ML models were created, one for each one of the chemical components.

The second ML model that was developed had 10 inputs and one output. The 10 inputs were temperature, oxygen concentration and the concentrations of eight of the nine components. The only component not included was oxalic acid because the measured concentrations from experiment A2-I were missing or too uncertain to include in the results. Therefore, oxalic acid was excluded as an input in the model. This was to include as much data as possible in the modelling of the reaction rates. However, the oxalic acid model had 11 inputs because the data for oxalic acid was included as an input. The output of the models was the rate of reaction of each of the different components. Also here, nine ML models were developed.

A few methods of calculating the modelled concentrations were tried out. The first method was to use the instantaneous rate, which is the rate at which a reaction is proceeding at a specific time.[29] The other method was to use the

average rate of each experiment as the reaction rate, $r_{C,n}$, assuming the rate is independent of the concentration levels of the degradation compounds. This was done to simplify the model and to attempt to make it more user-friendly. The goal was to develop a model that can be applied in different chemical absorption plants to indicate how the facility's components will degrade over time and how fast the degradation happens at the given conditions used in that specific plant.

## 3.2 Thermal degradation models

There was less available experimental data from the experiments performed by Davis (2009). Some measurements for the different degradation products were not available because of experimental difficulties and uncertainties. Two models were developed for predicting the rates of thermal degradation. The first model had 3 inputs and one output. The inputs were temperature, MEA-concentration and $CO_2$-concentration, and the output was the experimental reaction rate calculated with Equation 3.1. Also here, one model was developed for each of the four degradation compounds.

The second model that was developed used all the experimental data as input. In total, there were 6 inputs, temperature, MEA-concentration and $CO_2$-concentration, in addition to the concentration of HEIA, HEEDA and TriHEIA. Where experimental points were unavailable, the NaN (not a number) function in MATLAB was used for these values.

## 3.3 Assumptions and simplifications

As described in Section 2.1.2, there was some water loss that occurred in the duration of the oxidative degradation experiments. This resulted in concentration measurements that were too high and also some concentration jumps in the measured data. When the reaction rate of MEA was calculated with Equation 3.1, there were some positive values for the rate, indicating that MEA had been formed during the experiments. For the thermal degradation experiments, the same issues were seen with positive values for the reaction rates for MEA. These positive values were not wanted when developing the model. This is because, in this thesis, it is assumed that MEA is not formed, only consumed in oxidative and thermal degradation. Therefore, it was decided that the positive values for the reaction rate of MEA would not be included when developing the machine learning models that modelled the reaction rates of MEA. When making the

plots of the results, all the experimental data was included again.

After the ML models were developed, all experimental data, including the removed points before developing the model, were run through the model. This was to obtain as many reaction rates as possible to have more modelled predictions to compare with the experimental data. There was a problem with underprediction in the plotted results for MEA from the 3 input model with instantaneous rate. To avoid this, the data points or experiments where there were concentration jumps were removed altogether. Therefore, the plotted curve for the 3 input model with instantaneous rate is not included in many of the figures, or the first measurement point is missing, and the plot starts at the second measurement point. An example is Figure 4.2, where the ML model with three inputs and instantaneous rate, which is the purple line, starts at the second measurement point.

The average of the modelled rate was used when calculating the modelled concentration of the degradation products for one of the models. This assumes that the rate is independent of the concentration of MEA and results in a linear trend for the concentration curves. From previous research, it is seen that this is often not the case, as the concentration often has exponential growth, and the concentration will flatten out after reaching a maximum or react further and form other components.[5] Therefore, the concentration was also calculated by using the instantaneous rate to compare the two methods.

The density is assumed to be constant for the duration of the experiments. The density was measured at the beginning and end of every experiment. The change in density was around 1 % for all experiments, so it can be assumed that it does not significantly impact the results.

## 3.4 Developing a supervised shallow neural network model

Training a machine learning model is analogous to doing polynomial fitting, only that the optimization equations are more complex. In this section, the steps and considerations for making a supervised shallow neural network model are presented. Example MATLAB code is given in the appendix in Section C.

Before training the model with a dataset, one first has to choose what fraction of the data will be used for training, validation and testing. The data used for training will fit the model. The validation dataset is held back from the

model and used to evaluate and further fit the model. The testing dataset is for evaluating the fit of the final model compared to the training dataset. [30]

Then the number of neurons in the hidden layer is chosen. The more neurons there are in the hidden layer, the more computation is needed to solve the problem. The network often needs many neurons in the hidden layer to give an appropriate model for more complicated problems. The fitting performance of the model is then evaluated. If the model is overfitted, there are too many neurons in the hidden layer. This will result in a model that is too well fitted to the specific dataset, so its ability to generalize is negatively affected. When the model has not learned enough from the training data, its predictions are unreliable and not generalized. This is known as underfitting and will result in the model not capturing the dominant trend of the data. [31] If the model is overfitted or underfitted, it will cause problems when introducing new data to it. When finding the optimal number of neurons in the hidden layer where the model is not overfitted or underfitted, a trial and error method is a common approach.

There are two main optimization methods available in MATLAB's deep learning toolbox. Levenberg-Marquardt (LM) backpropagation algorithm or the Bayesian Regularization (BR) backpropagation algorithm. When the neural network is moderate-sized, LM is the fastest method. [32] The BR algorithm typically requires more time, but it has good generalization and prediction qualities and is a combination of the LM optimization method and Bayesian interpolation method. The BR algorithm can give good results for noisy or small datasets. [33]

Finally, the model can be trained with the chosen data and conditions. The goal is for the correlation coefficient, $R$, to be close to 1, which indicates a close relationship between the output and target variables. [4]

If the correlation coefficient is not optimal, the neural network can be retrained several times to see if the results improve. Each time the model is retrained, different solutions are obtained, and the outputs will therefore change even though the inputs are the same. One can often improve the accuracy of a model by retraining it several times. [34]

The models developed in this thesis are shallow neural network models with a single hidden layer. The number of neurons in the hidden layer was varied from model to model to optimize the fit. An example model with 3 inputs, four neurons in the hidden layer and one output is illustrated in Figure 3.1. Here

one can see that there is one hidden layer and one output layer. The sigmoid transformation of the input data happens in the hidden layer, and the linear transformation of the output variables happens in the output layer. The $w$ and $b$ represent the weight matrices and the biases, respectively.

For the machine learning models model in this thesis, the optimization method used was Bayesian Regularization with three or four neurons in the hidden layer, depending on the dataset. The number of neurons is determined by the complexity of the problem, not by the amount of data. However, the amount of data constrains the number of neurons that can be used. Because there was not a lot of data available, the percentage of data used for validation and testing was chosen to be 5-10 %, so most of the data would be used for training. This was to optimize the fitting and predictions of the models.

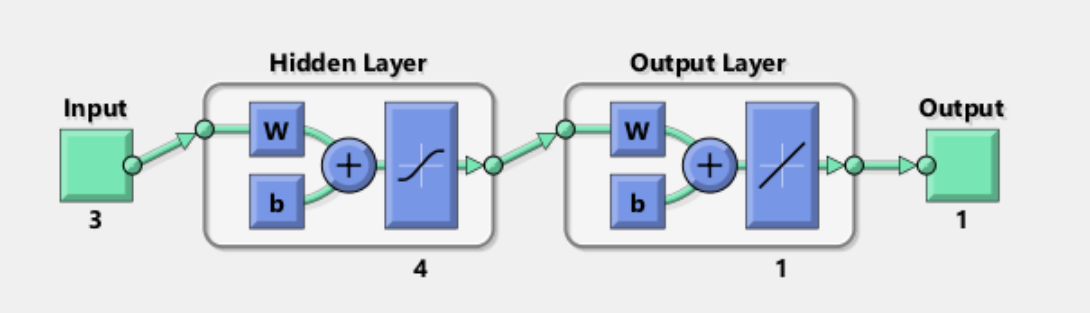


**Figure 3.1:** Flow sheet of the setup of a supervised shallow neural network with three input variables, four neurons in the hidden layer, one output layer and one output variable. The figure is from MATLAB.

## 3.5 Statistical analysis methods

Statistical analysis can be a helpful tool to help uncover patterns and trends in a dataset. In this thesis, the deviations that were calculated are average absolute relative deviation (AARD) and absolute average deviation (AAD). The AARD calculates the absolute average relative deviation between each data point in the dataset and the model prediction and tells how much each data point deviates from the mean of the data. AAD calculates the average absolute deviation between each data point in the dataset and the model prediction. The AARD was calculated with the following equation.

$$AARD = \frac{1}{N} \sum \left| \frac{c^e_{C,n} - c^{mod}_{C,n}}{c^e_{C,n}} \right| * 100\% \tag{3.3}$$

$N$ is the number of values in the dataset, $c^e$ is the experimental value of component $C$ at measurement point $n$, and $c^{mod}$ is the modelled value of component $C$ in the measurement point $n$. The AD was calculated with the following equation,

$$AAD = \frac{1}{N} \sum |c^e_{C,n} - c^{mod}_{C,n}| \tag{3.4}$$

# 4 Results and discussion

In this section, the main results and findings are presented and discussed. Also, a review of the advantages and disadvantages of the models, methods and assumptions made is done.

## 4.1 Oxidative degradation

In the following subsections, the experimental results from the oxidative degradation models are presented and discussed. Each degradation compound is discussed separately, and a comparison of the developed models is made. For each of the oxidative degradation components, some representative results are given. All other figures are given in the appendix in Subsection A.

Table 4.1 and 4.2 gives the mean AAD and AARD values of all experiments (A1-C4) for each one of the components for the three different ML-models. The complete tables with the AAD and AARD for each one of the experiments are given in the appendix in Subsection A.

**Table 4.1:** Mean AAD for experiment A1-C4 for each one of the components. (1) AAD between the experimental values and the model with 3 inputs and average rate. (2) AAD between experimental values and the model with 10 inputs. (3) AAD between the experimental values and the model with 3 inputs and instantaneous rate.

| Experiment | AAD (1) | AAD (2) | AAD (3) |
|---|---|---|---|
| MEA | 0.362 | 0.127 | 0.127 |
| Formate | 0.044 | 0.024 | 0.047 |
| Oxalic acid | 0.002 | 0.001 | 0.002 |
| HEGly | 0.003 | 0.001 | 0.002 |
| HEPO | 0.053 | 0.010 | 0.041 |
| HEF | 0.014 | 0.006 | 0.010 |
| HEA | 0.041 | 0.025 | 0.035 |
| BHEOX | 0.001 | 0.001 | 0.002 |
| HEI | 0.005 | 0.001 | 0.002 |

**Table 4.2:** Mean AARD for experiment A1-C4 for each on of the components. (1) AARDD between the experimental values and the model with 3 inputs and average rate. (2) AARD between the experimental values and the model with 10 inputs. (3) AARD between the experimental values and the model with 3 inputs and instantaneous rate.

| Experiment | AARD (1) [%] | AARD (2) [%] | AARD (3) [%] |
|---|---|---|---|
| MEA | 6.96 | 2.46 | 2.55 |
| Formate | 35.9 | 12.5 | 34.6 |
| Oxalic acid | 30.8 | 10.3 | 10.8 |
| HEGly | 18.1 | 6.56 | 11.5 |
| HEPO | 16.9 | 4.89 | 12.6 |
| HEF | 19.5 | 11.6 | 15.0 |
| HEA | 11.1 | 10.5 | 10.4 |
| BHEOX | 62.5 | 22.4 | 58.1 |
| HEI | 19.0 | 19.2 | 13.8 |

### 4.1.1 MEA

The modelling results for MEA is shown in Figure 4.1 and 4.2. The rest of the figures are given in the appendix in Subsection A.1.

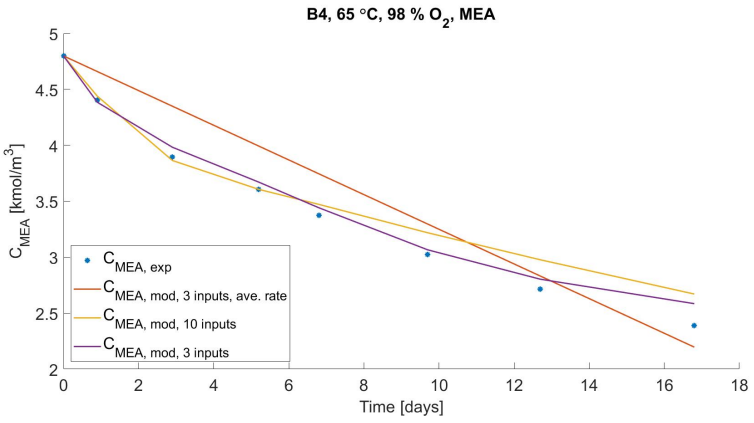


**Figure 4.1:** The figure shows the plotted results from experiment B4 for MEA conducted at 65°C and with 98% $O_2$. The blue dots are the experimental data points, the red line is the ML-model with 3 inputs and average reaction rate, the yellow line is the ML-model with 10 or 11 inputs, and the purple line is the ML-model with 3 inputs with instantaneous rate.

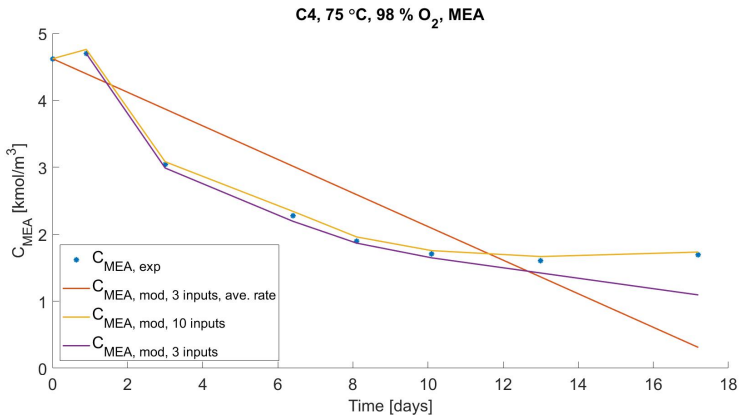


**Figure 4.2:** The figure shows the plotted results from experiment C4 for MEA conducted at 75°C and with 98% $O_2$. The blue dots are the experimental data points, the red line is the ML-model with 3 inputs and average reaction rate, the yellow line is the ML-model with 10 or 11 inputs, and the purple line is the ML-model with 3 inputs with instantaneous rate.

In Figure 4.1 experiment B4 is plotted. The experiment was performed at 65 °C with 98 % oxygen. One can see that all of the ML models have been able to predict the experimental data trend. The red line, which is the ML model with 3 inputs and average rate, is linear for all of the experiments. For the time span of the plot, the red curve has a reasonable development because the endpoint of the ML model is similar to the last experimental point. However, the experimental data has a curved shape, indicating that the degradation rate decreases over time. This is in accordance with the expected trend and what earlier research has shown. This trend will not be seen from the linear curve, where a constant degradation rate is assumed. Therefore, this model will have a limited validity range. The two other curves, the yellow and purple ones, have a decrease in degradation rate with time, and if the same trends continue, it seems as though these two curves will have a reasonable development over time.

Figure 4.2 shows the results from experiment C4, which was performed at 75 °C with 98% oxygen. Here, MEA degrades faster than in experiment B4, which is expected as the solvent degrades faster with increasing temperature. In this plot, the yellow and purple curves are similar to the curves in plot B4, where the degradation rate decreases with time. It seems that the ML models for most of the plots developed for MEA have captured the general trend for the data well.

The values for the AAD and AARD are shown in the appendix in Table B.1 and B.2. The AAD seems to increase with increasing temperature for the 3 input model, with some exceptions. This is probably because the reaction rate of MEA decreases faster with higher temperatures, and therefore has a more concave shape as the temperature and oxygen concentration increases. The 3 input model with average rate is linear and will not follow the same trend, so the AAD is expected to increase with increasing temperatures. From Table 4.1, it is seen that the mean AAD is lower for the model with 10 inputs than the model with 3 inputs and average rate. Several of the AADs for the 3 input model with instantaneous rate is missing because of missing modelled reaction rates. For the included values, results are promising, and the mean AAD is similar to the 10 input model. For the 10 input model, the AADs are good and steadily low for all the calculated values. This coincides with the plotted results from the ML model, which seemed to follow the experimental values well. The mean AARD is 6.96% for the 3 input model with an average rate, with a minimum value of 0.892% and a maximum value of 24.34%. For the 10 input model, the mean AARD is 2.46% with a minimum value of 0.761% and a maximum of 5.688%. For experiment B1, the AARD for the 3 input model with average rate deviates significantly from the experimental values. For the 3 input model with simultaneous rate, the mean value is similar to the 10 input model. The AARDs are low for all three models, but a simultaneous rate improves the fit, as seen in the plots and the deviations.

Because there were concentration jumps in the experimental data for MEA, values were removed from the data in the model with 3 inputs. This was done so that the data would have a decreasing concentration trend for the whole duration of the experiments. The ML models were then trained with this data. This was to support the assumption that MEA is only consumed, not formed, for the whole duration of the experiments, from the suggested reaction mechanisms for oxidative degradation. This is seen in Figure 4.2, where the purple line has one less experimental point than the other plots. This has altered the results compared to using the experimental data directly. However, if the concentration of MEA increased and decreased during the experiments, this would not make sense because MEA is not being formed in an absorber or simulated absorber conditions, only consumed. For the model with ten inputs, these experimental data points were not removed. As seen in Figure 4.2, the yellow curve does a jump in the beginning before decreasing in concentration for the remaining duration

of the experiment. This could indicate that the 10 input model is overfitted or is sensitive to outliers in the dataset.

The model with 3 and 10 inputs are similar in many cases. It seems like the model with ten inputs improved the overall fit of the model. This indicates that the degradation rate is not only dependent on the MEA-concentration; it is also dependent on the other degradation products that are formed.

### 4.1.2 Formate and oxalic acid

Selected results for formate are shown in Figure 4.3 and 4.4. These are the plotted results from experiment A1 and C4. The remaining plots are given in the appendix in Subsection A.2. In the ML model with three inputs, zero-values were removed from the data before training the model. In the model with 10 inputs, this was not done.

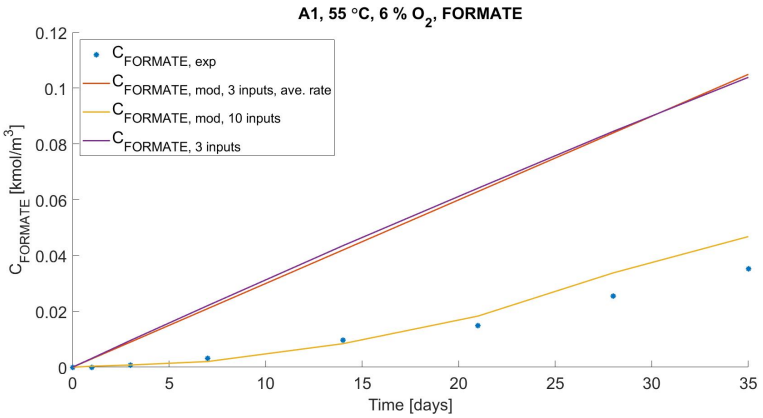


**Figure 4.3:** The figure shows the plotted results from experiment A1 for formate conducted at 55°C and with 6% $O_2$. The blue dots are the experimental data points, the red line is the ML-model with 3 inputs and average reaction rate, the yellow line is the ML-model with 10 inputs, and the purple line is the ML-model with 3 inputs with instantaneous rate.

The results of the ML model for formate are generally good. The values for the modelled reaction rates of the 3 input model were close to constant. This resulted in a concentration profile for the 3 input model with the instantaneous rate to be similar to the 3 input model with average rate. From the figures, it is seen that they are both close to linear. A similar linear trend for the 3 input models is seen for all the experiments. The trend of the experimental data is also linear, and it seems as though the ML model with 3 inputs has captured this linear trend well.

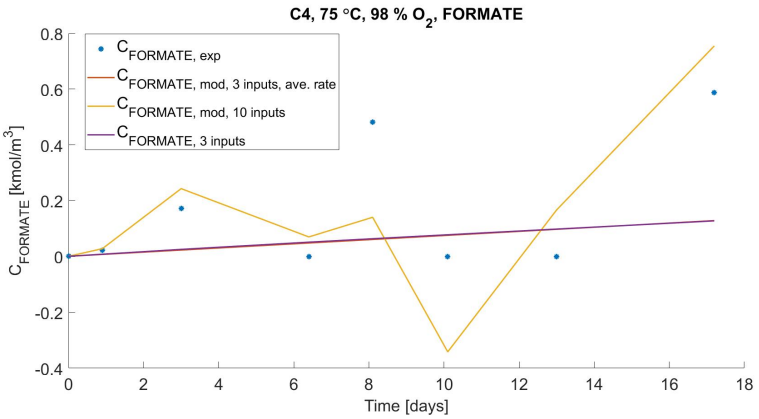


**Figure 4.4:** The figure shows the plotted results from experiment C4 for formate conducted at 75°C and with 98% $O_2$. The blue dots are the experimental data points, the red line is the ML-model with 3 inputs and average reaction rate, the yellow line is the ML-model with 10 inputs, and the purple line is the ML-model with 3 inputs with instantaneous rate.

From Figure 4.4 one can see that the yellow line, which is the 10 input model, has noticeable step changes in the reaction rate. Some experiments had zeros in the experimental data, such as in experiment C4, and these were not removed before training. This seems to have caused disturbances and shows that the ML model with ten inputs is sensitive to outliers in the dataset.

From reported results, the concentration levels and the reaction rate of formate are expected to increase for the whole duration of the experiments.[5] From the results, this trend is seen for most of the experiments. In experiment B3, C3 and C4, the concentration either decreases or has zeros where the concentration could not be measured, giving a negative rate for some points. This causes disturbances in the ML model with 10 inputs. Except for these outliers, the concentration has an increasing trend. When it comes to the reaction rate, the increase is linear for the model with 3 inputs. For the model with 10 inputs, the reaction rate has an even increase for many of the plots, and for other plots, it has a steeper growth.

From Table 4.1 it is seen that the mean AAD for formate is low for all ML models, and the AAD for the 10 input model is the lowest. From the mean AARD of formate in Table 4.2, there is a significant difference in the AARD for the 10 input model (12.5%) and the 3 input model with average (35.9%) and simultaneous rate (34.6%). This coincides with what is seen from the plotted results, where the 10 input model more easily follows the experimental data points than both of the plotted lines from the 3 input model, thus deviating more from the mean

of the data.

The plotted results from experiment B2-II and C2 for oxalic acid are shown in Figure 4.5 and 4.6. The remaining plots are given in the appendix in Subsection A.3.

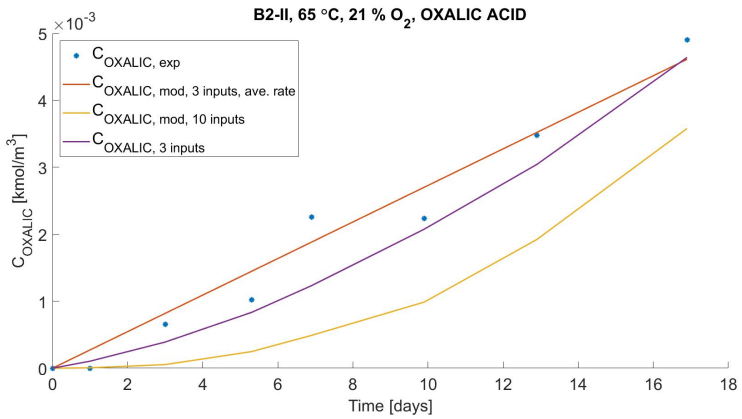


**Figure 4.5:** The figure shows the plotted results from experiment B2-II for oxalic acid conducted at 65°C and with 21% $O_2$. The blue dots are the experimental data points, the red line is the ML-model with 3 inputs and average reaction rate, the yellow line is the ML-model with 11 inputs, and the purple line is the ML-model with 3 inputs with instantaneous rate.

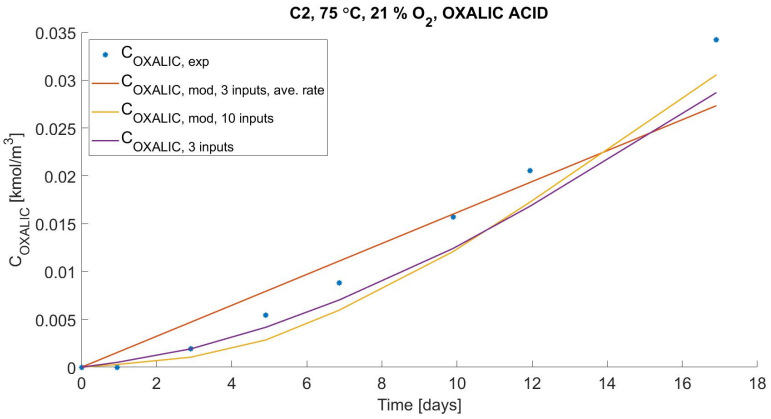


**Figure 4.6:** The figure shows the plotted results from experiment C2 for oxalic acid conducted at 75°C and with 21% $O_2$. The blue dots are the experimental data points, the red line is the ML-model with 3 inputs and average reaction rate, the yellow line is the ML-model with 11 inputs, and the purple line is the ML-model with 3 inputs with instantaneous rate.

From the results, one can see that the fit is suitable for all the plots. In Figure 4.5 the red line has a very nice development, and the same applies to the purple line. The yellow line, the 11 input model, is underpredicted, meaning that it

predicts too low values. This can be because, in the experimental data, the first two values are zero. As also seen from the formate results, the 10 or 11 input model is sensitive to outliers and zero-values in the dataset. In Figure 4.6 all three curves have a good fit. The yellow and purple lines have a curved shape, which follows the pattern of the experimental data points. It seems like these curves will have a reasonable development over time.

It seems as though the fit improves with increasing temperature and oxygen concentration. When looking at the order of magnitude, the concentration levels are around 10 times larger for the experiments performed at 55 °C and 75 °C, so an error is more visible for the experiments performed at lower temperatures than the higher ones. When looking at Table 4.1 with the mean AAD, the average absolute deviation is very low for all models. This indicates that the fit is good for both the ML models, and errors are more visible for the lower temperatures in the graphs. From Table 4.2 with the AARD, the mean is much higher for the 3 input model with the average rate (30.8%), with the highest value being 153.1% for A2-II, than the models with simultaneous rates with 11 inputs (10.3%) and 3 inputs (10.8%). This indicates that the modelled rates from the models with simultaneous rates follow the experimental data better than with an average rate. A reason for high AARD values can be because the order of magnitude for oxalic acid is relatively low, as mentioned earlier. Therefore, the absolute average relative deviation will be more visible because a deviation from the mean of the data will make a more significant difference when the concentration levels are lower.

### 4.1.3 HEGly and HEPO

The results from the plots of experiment A2-II and C2 for HEGly are shown in Figure 4.7 and 4.8. The remaining plots are given in the appendix in Subsection A.4.

HEGly is a major degradation compound found in pilot plants, and it has a strong temperature dependency. From the results of the ML models, there is an apparent increase in the concentration levels of HEGly with increasing temperature. There is also a decrease in the concentration levels with increasing oxygen content, coinciding with the expected development from research. [5] This indicates that ML models have been able to capture the general trend of the data.

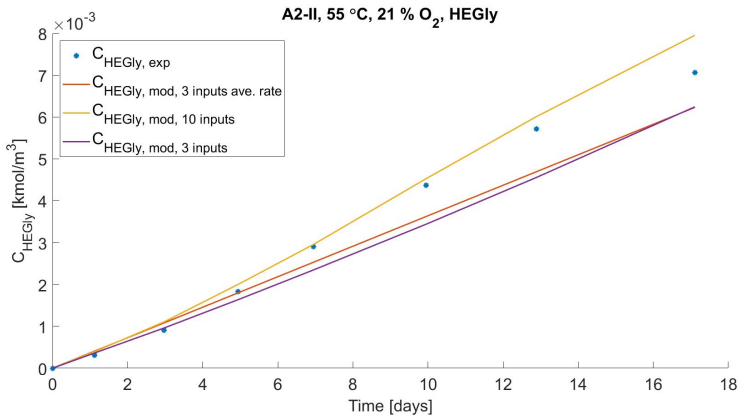


**Figure 4.7:** The figure shows the plotted results from experiment A2-II for HEGly conducted at 55°C and with 21% $O_2$. The blue dots are the experimental data points, the red line is the ML-model with 3 inputs and average reaction rate, the yellow line is the ML-model with 10 inputs, and the purple line is the ML-model with 3 inputs with instantaneous rate.

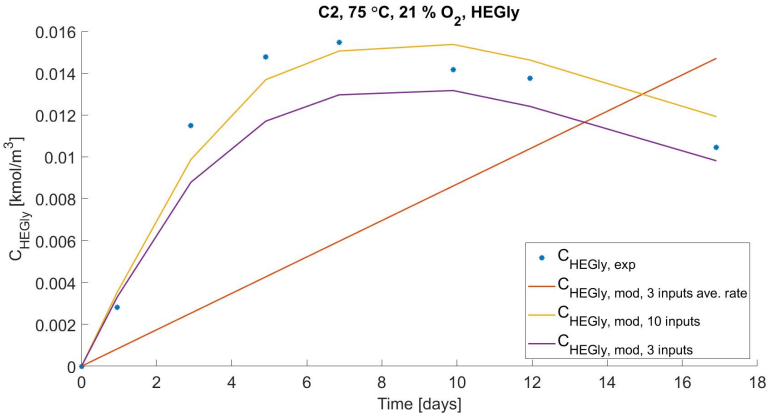


**Figure 4.8:** The figure shows the plotted results from experiment C2 for HEGly conducted at 75°C and with 21% $O_2$. The blue dots are the experimental data points, the red line is the ML-model with 3 inputs and average reaction rate, the yellow line is the ML-model with 10 inputs, and the purple line is the ML-model with 3 inputs with instantaneous rate.

For Figure 4.8 one can see a decrease in the concentration after around 6 days. From the theory, HEGly is believed to be consumed as the reactant in other reactions.[5] This is more visible for the highest temperature in the experimental data, and the ML models seem to follow a similar trend. Also, the red line, plotted with the average reaction rate, will have a limited validity range because it has a linear development the whole time, and HEGly is expected to decrease or stagnate in concentration levels. For the results for 55 °C and the experiments done with 6 % oxygen for 65 and 75 °C, the results show a linear trend,

similar to Figure 4.7. This is because the reactions with HEGly as an intermediate are believed to be reached faster for higher temperature and oxygen levels, and the decrease in HEGly concentration is therefore not observed at the lower temperature and oxygen levels.

Figure 4.9, 4.10 and 4.11 show the results from the ML models of experiment A1, B1 and C3 for HEPO. The remaining figures are given in the appendix in Subsection A.5. The majority of the results have a good fit, similar to B1 in Figure 4.10.

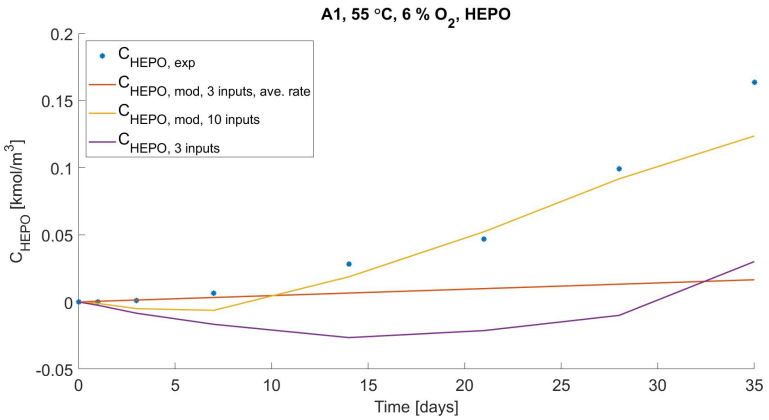


**Figure 4.9:** The figure shows the plotted results from experiment A1 for HEPO conducted at 55°C and with 6% $O_2$. The blue dots are the experimental data points, the red line is the ML-model with 3 inputs and average reaction rate, the yellow line is the ML-model with 10 inputs, and the purple line is the ML-model with 3 inputs with instantaneous rate.

For almost all cases, the two models gave very similar results. For experiment C3, in Figure 4.11 it is seen that the 10 input model is sensitive to concentration jumps in the experimental data and outlier points. The model with 3 inputs has a better-adjusted fit. The exception is Figure 4.9 where the 3 input model gives negative values and low average rates. This may be because the first few data points of the experimental data are low, and this seems to affect the modelled rates a lot.

Lab-scale experiments do not seem to capture HEPO's behaviour in pilot plants, [5] therefore, experimental data from pilot plants or larger scale plants is needed for models to be applicable to an industrial plant. However, since the models seemed to easily capture the trends of the lab-scale experimental data for HEPO, this is promising also for a model developed based on data from a pilot or a large-scale capture plant.

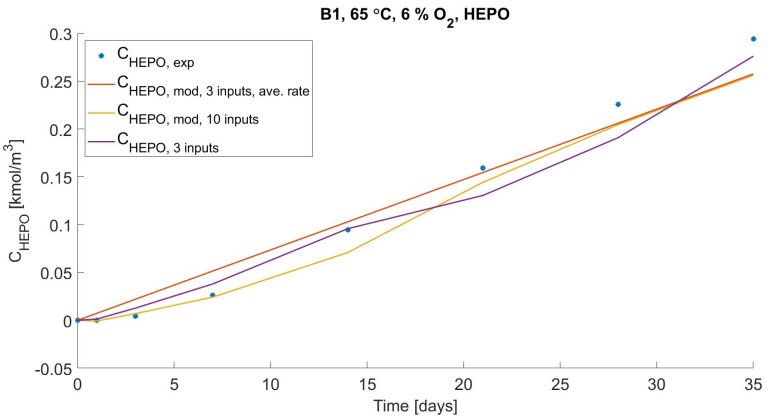


**Figure 4.10:** The figure shows the plotted results from experiment B1 for HEPO conducted at 65°C and with 6% $O_2$. The blue dots are the experimental data points, the red line is the ML-model with 3 inputs and average reaction rate, the yellow line is the ML-model with 10 inputs, and the purple line is the ML-model with 3 inputs with instantaneous rate.

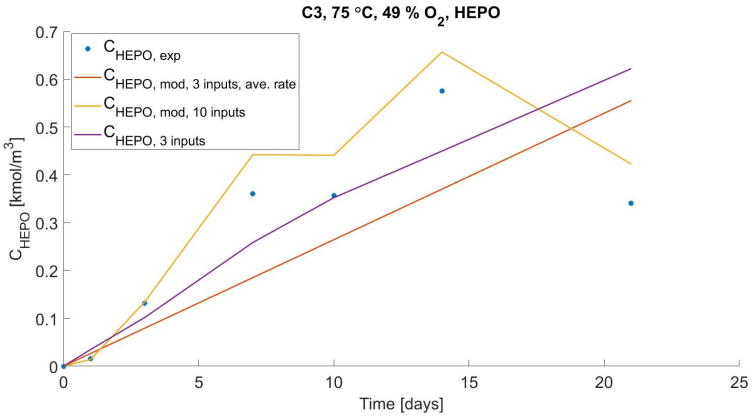


**Figure 4.11:** The figure shows the plotted results from experiment C3 for HEPO conducted at 75°C and with 49% $O_2$. The blue dots are the experimental data points, the red line is the ML-model with 3 inputs and average reaction rate, the yellow line is the ML-model with 10 inputs, and the purple line is the ML-model with 3 inputs with instantaneous rate.

The mean AAD, as seen in Table 4.1, for both HEGly and HEPO are the smallest for the 10 input models for both components. The values for the AAD are around 10 times higher for all models for HEPO than HEGly, and this is believed to be because HEPO is formed in more significant concentrations than HEGly, and this will have a greater impact on the absolute average deviations. The mean AARD for HEGly and HEPO, as seen in Table 4.2, have a similar pattern, where they are highest for the 3 input model with average rates (18.1% and 16.9%) than the models with simultaneous rates with 10 inputs (6.56 and 4.89%) and 3 inputs

(11.5 % and 12.6%). This is again because the model with an average rate will have a linear development. The two other plotted lines will curve and thus follow the development of the experimental data more accurately.

### 4.1.4 HEF, HEA and BHEOX

The result from HEA experiment C3 is shown in Figure 4.12, and the result from HEF experiment C4 is shown in Figure 4.13. Both of these plots give a general idea of how the plotted results of all the experiments turned out. The remaining plots for HEF and HEA are given in the appendix in Subsection A.6 and A.7.

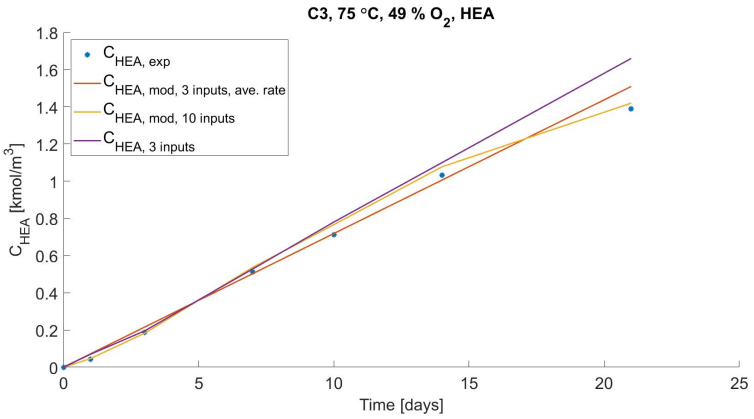


**Figure 4.12:** The figure shows the plotted results from experiment C3 for HEA conducted at 75°C and with 49% $O_2$. The blue dots are the experimental data points, the red line is the ML-model with 3 inputs and average reaction rate, the yellow line is the ML-model with 10 inputs, and the purple line is the ML-model with 3 inputs with instantaneous rate.

For both HEF and HEA, the fit is good, although there are few outlier plots. The models tend to overpredict and underpredict the concentrations, but this also applies to several other degradation compounds. HEA has a similar trend as the formate compound. The model with three inputs and average rate and the model with three inputs and instantaneous rate are similar and follow an almost identical path. From Table 4.1 and 4.2 with the mean AAD and AARD, the values follow the trends that have also been seen for most of the other compounds, where the deviations are lower for the model with 10 inputs than the model with 3 inputs.

Figure 4.14 and 4.15 show the results of experiment B4 and C3 for BHEOX. The results were more varying than many of the plotted results for other compounds. The remaining plots are given in the appendix in Subsection A.8.

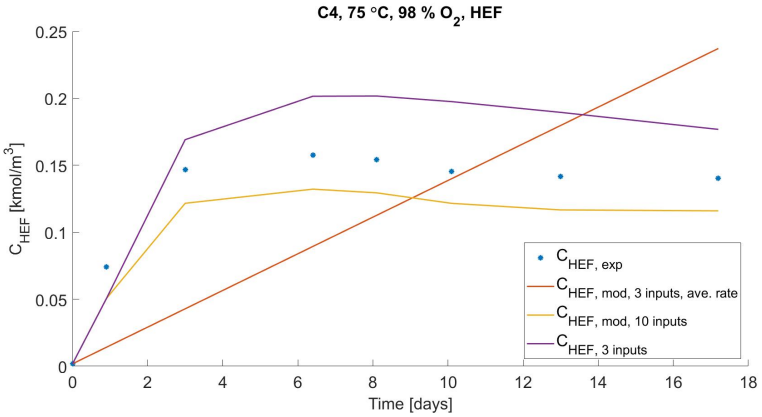


**Figure 4.13:** The figure shows the plotted results from experiment C4 for HEF conducted at 75°C and with 98% $O_2$. The blue dots are the experimental data points, the red line is the ML-model with 3 inputs and average reaction rate, the yellow line is the ML-model with 10 inputs, and the purple line is the ML-model with 3 inputs with instantaneous rate.

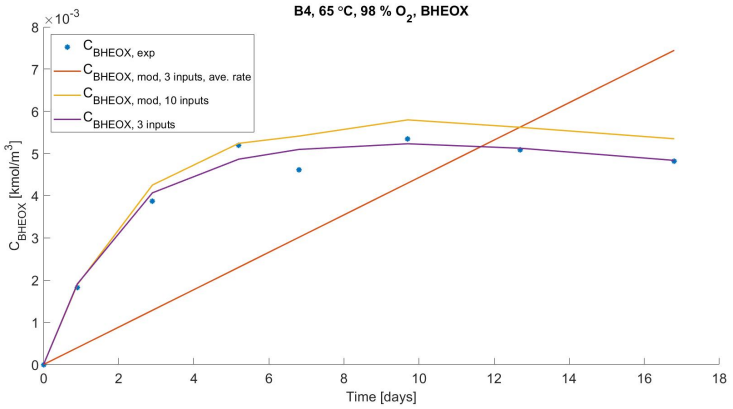


**Figure 4.14:** The figure shows the plotted results from experiment B4 for BHEOX conducted at 65°C and with 98% $O_2$. The blue dots are the experimental data points, the red line is the ML-model with 3 inputs and average reaction rate, the yellow line is the ML-model with 10 inputs, and the purple line is the ML-model with 3 inputs with instantaneous rate.

It is observed that the measured experimental concentrations of BHEOX are low for all the experiments. From theory, it is known that BHEOX is not a major degradation product. It is formed from oxalic acid, which is produced through several and often non-favoured reaction steps.[5] The concentration development will therefore be low. Because the concentrations levels are low, an error will be more visible, as seen from other components with low concentration levels. From Table B.16 the values for the AARD are high for many of the experiments. Nevertheless, from Table B.15 it is seen that the AAD between each data point and

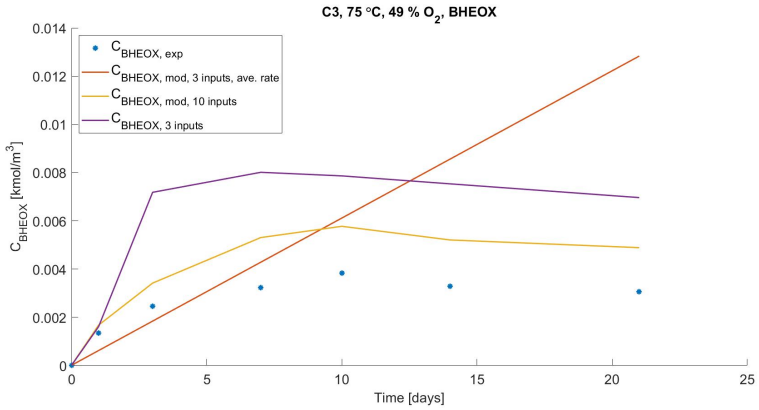


**Figure 4.15:** The figure shows the plotted results from experiment C3 for BHEOX conducted at 75°C and with 49% $O_2$. The blue dots are the experimental data points, the red line is the ML-model with 3 inputs and average reaction rate, the yellow line is the ML-model with 10 inputs, and the purple line is the ML-model with 3 inputs with instantaneous rate.

the model prediction is low for all the values. From Figure 4.14 the inaccuracy of the plotted red line with average, constant rate of reaction is also very visible.

### 4.1.5 HEI

Figure 4.16 and 4.17 show the results from experiment A1 and B4 for HEI, respectively. The remaining plots are given in the appendix in Subsection A.9.

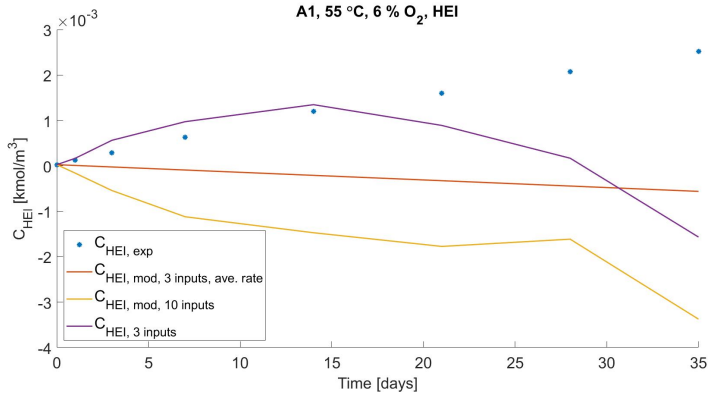


**Figure 4.16:** The figure shows the plotted results from experiment A1 for HEI conducted at 55°C and with 6% $O_2$. The blue dots are the experimental data points, the red line is the ML-model with 3 inputs and average reaction rate, the yellow line is the ML-model with 10 inputs, and the purple line is the ML-model with 3 inputs with instantaneous rate.

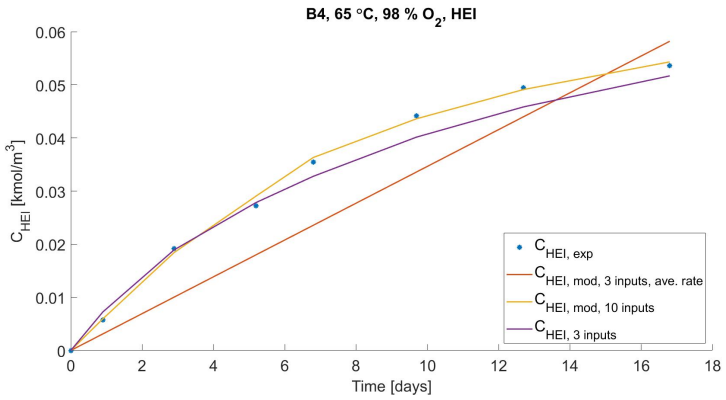


**Figure 4.17:** The figure shows the plotted results from experiment B4 for HEI conducted at 65°C and with 98% $O_2$. The blue dots are the experimental data points, the red line is the ML-model with 3 inputs and average reaction rate, the yellow line is the ML-model with 10 inputs, and the purple line is the ML-model with 3 inputs with instantaneous rate.

Experiment B4 has a positive development and flattens out after some time, and this is also representative of many of the other plots. All the ML models have a good development. As expected, the red line, with average, constant reaction rate, is not as accurate as the models with instantaneous rates. From Table B.18 one can see that the average absolute relative deviation is 20.05 % for the red line, 1.479 % and 4.281 % for the yellow and purple line, respectively. The AARD for the red line is larger than the other models, indicating that it is not as accurate, as also seen from the figure. The absolute average deviation, seen in Table B.17 is also larger for the model with average rate than the other two models. The fit for the 3 input model and 10 input model with instantaneous rates are similar, and they follow the experimental data points well.

For experiment A1 all the curves have a negative development over time. The purple line, which is the model with three inputs and instantaneous rate, has a positive development in the beginning before becoming negative after about 15 days. One of the reasons for the inaccuracies shown in Figure 4.16 could be caused by the discrepancy in the order of magnitude of the experimental data. The order of magnitude varies substantially for the experimental data, which will influence the modelled rate. The experimental values for A1 are low, impacting the results notably. The experimental values are low for the other experiments conducted at 55°C, but it seems only to have affected A1.

### 4.1.6 Comparison of the models

Two machine learning models describing the oxidative degradation of MEA have been developed in this thesis. The first model was trained with 3 inputs (MEA-concentration, temperature and $O_2$-concentration) and one output (the calculated experimental reaction rate of a component). The modelled rates were obtained from this model, and the modelled concentrations were calculated in two different ways, one with the average of the modelled rates, so a constant rate, and one with the instantaneous rate.

From the results, it was seen that the plotted line with average rate is linear, and it will therefore have a limited validity range. From previous experiments and research, the degradation rates for MEA and reaction rates for the degradation products are expected to decrease with time. When there is less MEA, there will also be less formation of degradation products. Therefore, the linear model will not be valid over time. Therefore it is not relevant to assume a constant reaction rate. From the plotted line with instantaneous rate, it is seen that the results improve substantially, and the curves have better accuracy and behaviour, with some exceptions.

A second model was proposed to see if there was a dependency between the reaction rates of MEA and the degradation products. In addition to the three inputs from the first model, the experimental concentrations of formate, HEF, HEI, BHEOX, HEGly, HEA and HEPO were also inputs. Oxalic acid was not included as an input because the data from experiment A2-I was not available. In the ML model for oxalic acid, all available data were included in the model. For many of the results, the extra inputs seemed to give an improved fit. Looking at the AAD and AARD for the experiments, the error is lowest for the 10 input models in all cases. Because of improved results and lower deviations for the 10 input model, there is an indication that there is a dependency between the degradation compounds.

It seems like the model with 10 inputs will give the most accurate results. This indicates that the more data is available, the better. In machine learning, a model will have better predictions if more data is available. More experimental data could help improve the performance of the ML model. However, it is also seen that the 10 input model is sensitive to outliers in the dataset. A screening of the data and removal of apparent outliers could improve the fit of the model.

One of the goals of this thesis was to see if machine learning can model the oxidative degradation of MEA and the formation of degradation products in an acceptable way. It could also be interesting to see if there is a possibility of developing a model that could be applied in different $CO_2$-capture plants. The model is data-driven and requires experimental data from many degradation compounds to obtain the modelled rates and accurate predictions. A model that only requires plant conditions and kinetics as inputs would be optimal. Further understanding of the chemical reactions and how conditions of the plant affect the degradation is needed for this to be possible.

## 4.2 Thermal degradation

In this section, a selection of the plotted results is shown. The rest of the results are given in the appendix in Subsection B. Table 4.3 and 4.4 gives the mean AAD and AARD values from both of the ML models for each one of the components for all experiments (E1-F9). The tables of AAD and AARD for each experiment is given in the appendix in Subsection B.

**Table 4.3:** Mean AAD for all experiments (E1-E9) for each one of the thermal degradation components. (1) AAD between the experimental values and the ML model with 3 inputs. (2) AAD between the experimental values and the model with 6 inputs.

| Compound | AAD (3) | AAD (6) |
|---|---|---|
| MEA | 0.235 | 0.153 |
| HEIA | 0.027 | 0.020 |
| HEEDA | 0.012 | 0.034 |
| TriHEIA | 0.015 | 0.003 |

**Table 4.4:** Mean AARD for all experiments (E1-E9) for each one of the thermal degradation components. (1) AARD between the experimental values and the ML model with 3 inputs. (2) AARD between the experimental values and the model with 6 inputs.

| Compound | AARD (1) [%] | AARD (2) [%] |
|---|---|---|
| MEA | 5.3 | 3.8 |
| HEIA | 14.0 | 11.4 |
| HEEDA | 28.9 | 16.4 |
| TriHEIA | 38.8 | 7.7 |

### 4.2.1 Modelling results

Figure 4.18 shows the plotted results for experiment E6 for MEA at 120°C and a $CO_2$-loading of 0.5. Figure 4.19 shows the plotted results for experiment F6 for HEEDA at 135°C and a $CO_2$-loading of 0.5. Figure 4.20 shows the plotted results for experiment F6 for HEIA at 135°C and a $CO_2$-loading of 0.5. Figure 4.21 shows the plotted results for experiment E6 for TriHEIA at 120°C and a $CO_2$-loading of 0.5. All the experiments had an initial MEA concentration of 4.9 kmol/$m^3$. The figures show the concentration of MEA plotted against time. The experimental data points are the blue dots in the plot. The red line is the ML model with 3 inputs and one output, and the yellow line is the ML model with 6 inputs and one output. The remaining plots are given in the appendix in Subsection B.1, B.2, B.3 and B.4.

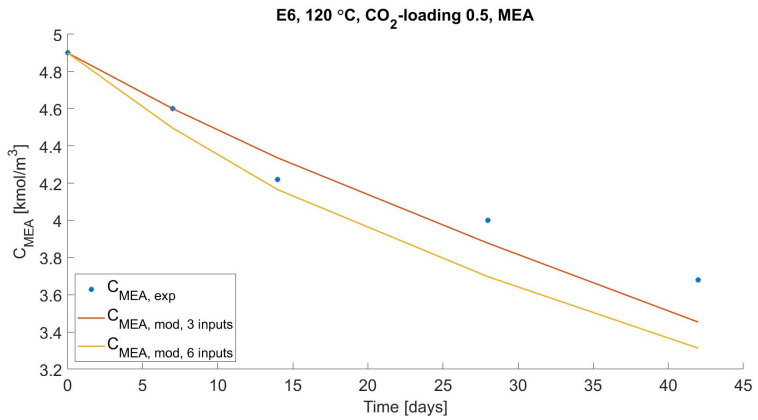


**Figure 4.18:** The figure shows the plotted results from experiment E6 for MEA conducted at 120°C and with a $CO_2$-loading of 0.5. The blue dots are the experimental datapoints, the red line is the ML-model with 3 inputs, and the yellow line is the ML-model with 6 inputs.

From the thermal degradation models for MEA, a good fit is observed for most of the experiments. The curves have the expected development, a decreasing reaction rate with time, and a decreasing concentration of MEA over time. For many of the experiments, the model with three inputs and six inputs had similar fits. The model with six inputs gave slightly better results for some of the cases, but all in all, there is not a significant difference. Figure 4.18 represents the results well and is a good indication of how most of the plots for MEA turned out. From Table 4.4 with the mean AARD, the observations from the plotted results are confirmed, as the model with 6 inputs has a lower mean AARD (3.8%) than the 3 input model (5.3%).

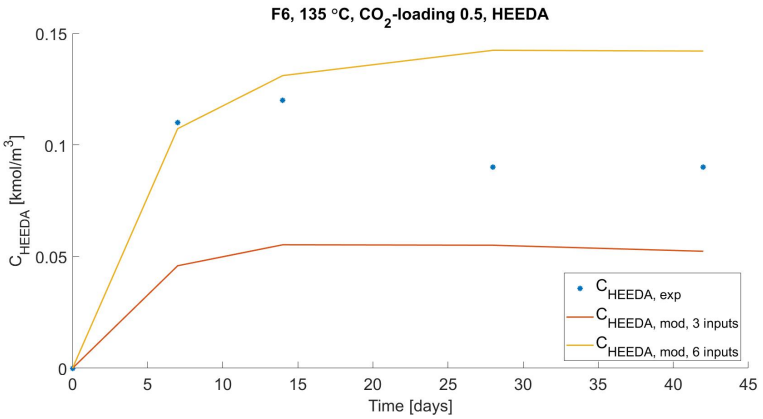


**Figure 4.19:** The figure shows the plotted results from experiment F6 for HEEDA conducted at 135°C and with a $CO_2$-loading of 0.5. The blue dots are the experimental datapoints, the red line is the ML-model with 3 inputs, and the yellow line is the ML-model with 6 inputs.

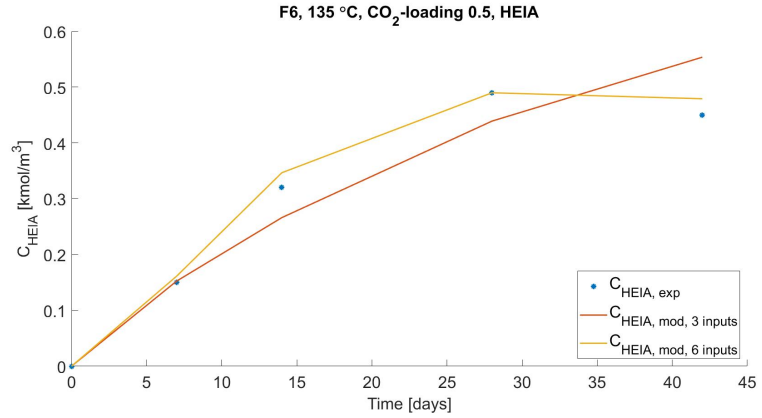


**Figure 4.20:** The figure shows the plotted results from experiment F6 for HEIA conducted at 135°C and with a $CO_2$-loading of 0.5. The blue dots are the experimental datapoints, the red line is the ML-model with 3 inputs, and the yellow line is the ML-model with 6 inputs.

For several of the experiments, some of the data points were not available for HEIA, HEEDA and TriHEIA. Therefore, for some of the experiments, the ML models are not complete or not available. For all of the measured compounds, it is seen that the model captures the trend of the data relatively well, but there is also too little experimental data to make an optimal model. However, compared to the amount of available data, the results are promising.

For HEEDA and HEIA, the trends have, for the majority of the results, an increasing reaction rate in the beginning before it starts to decrease after some time. This applies mainly to HEEDA, where almost all the curves have a concave

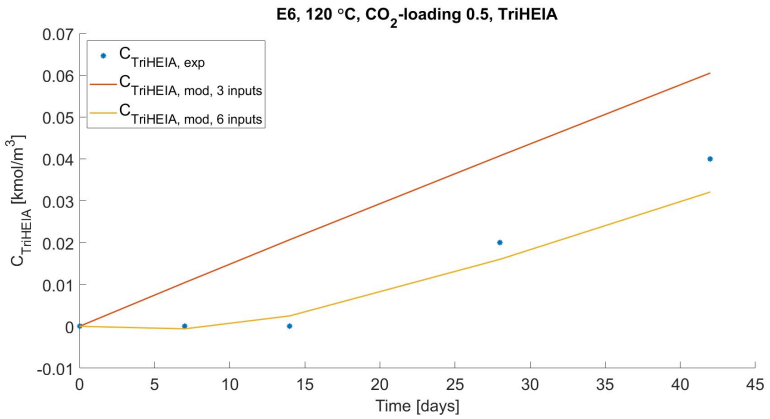


**Figure 4.21:** The figure shows the plotted results from experiment E6 for TriHEIA conducted at 120°C and with a $CO_2$-loading of 0.5. The blue dots are the experimental datapoints, the red line is the ML-model with 3 inputs, and the yellow line is the ML-model with 6 inputs.

shape. The results for HEIA are primarily linear, but the curves are more concave shaped with increasing temperature. As mentioned in Subsection 2.2.1, HEIA is believed to be formed from HEEDA, which could explain the decrease in the concentration levels of HEEDA over time. For HEIA, this conversion is not as rapid. HEIA does react further in the system, but this is more visible at higher temperatures.[6;24]

The accuracy of the TriHEIA results varies significantly. Some of the plotted lines have increasing trends, some of the lines have decreasing trends, some are linear, and some are curved. Figure 4.21 shows one of the plotted results that had a reasonable development of the curves. The yellow line, which is the model with 6 inputs, has a much better fit than the red line, which is the model with 3 inputs. Because data was missing in the datasets, it has caused disturbances in the models' ability to capture a trend. From the mean AARD in Table 4.4, it is significantly smaller for the 6 input model (7.7%) compared to the 3 input model (38.8%).

### 4.2.2 Comparison of the models

It is observed that the ML model with 6 inputs gives an improved trend. The model follows the experimental data points better than the 3 input model for most models. The model with 6 inputs was made because, as for the oxidative degradation model, it was interesting to see if there was any correlation between the concentration levels of the degradation compounds.

The AAD and AARD are lower or similar for the model with six inputs than for the model with three inputs for most of the cases, as seen in the tables in Subsection B in the appendix. This indicates that the fit of the second model is better than the first one and that there is a correlation between the different degradation compounds.

Models of thermal degradation have already been developed. These models are mechanistic and often complex. A machine learning model can potentially simplify such a model while still giving good model predictions if there is enough data. If one has an accurate mechanistic model available, many data points could be generated and used to make a relatively simple ML model. For the model developed in this thesis, only experimental data was used. There was not much data available, so the model is too simple to give satisfactory and accurate predictions. However, the model that was developed shows potential. If more data were available, the model would improve substantially.

## 4.3 Characteristics of the machine learning models

There are several advantages and disadvantages in the developed models, the chosen modelling approach, and the simplifications and assumptions that were made. In this subsection, this will be discussed further.

One of the main characteristics of the machine learning models is that they are data-driven. Hence, they require a significant amount of experimental data. The inputs of the model are experimental concentrations from experiments performed in lab scale. To recreate or make a similar model to be used in predictive analysis of degradation that can be applied to $CO_2$-capture plants, it would require similar experiments to be performed on a larger scale. Application to a larger scale would require further adaptations.

The predictions of the models are not generalized due to their data-driven nature, leading to a variation in the quality of the results. Within the same experiment, some of the plotted results have a good trend, and some results have a trend that does not follow the trend of the experimental data. This indicates that there is a lack of generalization in the model.

The developed models are empirical, so reaction equations or equations of state have not been taken into account. The models are based purely on experimental data. A mechanistic approach with kinetic knowledge, experimental data

performed at a broader period, and different conditions would help make the model more generalized. However, in a mechanistic model, we extrapolate data measured from experiments and assume that the information available is valid. With both an empirical and a mechanistic approach to modelling degradation, with the current data and knowledge available, an ML model will not be applicable in a larger time scale before more research is done on a larger time frame and a broader understanding of oxidative degradation. Also, the experiments performed are done with increased speed and higher oxygen levels than usual in a large scale plant, so what is seen from the results may not be what is the expected development in an industrial plant.

One advantage of developing a simple machine learning model such as the ones in this thesis is that it helps smoothen the data. Smoothening data is a way to identify and eliminate outliers in a dataset and recognize patterns in a dataset. [35] This method is ideal when developing a predictive model. It can help find suitable patterns, and it is a good start, as it can find trends in the dataset. Identifying outliers and finding patterns in a dataset is helpful if a mechanistic model is to be developed in the future.

When developing the ML models describing oxidative and thermal degradation, it was seen that outliers in the dataset were easier to identify. If one had a lot more experimental data, the pattern and trends of the different degradation products and MEA would be easier to spot. The model was able to find a correlation between the different components because an improvement of the models was seen when more inputs were included. This smoothening of the data, as mentioned earlier, can be helpful when developing a predictive model. It will be easier to fit a mechanistic model when the expected development of the degradation is known. When it comes to a thermal degradation model, the mechanisms and the process is more well known, so it would be easier to develop a machine learning model that can predict the degradation over a wider time frame. Much research is still needed for oxidative degradation, but the ML models developed is a promising start. With more research and understanding of oxidative degradation, the predictive abilities of the ML models are expected to improve.

Measures can be taken to improve the models' generalization abilities. Including more parameters can help make the model more accurate. The model is only based on experimental data, so including kinetic information into the neural

network could be helpful. Another measure that can be taken is to include even more experimental data from experiments conducted at the same or other conditions. This will improve the learning abilities of the ML model.

The equation used to calculate the rate is a common way of calculating the reaction rate for a compound. Because of the large amount of available experimental data, this method was a good basis for further calculations and the development of a model. However, it has the drawback that the numerical derivative may provide additional uncertainties. Nevertheless, the method used seems to give adequate modelled reaction rates and a satisfying result for most of the experiments.

Several modelled rates for the experiments gave an uneven fit, and it seems that the model is sensitive to outliers in the dataset. In the model developed with 3 inputs, obvious outlier points were removed before developing the ML models, but all data was included in the model with 10 inputs. Therefore, some of the modelled results from the 10 input model are uneven when there were zero-points or concentration jumps in the dataset. Something that could improve the machine learning models would be to conduct several parallels for the experiments, making it easier to identify outliers points in the experimental data.

When removing outliers in the experimental data, the results are altered to get a better fit, and the results obtained may not be similar to reality. However, the data was removed because it had some underlying issues and did not represent what wanted to be measured. If the concentration profile of MEA did not decrease for the whole duration of the experiments, this would not coincide with what is known from theory and previous research; that MEA is not formed, only consumed, in oxidative and thermal degradation. It seems as this is a reasonable assumption to make. If more data had been included in the model, the ML model would identify the outliers in the datasets more efficiently. Therefore, when considering the size of the available datasets, removing the obvious outliers in the experimental data is further supported as something that will optimize the model's parameters.

The results showed that assuming an average degradation rate for the degradation compounds will limit the model's validity range. For MEA, as an example, the concentration will decrease rapidly and eventually go below zero. As has been mentioned earlier, the expected development of the concentration is not

linear. However, for many of the modelled results, the model's predictions with a linear rate were good. For a short interval of time, it can therefore be ok to assume a linear reaction rate.

# 5 Conclusion

The objective of this work was to see if there was potential for using machine learning to model the oxidative and thermal degradation of MEA. Machine learning models have been developed by modelling the reaction rates of MEA and known degradation compounds. The data used for the modelling is experimental data from experiments performed at lab-scale. The experiments were conducted by Vevelstad et al. (2016) and Davis (2009). The modelled degradation rates were used to calculate the concentration profiles of the components, and the modelled concentrations were compared to the experimental values.

From the results of the oxidative degradation modelling, it is seen that the results are generally good. For the oxidative degradation model with three inputs, the modelled concentration was calculated in two different ways. The first method used the average of the modelled rates to calculate the concentrations, resulting in a linear curve. However, for MEA and the degradation compounds, a linear development will not be relevant over a longer time frame; thus, the validity range will be limited. Therefore, the simultaneous rate was also used to calculate the concentrations. This improved the model predictions and provided concentration profiles and trends closer to what was seen in the experimental data. The second model developed used all the available ten or eleven parameters as an input. This was to see if the machine learning model would find a correlation between the measured degradation compounds. This model improved the fit for many of the plotted results, and the curves seem to follow the experimental data points more accurately than the model with three inputs. However, the results show that the second model is more sensitive to outliers or zero-values than the first model, thus having more outlier plots than seen from the 3 input model.

More understanding of the chemical reactions and effect of the conditions used are needed to improve the oxidative degradation modelling. In addition, more experimental data could also improve the prediction abilities of the model. Nevertheless, the results from the modelling are promising, and there is potential for making a model that can predict oxidative degradation in a chemical absorption plant.

There was less experimental data available for thermal degradation than for oxidative degradation, but still, the results show potential. Also here two models were developed. The first model had three inputs, and the second model used all

the available six parameters as inputs. The fit improved for the 6 input model, and the curves seem to follow the experimental data points better than for the model with three inputs.

Thermal degradation is, as mentioned, better understood than oxidative degradation. Therefore, to improve the predictions of the thermal degradation model, one could include more existing experimental data. Also, it would be interesting to develop a mechanistic model in addition to the empirical model since the reactions and products formed are more well known.

One of the main characteristics of the models is that they are data-driven and require experimental data. This can be disadvantageous, and it will be challenging to apply the models to other plants because it would require experimental data from each specific plant performed at its given conditions for the model to give good model predictions. To make an ML model that would not require experimental data, only parameters such as initial concentration of the solvent, temperature, oxygen concentration and $CO_2$-loading would simplify the modelling and make the models more applicable to a larger variety of industrial plants. Furthermore, from the results, outliers in the data are more easily identified. This is, as mentioned, called smoothening of data and can help identify outliers and patterns in the dataset. This is one of the advantages of making a simple model such as the ones developed in this thesis.

There is still much work to do on both models, and as mentioned, more research and understanding of the degradation process is needed to improve the models. Also, understanding how oxidative and thermal degradation is connected is essential if a model describing both processes in an industrial plant can be developed. However, the developed models in this thesis have potential, and they are a good start and basis for further work.

# 6 Further work

The results presented in this thesis are promising and show great potential for further modelling of oxidative and thermal degradation with machine learning. However, some issues were observed with the chosen modelling approach. In this chapter, some recommendations and suggestions that could improve the models' prediction abilities and ideas that would be interesting to implement in a future model are given.

The developed models in this thesis are empirical, and as mentioned earlier, the validity range is low. Therefore, there is a need for more experimental data to increase the validity range and accuracy of the models. It will also be beneficial if this experimental data is from experiments conducted for a wider time interval and at a large variety of conditions.

As mentioned in the introduction of this thesis, the ultimate goal of this work would be to make a model that ties oxidative and thermal degradation together. The models developed in this thesis describing either the oxidative or thermal degradation of MEA will not be applicable to a large scale plant because both oxidative and thermal degradation will occur in the system. For this model to have good prediction abilities, there is a need to understand how these two types of degradation are connected and affect each other. A model that could describe the two types of degradation could help understand the process further and potentially save the plant money and reduce yearly expenses connected to the degradation of the solvent. As of now not, such a model is not likely to be developed any time soon, but it is a fascinating idea.

The models developed in this thesis are supervised, shallow neural network models. Another approach would be deep learning, meaning having several hidden layers in the neural network. Deep learning is even more complex than shallow neural and can generalize and recognize patterns in data even better than shallow neural networks.[15] The method is complicated and would require research, but it has the potential to improve the results substantially.

# References

[1] Center for Climate and Energy Solutions. Ipcc fifth assessment report. URL https://www.c2es.org/content/ipcc-fifth-assessment-report/. Found 13.12.2020.

[2] B. Dutcher, M. Fan, and A. G. Russell. Amine-based co2 capture technology development from the beginning of 2013—a review. *ACS Applied Materials & Interfaces*, 7(4):2137–2148, 2015. doi: 10.1021/am507465f.

[3] F. F. Henriksen. Modelling of amine degradation. *Master thesis, Department of Chemical Engineering, NTNU*, 2012.

[4] Andres Carranza-Abaid, Hallvard F. Svendsen, and Jana P. Jakobsen. Surrogate modelling of VLE: Integrating machine learning with thermodynamic constraints. *Chemical Engineering Science: X*, 8, 2020. URL https://doi.org/10.1016/j.cesx.2020.100080.

[5] Solrun Johanne Vevelstad, Maren T. Johansen, Hanna Knuutila, and Hallvard F. Svendsen. Extensive dataset for oxidative degradation of ethanolamine at 55–75°c and oxygen concentrations from 6 to 98%. *International Journal of Greenhouse Gas Control*, 50:158–178, 2016. ISSN 1750-5836. doi: https://doi.org/10.1016/j.ijggc.2016.04.013. URL https://www.sciencedirect.com/science/article/pii/S1750583616301803.

[6] Jason Davis. Thermal degradation of aqueous amines used for carbon dioxide capture. 01 2009. URL https://www.researchgate.net/publication/37984597$_{\mathrm{T}}$hermal$_{\mathrm{D}}$egradation$_{\mathrm{o}}$f$_{\mathrm{A}}$queous$_{\mathrm{A}}$mines$_{\mathrm{U}}$sed$_{\mathrm{f}}$or$_{\mathrm{C}}$arbon$_{\mathrm{D}}$ioxide$_{\mathrm{C}}$apture.

[7] ALFA Chemistry. URL https://www.alfa-chemistry.com/. Found 31.05.2021.

[8] D. Attenborough. Netflix documentary: A life on our planet, 2020. URL https://www.netflix.com/title/80216393. Found: 03.11.2020.

[9] B. M. Waggoner. The holocene epoch, 1996. URL https://ucmp.berkeley.edu/quaternary/holocene.php. Found: 01.05.2021.

[10] M. Bagley. Holocene epoch: The age of man, 2013. URL https://www.livescience.com/28219-holocene-epoch.html. Found: 01.05.2021.

[11] T.V. Verheyen A.J. Reynolds and E. Meuleman. 16 - degradation of amine-based solvents. In *Absorption-Based Post-combustion Capture of Carbon Dioxide*, pages 399–423. Woodhead Publishing, 2016. ISBN 978-0-08-100514-9. doi: https://doi.org/10.1016/B978-0-08-100514-9.00016-0.

[12] E. F. Da Silva, H. Lepaumier, A. Grimstvedt, S. J. Vevelstad, A. Einbu, K. Vernstad, H. F. Svendsen, and K. Zahlsen. Understanding 2-ethanolamine degradation in postcombustion CO 2 capture. *Industrial and Engineering Chemistry Research*, 51:13329–13338, 2012. doi: 10.1021/ie300718a.

[13] E. S. Rubin A. B. Rao. A technical, economic, and environmental assessment of amine-

based co2 capture technology for power plant greenhouse gas control. *Environmental Science Technology*, 36:4467–4475, 2002. doi: http://dx.doi.org/10.1021/es0158861.

[14] D. Lawson G. Marion. An introduction to mathematical modelling. *Bioinformatics and Statistics Scotland*, 2008.

[15] IBM. Data science and machine learning. URL `https://www.ibm.com/analytics/machine-learning`. Found: 15.09.2020.

[16] Eirik F. da Silva, Hélène Lepaumier, Andreas Grimstvedt, Solrun Johanne Vevelstad, Aslak Einbu, Kai Vernstad, Hallvard F. Svendsen, and Kolbjørn Zahlsen. Understanding 2-ethanolamine degradation in postcombustion co2 capture. *Industrial & Engineering Chemistry Research*, 51(41):13329–13338, 2012. doi: 10.1021/ie300718a.

[17] T. W. Brodtkorb. Modeling of mea degradation. *Master thesis, Department of Chemical Engineering, NTNU*, 2013.

[18] Camille Gouedard. Novel degradation products of ethanolamine ( MEA ) in CO2 capture conditions : identification , mechanisms proposal and transposition to other amines. 2014. URL `https://tel.archives-ouvertes.fr/tel-01081315`.

[19] S. J. Vevelstad, A. Grimstvedt, J. Elnan, E. Falck da Silva, and H. F. Svendsen. Oxidative degradation of 2-ethanolamine: The effect of oxygen concentration and temperature on product formation. *International Journal of Greenhouse Gas Control*, 18:88–100, 2013. ISSN 1750-5836. doi: https://doi.org/10.1016/j.ijggc.2013.06.008.

[20] P.C. Rooney, M.S. DuPont, and T.R. Bacon. Oxygen's role in alkanolamine degradation. *Hydrocarbon Process.*, pages 109–113, 1998.

[21] G. Léonard, D. Toye, and G. Heyen. Experimental study and kinetic model of monoethanolamine oxidative and thermal degradation for post-combustion co2 capture. *International Journal of Greenhouse Gas Control*, 30:171–178, 2014. ISSN 1750-5836. doi: https://doi.org/10.1016/j.ijggc.2014.09.014.

[22] Mahla Rashidian. Thermal degradation study by continuous thermal stability rig. 2013. URL `https://ntnuopen.ntnu.no/ntnu-xmlui/bitstream/handle/11250/248572/655063_FULLTEXT01.pdf?sequence=1`.

[23] et al. L. D. Polderman, C. P. Dillon. Why monoethanolamine solution breaks down in gas treating service. *Proc. Gas Conditioning Conf.*, pages 49–56, 1955.

[24] J. Davis and G. Rochelle. Thermal degradation of monoethanolamine at stripper conditions. *Energy Procedia*, 1:327–333, 2009. ISSN 1876-6102. doi: https://doi.org/10.1016/j.egypro.2009.01.045. URL `https://www.sciencedirect.com/science/article/pii/S1876610209000460`. Greenhouse Gas Control Technologies 9.

[25] Ted Vrountas. 5 examples that show how machine learning is changing digital advertising, 2019. URL `https://instapage.com/blog/machine-learning-in-advertising`. Found 25.11.2020.

[26] M I Jordan and T M Mitchell. Machine learning: Trends, perspectives, and prospects. 349(6245), 2015.

[27] W. Pitts W. S. McCulloch. A Logical Calculus of the Ideas Immanent in Nervous Activity. *Bulletin of Mathematical Biophysics*, 5:115–133, 1943. doi: https://doi.org/10.1007/BF02478259.

[28] MATLAB MathWorks Help Center. tansig, hyperbolic tangent sigmoid transfer function, . URL `https://se.mathworks.com/help/deeplearning/ref/tansig.html`. Found 22.11.2020.

[29] R. Langley et al. P. Flowers, K. Theopold. *Chemistry*. 2012. URL `https://opentextbc.ca/chemistry2eopenstax/chapter/chemical-reaction-rates/`.

[30] T. Shah. About train, validation and test sets in machine learning, 2017. URL `https://towardsdatascience.com/train-validation-and-test-sets-72cb40cba9e7`. Found: 29.09.2020.

[31] A. Al-Masri. What are overfitting and underfitting in machine learning?, 2019. URL `https://towardsdatascience.com/what-are-overfitting-and-underfitting-in-machine-learning-a96b30864690`. Found 02.10.2020.

[32] MATLAB MathWorks Help Center. trainlm, levenberg-marquardt backpropagation, . URL `https://se.mathworks.com/help/deeplearning/ref/trainlm.html`. Found 02.10.2020.

[33] MATLAB MathWorks Help Center. trainbr, bayesian regularization backpropagation, . URL `https://se.mathworks.com/help/deeplearning/ref/trainbr.html`. Found 01.10.2020.

[34] MATLAB MathWorks Help Center. Fit data with a shallow neural network, . URL `https://se.mathworks.com/help/deeplearning/gs/fit-data-with-a-neural-network.html`. Found 27.10.2020.

[35] CFI. Data smoothing. URL `https://corporatefinanceinstitute.com/resources/knowledge/other/data-smoothing/`. Found: 20.05.2021.

# Appendix

# A Figures

## A Oxidative degradation

### A.1 MEA

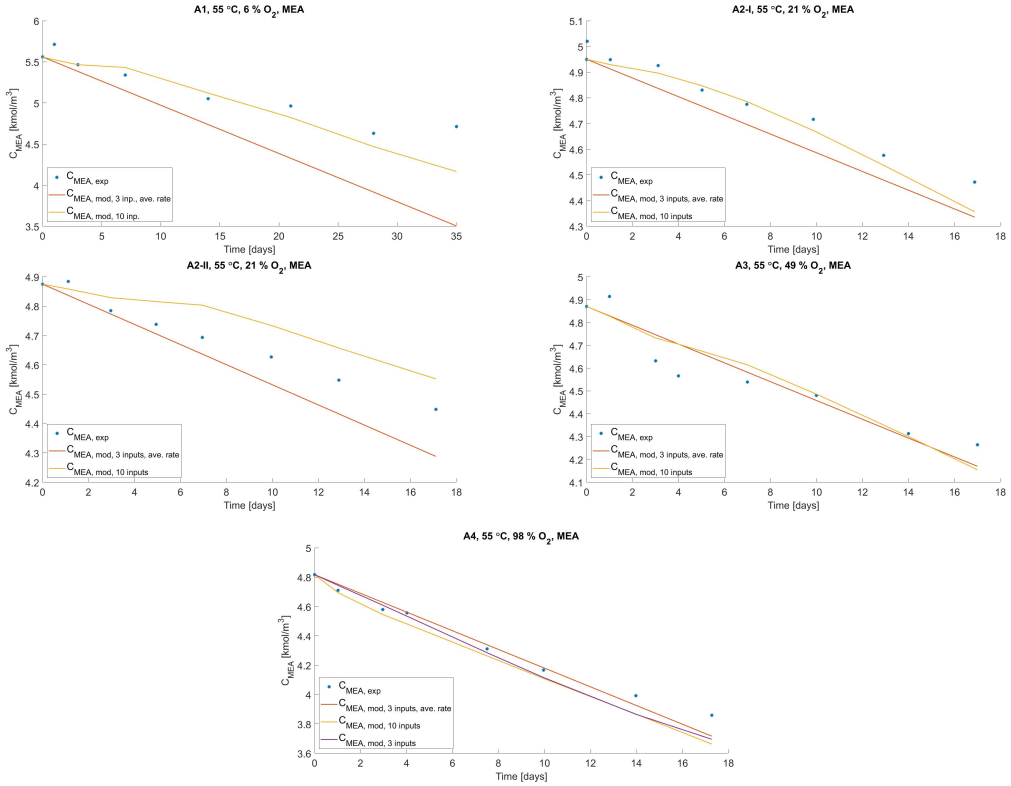


**Figure A.1:** Plotted results for experiment A1, A2-I, A2-II, A3 and A4 done at 55°C for MEA. The blue dots are the experimental datapoints, the red line is the ML-model with 3 inputs and average reaction rate, the yellow line is the ML-model with 10 inputs, and the purple line is the ML-model with 3 inputs with instantaneous rate.

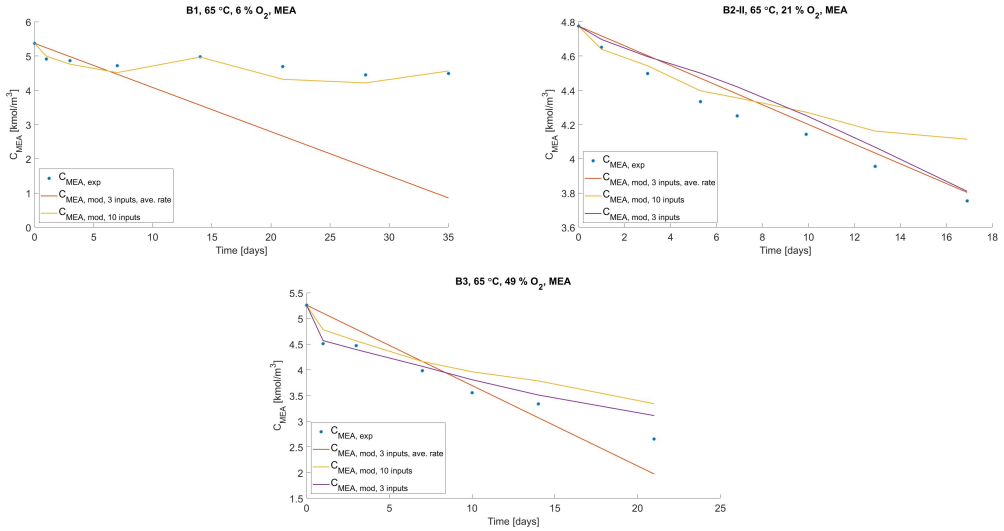


**Figure A.2:** Plotted results for experiment B1, B2-II and B3 done at 65°C for MEA. The blue dots are the experimental data points, the red line is the ML-model with 3 inputs and average reaction rate, the yellow line is the ML-model with 10 inputs, and the purple line is the ML-model with 3 inputs with instantaneous rate.

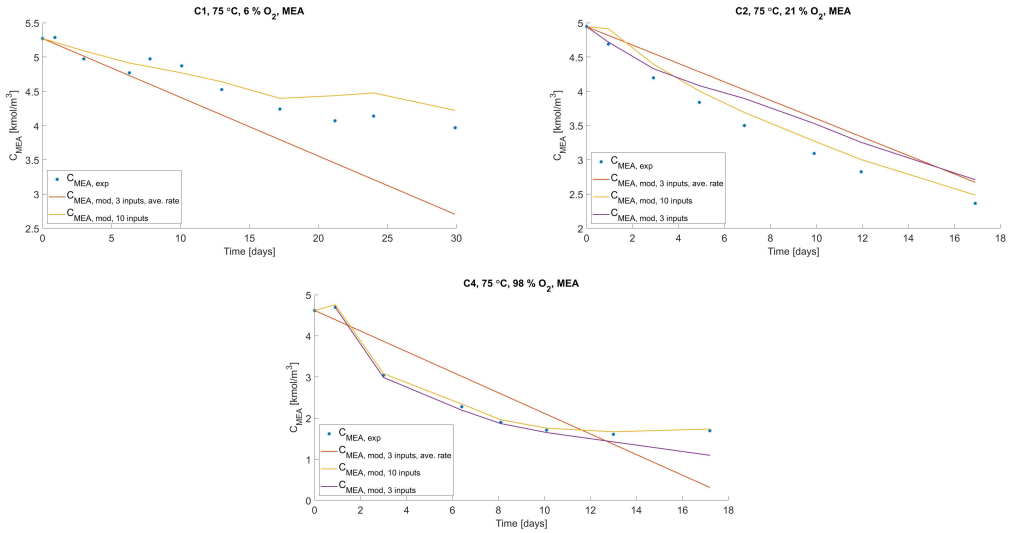


**Figure A.3:** Plotted results for experiment C1, C2 and C4 done at 75°C for MEA. The blue dots are the experimental data points, the red line is the ML-model with 3 inputs and average reaction rate, the yellow line is the ML-model with 10 inputs, and the purple line is the ML-model with 3 inputs with instantaneous rate.

## A.2 Formate

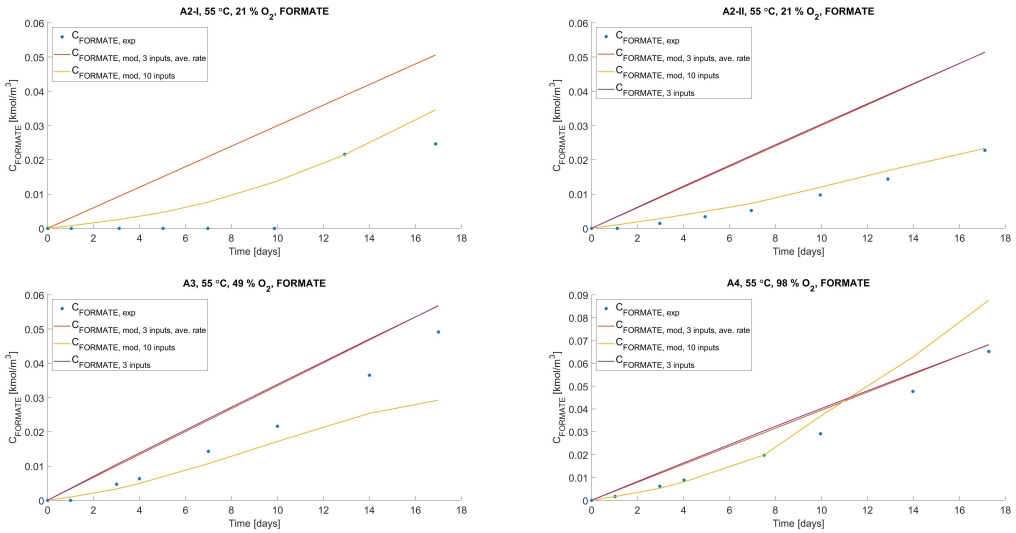


**Figure A.4:** Plotted results for experiment A2-I, A2-II, A3 and A4 done at 55°C for formate. The blue dots are the experimental data points, and the red line is the ML-model with 3 inputs and average reaction rate, the yellow line is the ML-model with 10 inputs, the purple line is the ML-model with 3 inputs with instantaneous rate.

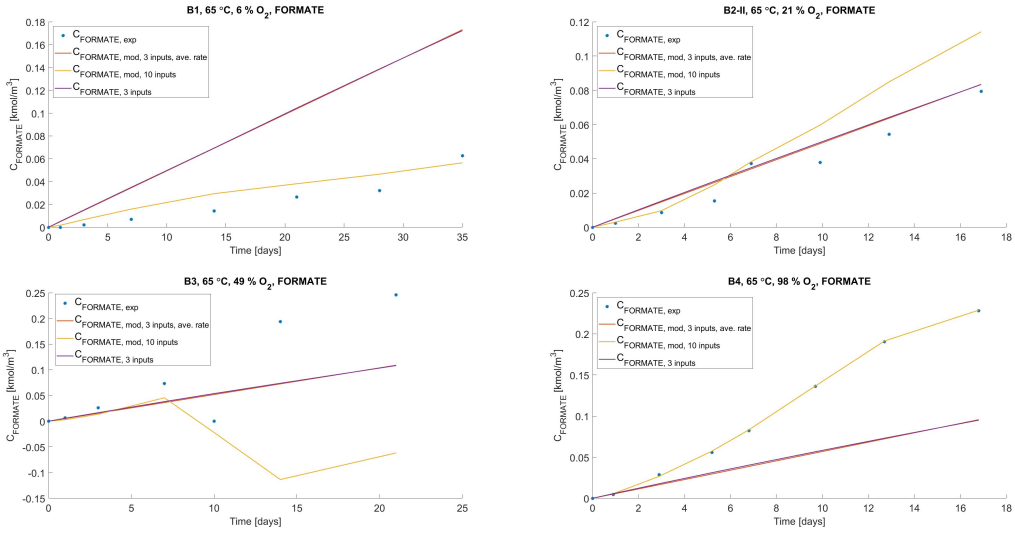


**Figure A.5:** Plotted results for experiment B1, B2-II, B3, B4 done at 65°C for formate. The blue dots are the experimental data points, and the red line is the ML-model with 3 inputs and average reaction rate, the yellow line is the ML-model with 10 inputs, the purple line is the ML-model with 3 inputs with instantaneous rate.

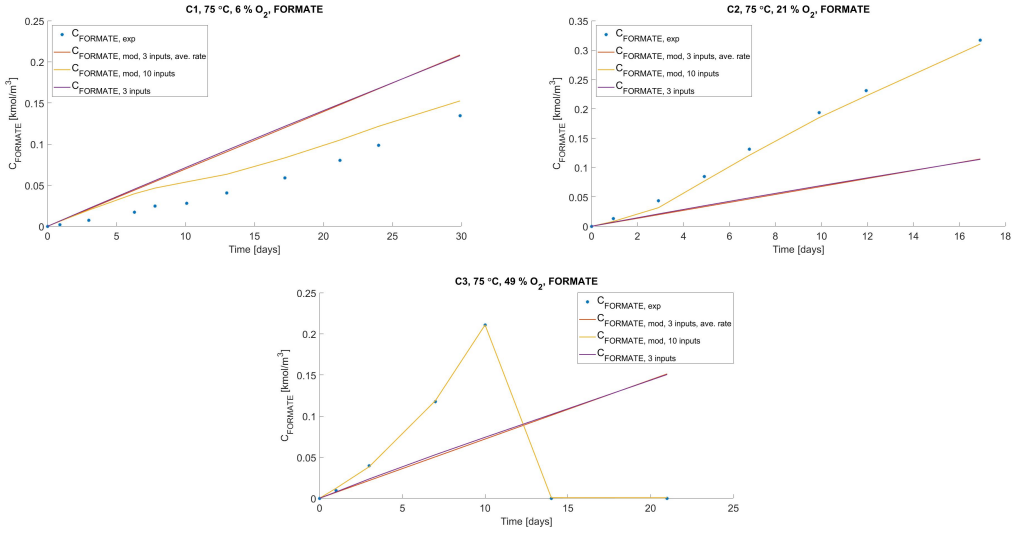


**Figure A.6:** Plotted results for experiment C1, C2 and C3 done at 75°C for formate. The blue dots are the experimental data points, the red line is the ML-model with 3 inputs and average reaction rate, the yellow line is the ML-model with 10 inputs, and the purple line is the ML-model with 3 inputs with instantaneous rate.

## A.3 Oxalic acid

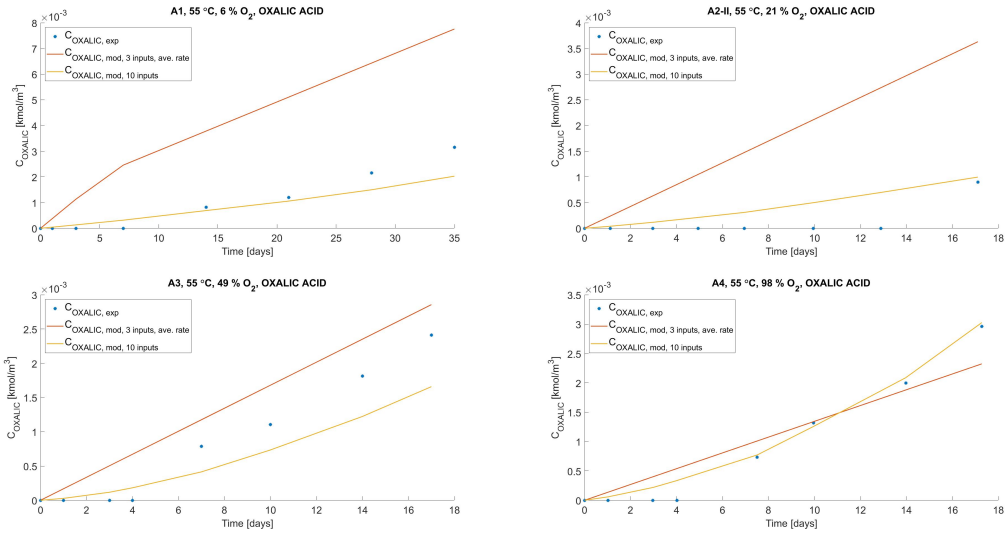


**Figure A.7:** Plotted results for experiment A1, A2-II, A3 and A4 done at 55°C for oxalic acid. The blue dots are the experimental data points, the red line is the ML-model with 3 inputs and average reaction rate, the yellow line is the ML-model with 11 inputs, and the purple line is the ML-model with 3 inputs with instantaneous rate.

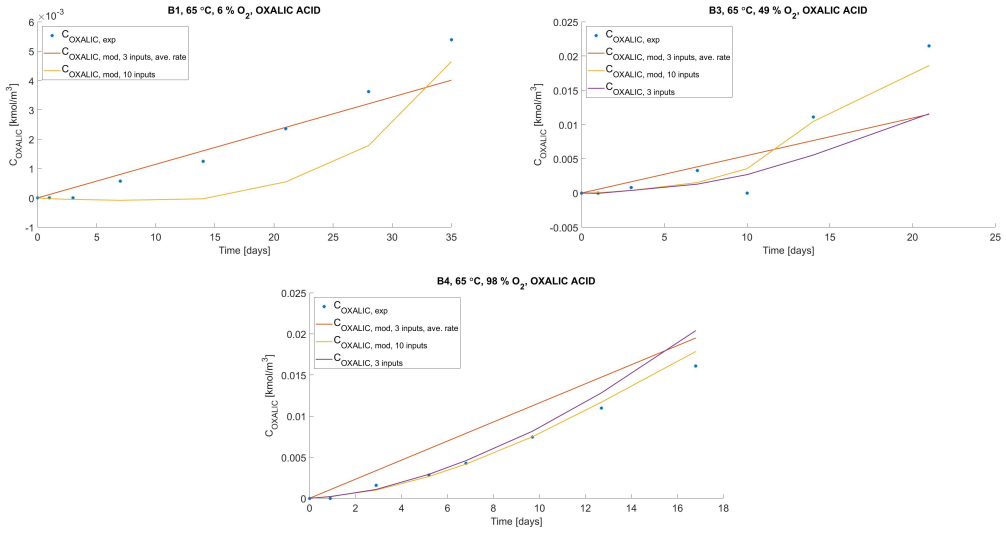


**Figure A.8:** Plotted results for experiment B1, B3 and B4 done at 65°C for oxalic acid. The blue dots are the experimental data points, the red line is the ML-model with 3 inputs and average reaction rate, the yellow line is the ML-model with 11 inputs, and the purple line is the ML-model with 3 inputs with instantaneous rate.

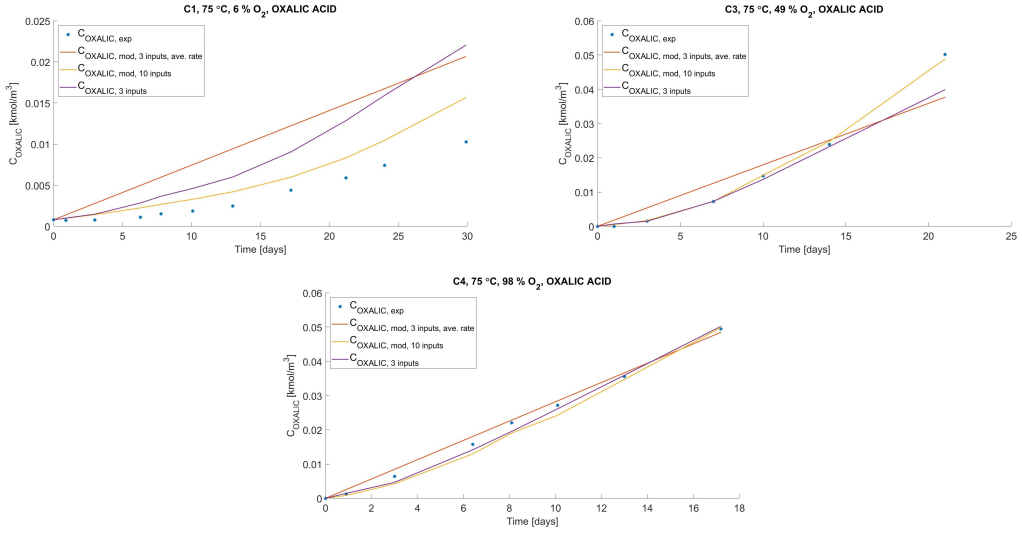


**Figure A.9:** Plotted results for experiment C1, C3 and C4 done at 75°C for oxalic acid. The blue dots are the experimental data points, the red line is the ML-model with 3 inputs and average reaction rate, the yellow line is the ML-model with 11 inputs, and the purple line is the ML-model with 3 inputs with instantaneous rate.

## A.4 HEGly

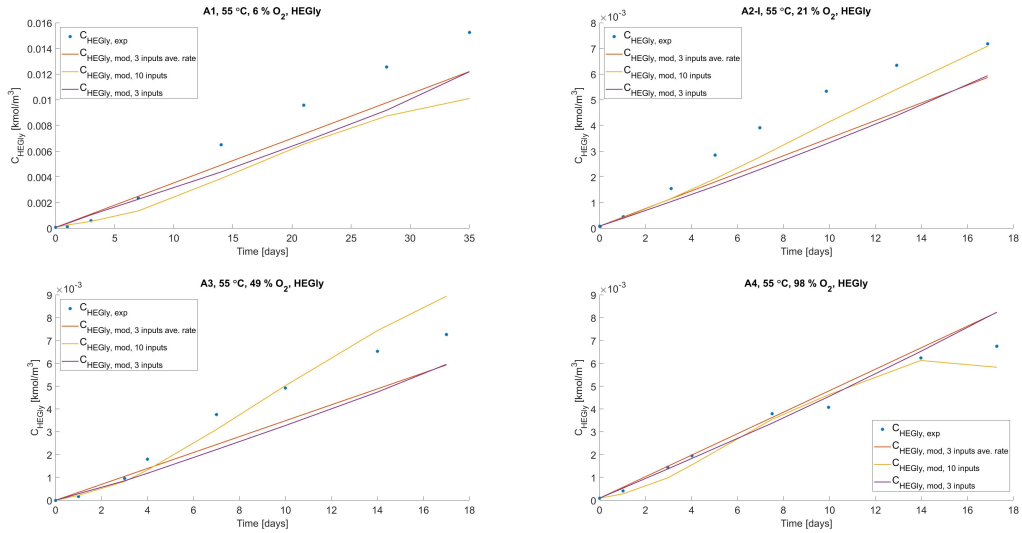


**Figure A.10:** Plotted results for experiment A1, A2-I, A3 and A4 done at 55°C for HEGly. The blue dots are the experimental data points, the red line is the ML-model with 3 inputs and average reaction rate, the yellow line is the ML-model with 10 inputs, and the purple line is the ML-model with 3 inputs with instantaneous rate.

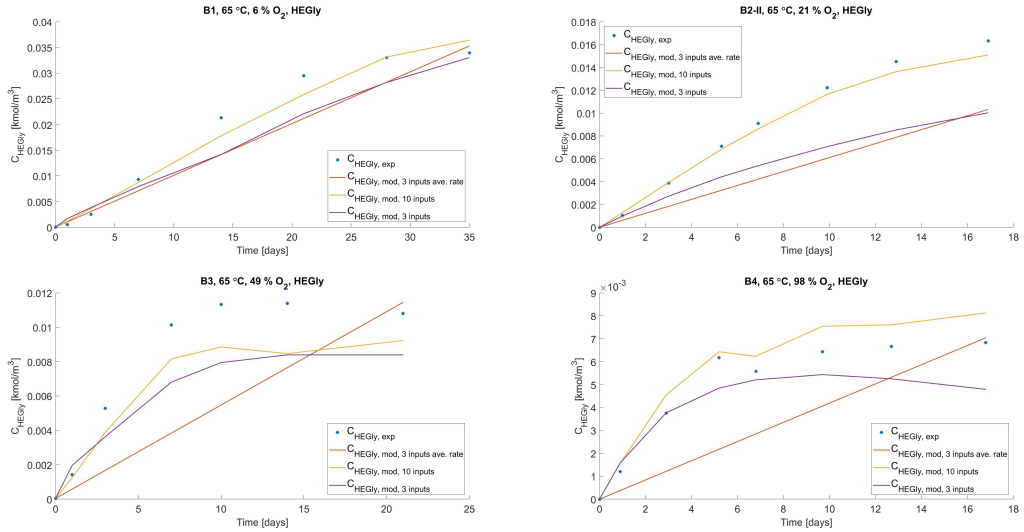


**Figure A.11:** Plotted results for experiment B1, B2-II, B3 and B4 done at 65°C for HEGly. The blue dots are the experimental data points, the red line is the ML-model with 3 inputs and average reaction rate, the yellow line is the ML-model with 10 inputs, and the purple line is the ML-model with 3 inputs with instantaneous rate.

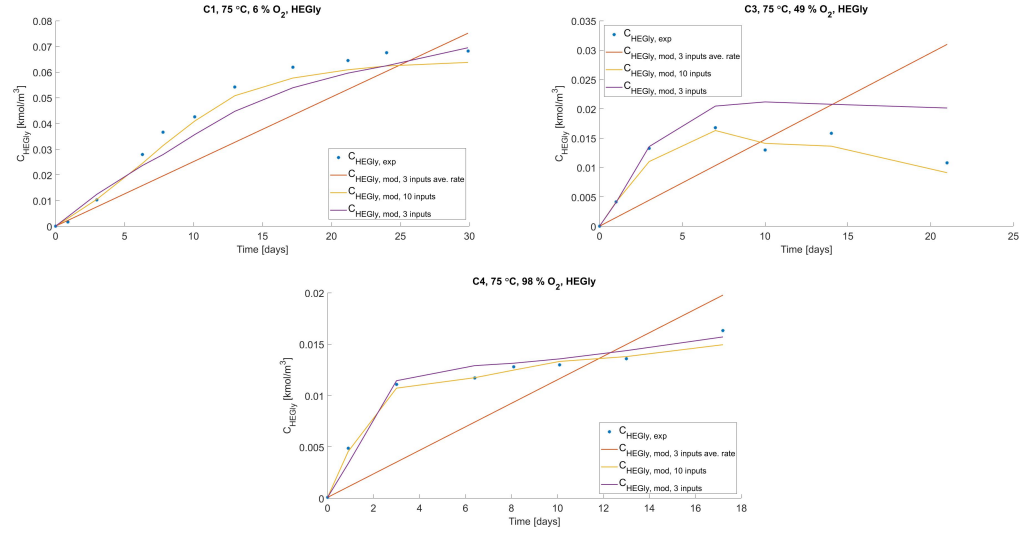


**Figure A.12:** Plotted results for experiment C1, C3 and C4 done at 75°C for HEGly. The blue dots are the experimental data points, the red line is the ML-model with 3 inputs and average reaction rate, the yellow line is the ML-model with 10 inputs, and the purple line is the ML-model with 3 inputs with instantaneous rate.

## A.5 HEPO

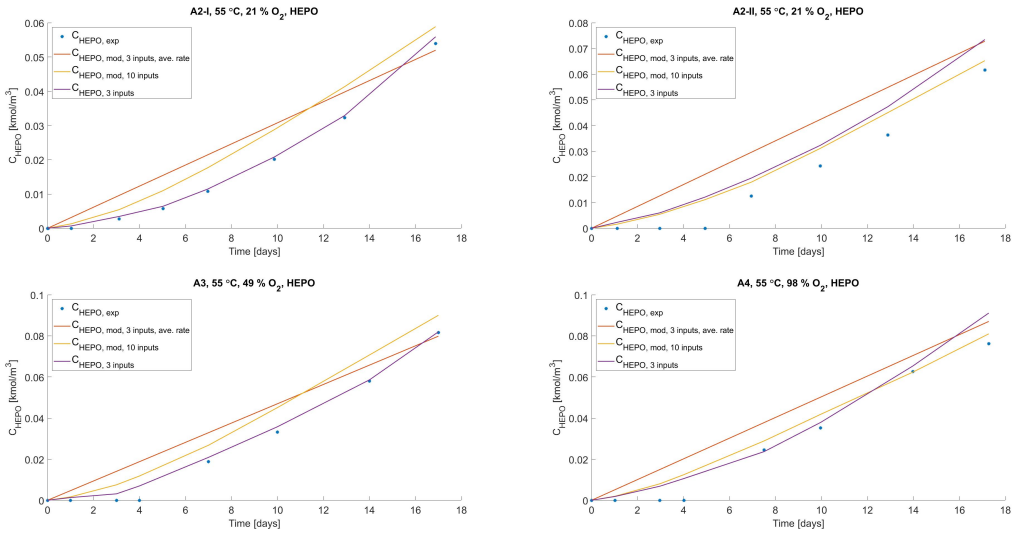


**Figure A.13:** Plotted results for experiment A2-I, A2-II, A3 and A4 done at 55°C for HEPO. The blue dots are the experimental data points, the red line is the ML-model with 3 inputs and average reaction rate, the yellow line is the ML-model with 10 inputs, and the purple line is the ML-model with 3 inputs with instantaneous rate.

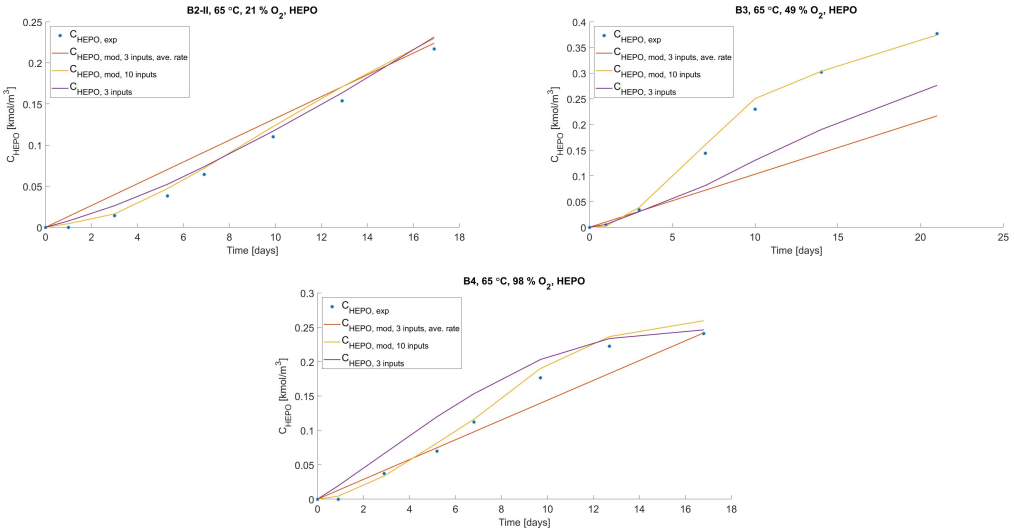


**Figure A.14:** Plotted results for experiment B2-II, B3 and B4 done at 65°C for HEPO. The blue dots are the experimental data points, the red line is the ML-model with 3 inputs and average reaction rate, the yellow line is the ML-model with 10 inputs, and the purple line is the ML-model with 3 inputs with instantaneous rate.

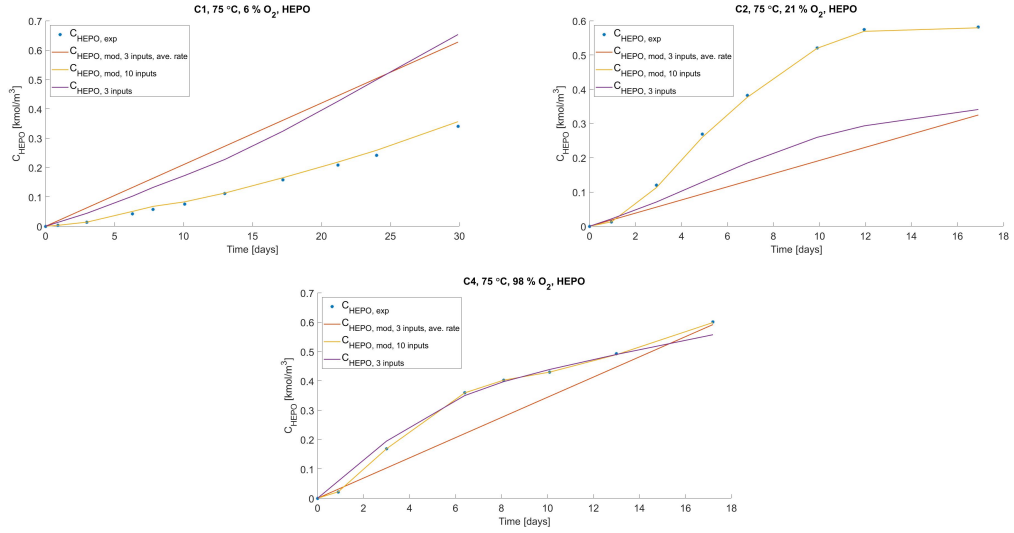


**Figure A.15:** Plotted results for experiment C1, C2 and C4 done at 75°C for HEPO. The blue dots are the experimental data points, the red line is the ML-model with 3 inputs and average reaction rate, the yellow line is the ML-model with 10 inputs, and the purple line is the ML-model with 3 inputs with instantaneous rate.

## A.6 HEF

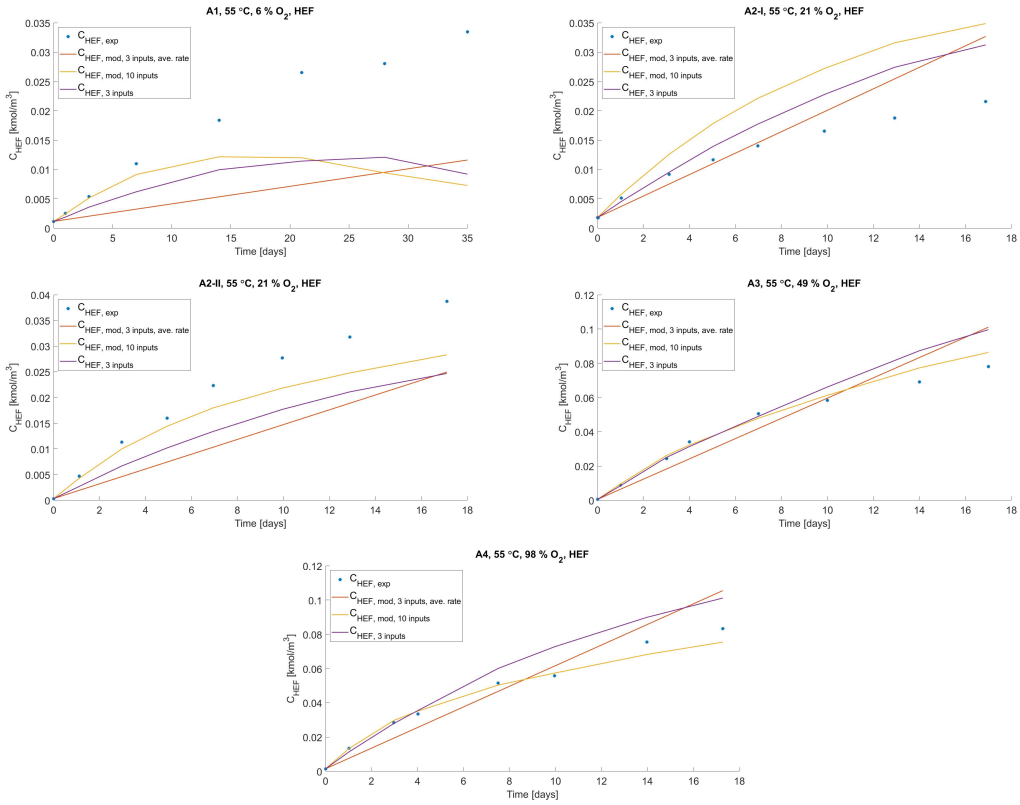


**Figure A.16:** Plotted results for experiment A1, A2-I, A2-II, A3 and A4 done at 55°C for HEF. The blue dots are the experimental data points, the red line is the ML-model with 3 inputs and average reaction rate, the yellow line is the ML-model with 10 inputs, and the purple line is the ML-model with 3 inputs with instantaneous rate.

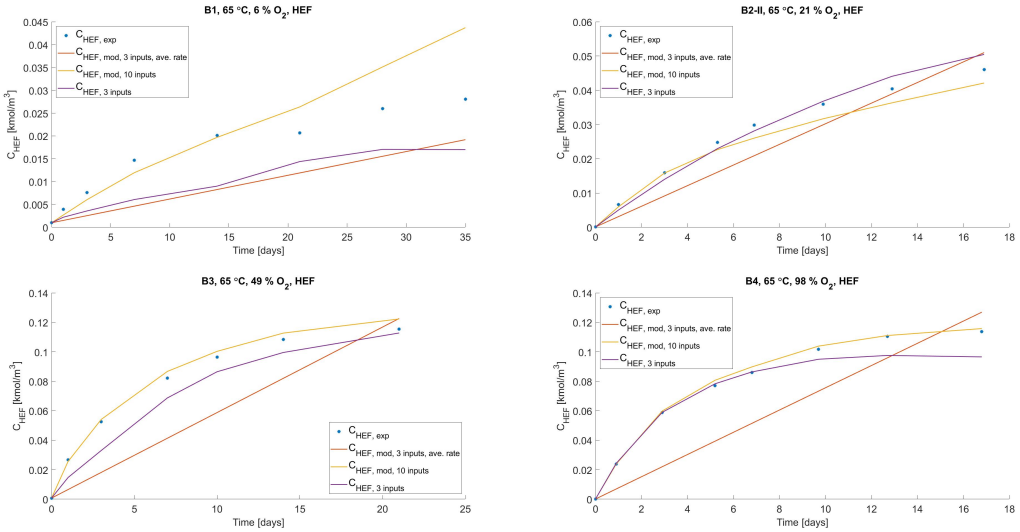


**Figure A.17:** Plotted results for experiment B1, B2-II, B3 and B4 done at 65°C for HEF. The blue dots are the experimental data points, the red line is the ML-model with 3 inputs and average reaction rate, the yellow line is the ML-model with 10 inputs, and the purple line is the ML-model with 3 inputs with instantaneous rate.

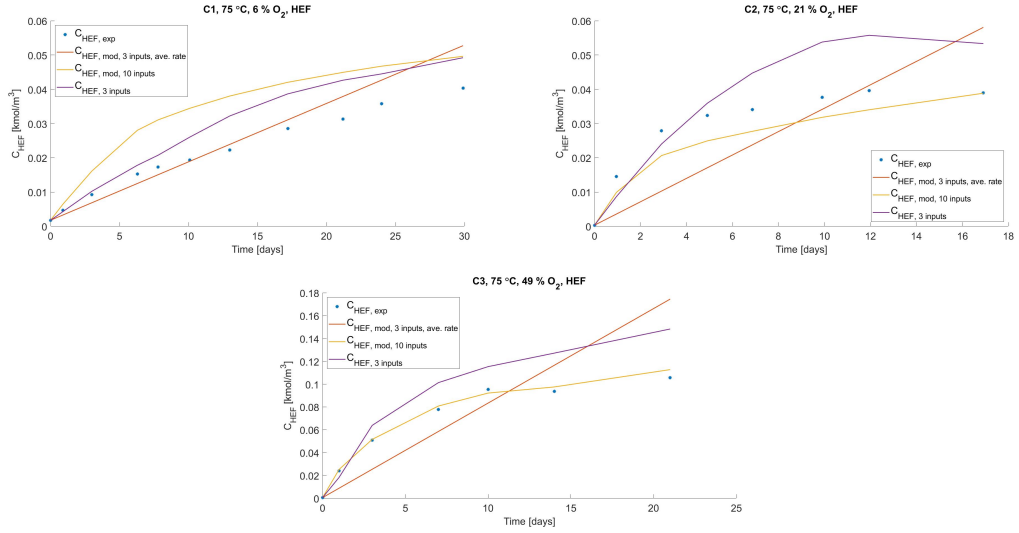


**Figure A.18:** Plotted results for experiment C1, C2 and C3 done at 75°C for HEF. The blue dots are the experimental data points, the red line is the ML-model with 3 inputs and average reaction rate, the yellow line is the ML-model with 10 inputs, and the purple line is the ML-model with 3 inputs with instantaneous rate.

## A.7 HEA

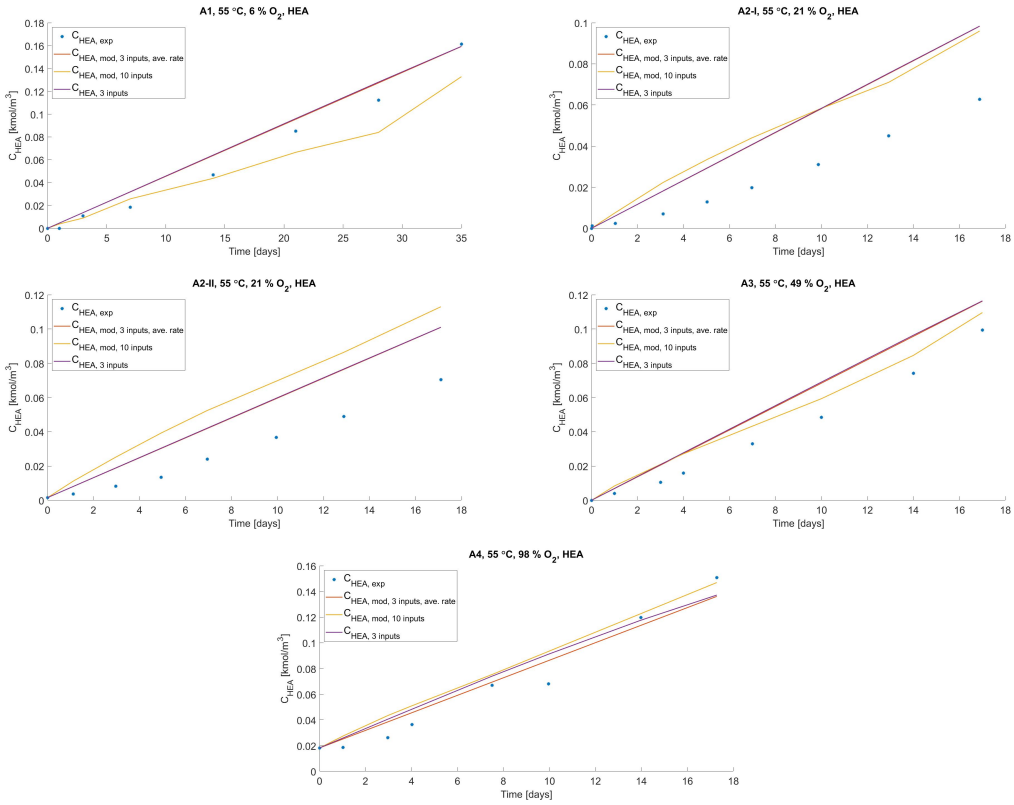


**Figure A.19:** Plotted results for experiment A1, A2-I, A2-II, A3 and A4 done at 55°C for HEA. The blue dots are the experimental data points, the red line is the ML-model with 3 inputs and average reaction rate, the yellow line is the ML-model with 10 inputs, and the purple line is the ML-model with 3 inputs with instantaneous rate.

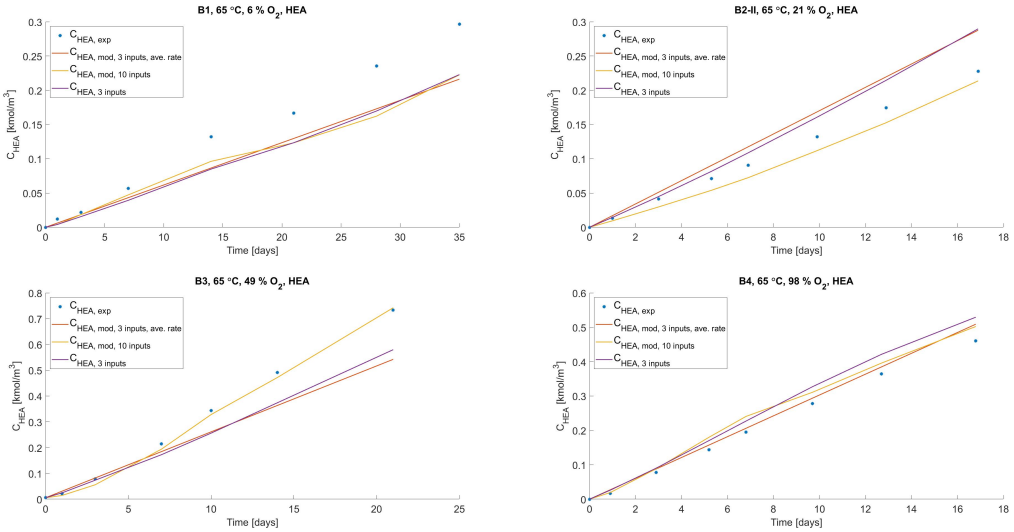


**Figure A.20:** Plotted results for experiment B1, B2-II, B3 and B4 done at 65°C for HEA. The blue dots are the experimental data points, the red line is the ML-model with 3 inputs and average reaction rate, the yellow line is the ML-model with 10 inputs, and the purple line is the ML-model with 3 inputs with instantaneous rate.

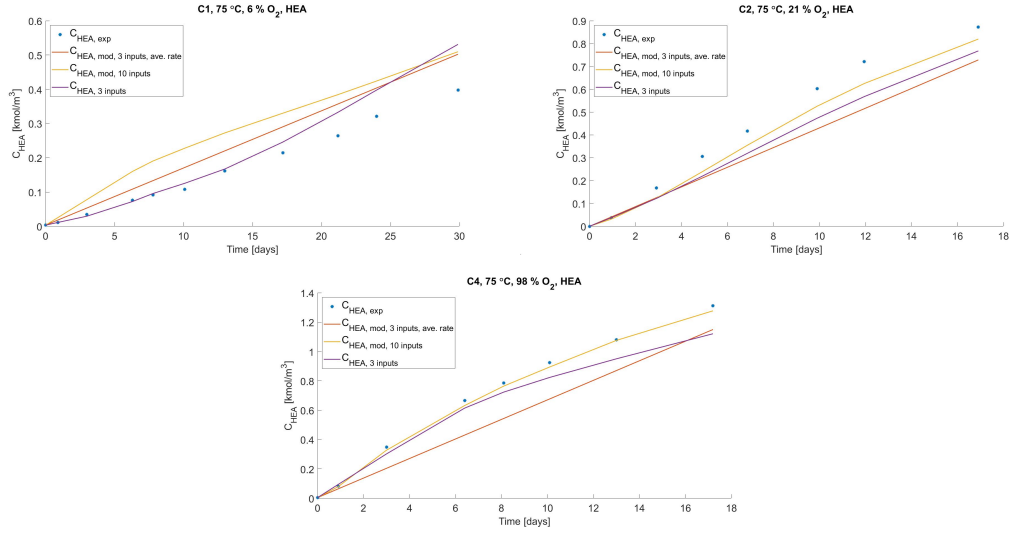


**Figure A.21:** Plotted results for experiment C1, C2 and C4 done at 75°C for HEA. The blue dots are the experimental data points, the red line is the ML-model with 3 inputs and average reaction rate, the yellow line is the ML-model with 10 inputs, and the purple line is the ML-model with 3 inputs with instantaneous rate.

## A.8 BHEOX

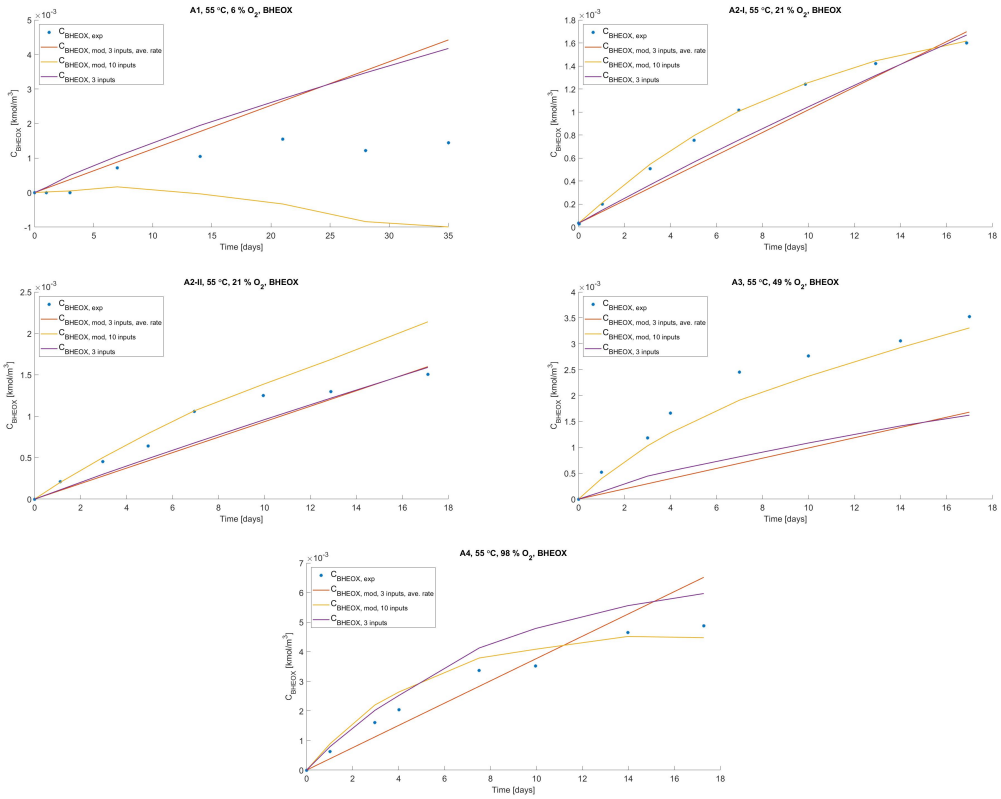


**Figure A.22:** Plotted results for experiment A1, A2-I, A2-II, A3 and A4 done at 55°C for BHEOX. The blue dots are the experimental data points, the red line is the ML-model with 3 inputs and average reaction rate, the yellow line is the ML-model with 10 inputs, and the purple line is the ML-model with 3 inputs with instantaneous rate.

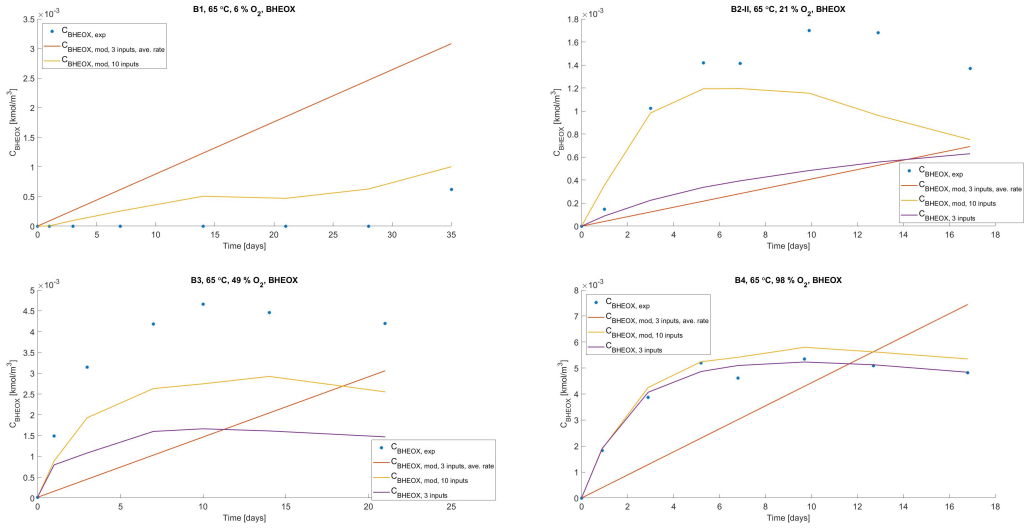


**Figure A.23:** Plotted results for experiment B1, B2-II, B3 and B4 done at 65°C for BHEOX. The blue dots are the experimental data points, the red line is the ML-model with 3 inputs and average reaction rate, the yellow line is the ML-model with 10 inputs, and the purple line is the ML-model with 3 inputs with instantaneous rate.

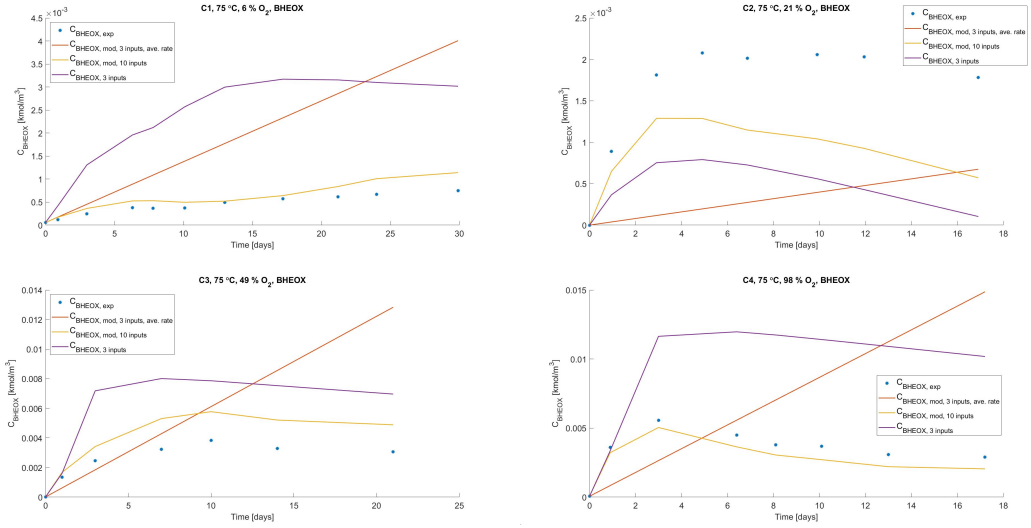


**Figure A.24:** Plotted results for experiment C1, C2, C3 and C4 done at 75°C for BHEOX. The blue dots are the experimental data points, the red line is the ML-model with 3 inputs and average reaction rate, the yellow line is the ML-model with 10 inputs, and the purple line is the ML-model with 3 inputs with instantaneous rate.

## A.9 HEI

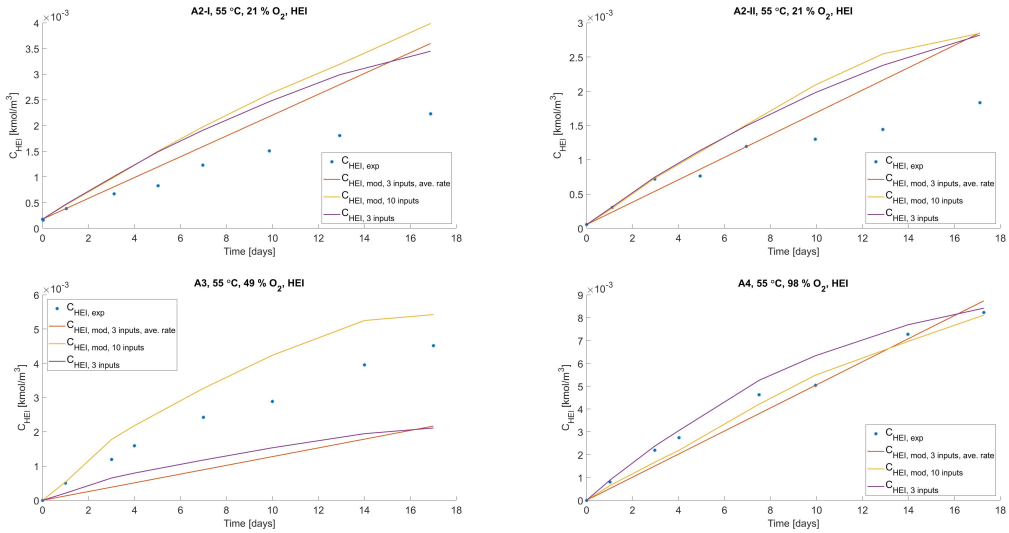


**Figure A.25:** Plotted results for experiment A2-I, A2-II, A3 and A4 done at 55°C for HEI. The blue dots are the experimental data points, the red line is the ML-model with 3 inputs and average reaction rate, the yellow line is the ML-model with 10 inputs, and the purple line is the ML-model with 3 inputs with instantaneous rate.

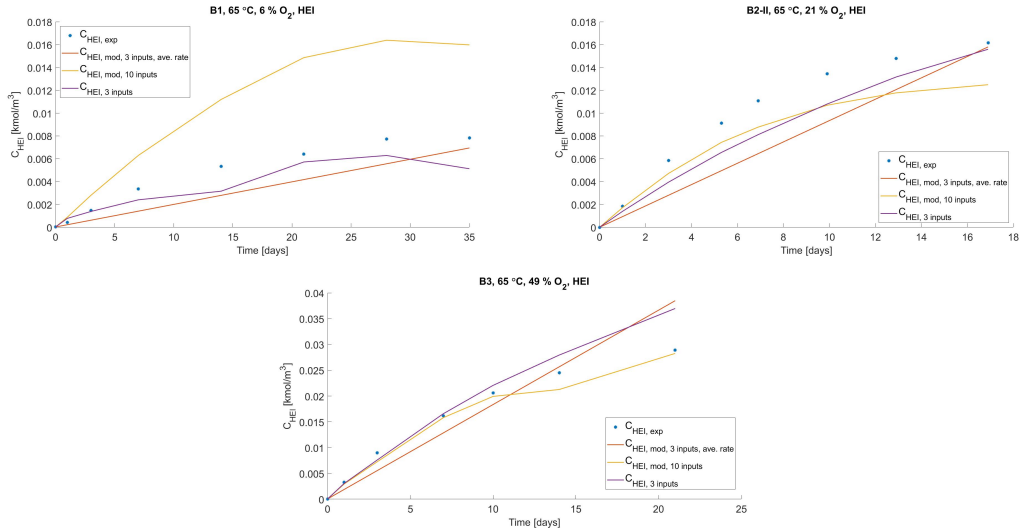


**Figure A.26:** Plotted results for experiment B1, B2-II and B3 done at 65°C for HEI. The blue dots are the experimental data points, the red line is the ML-model with 3 inputs and average reaction rate, the yellow line is the ML-model with 10 inputs, and the purple line is the ML-model with 3 inputs with instantaneous rate.

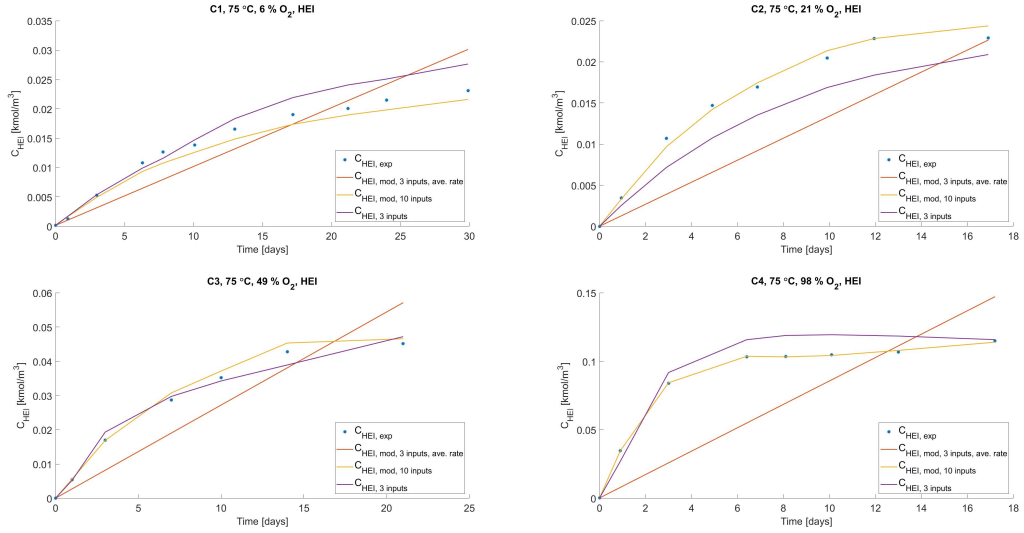


**Figure A.27:** Plotted results for experiment C1, C2, C3 and C4 done at 75°C for HEI. The blue dots are the experimental data points, the red line is the ML-model with 3 inputs and average reaction rate, the yellow line is the ML-model with 10 inputs, and the purple line is the ML-model with 3 inputs with instantaneous rate.

# B Thermal degradation

## B.1 MEA

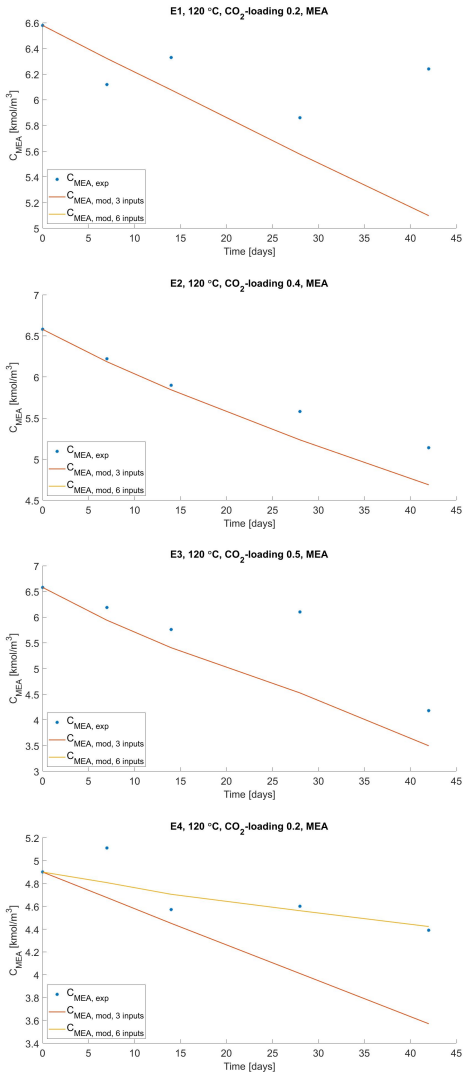


**Figure A.28:** Plotted results for experiment E1, E2, E3 and E4 done at 120°C for MEA. The blue dots are the experimental data points, the red line is the ML-model with 3 inputs, and the yellow line is the ML-model with 6 inputs.

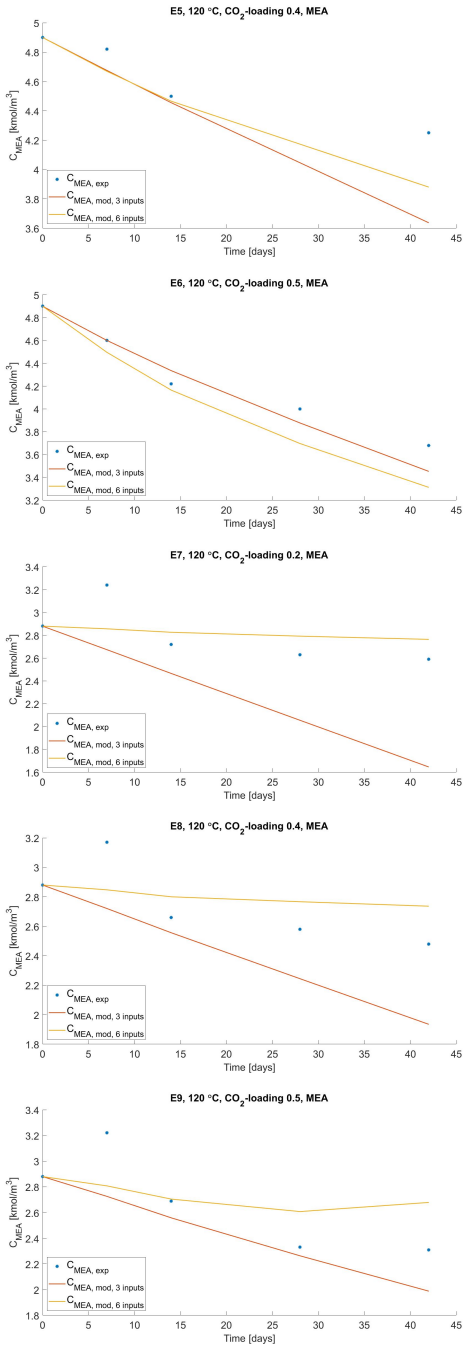


**Figure A.29:** Plotted results for experiment E5, E6, E7, E8 and E9 done at 120°C for MEA. The blue dots are the experimental data points, the red line is the ML-model with 3 inputs, and the yellow line is the ML-model with 6 inputs.

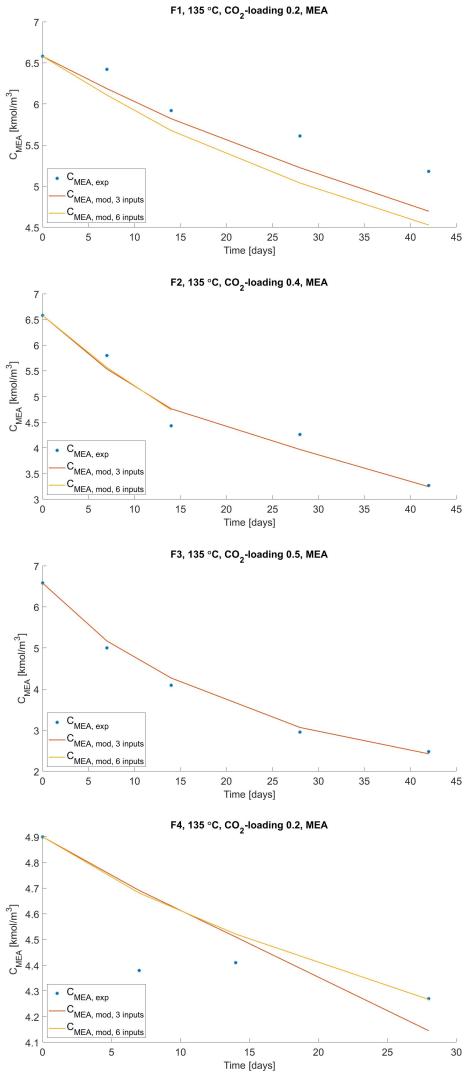


**Figure A.30:** Plotted results for experiment F1, F2, F3 and F4 done at 135°C for MEA. The blue dots are the experimental data points, the red line is the ML-model with 3 inputs, and the yellow line is the ML-model with 6 inputs.

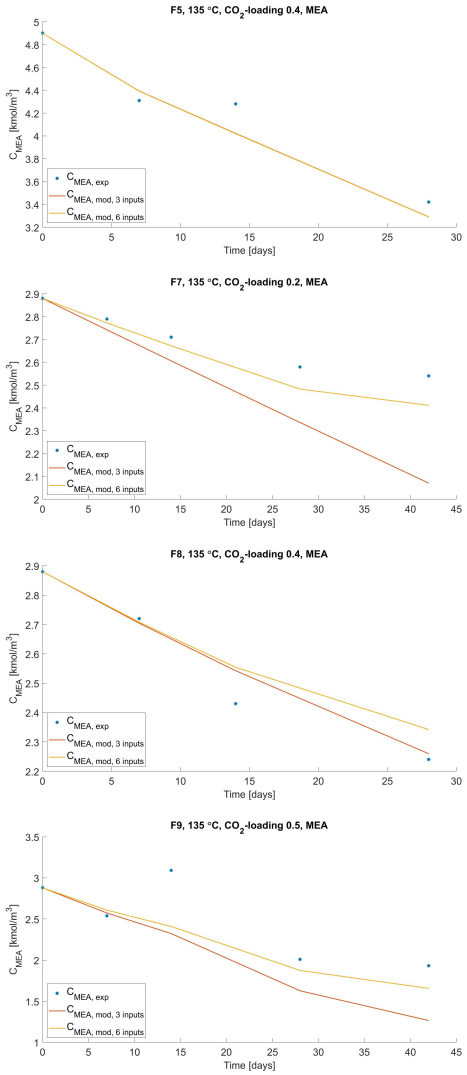


**Figure A.31:** Plotted results for experiment F5, F7, F8 and F9 done at 135°C for MEA. The blue dots are the experimental data points, the red line is the ML-model with 3 inputs, and the yellow line is the ML-model with 6 inputs.

## B.2 HEEDA

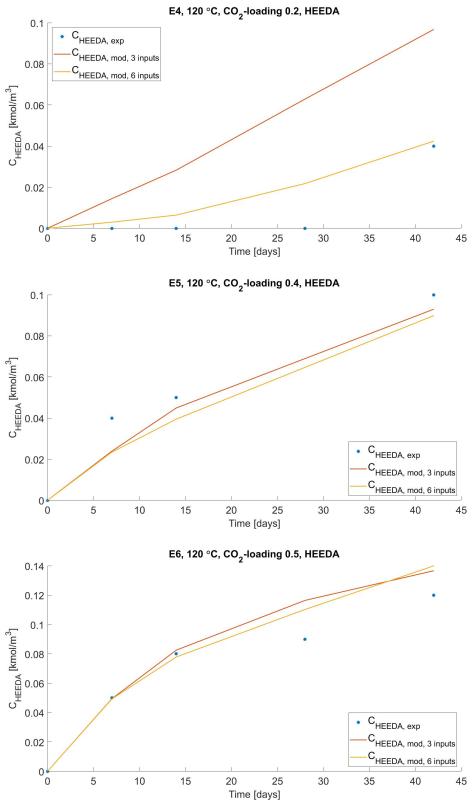


**Figure A.32:** Plotted results for experiment E4, E5 and E6 done at 120°C for HEEDA. The blue dots are the experimental data points, the red line is the ML-model with 3 inputs, and the yellow line is the ML-model with 6 inputs.

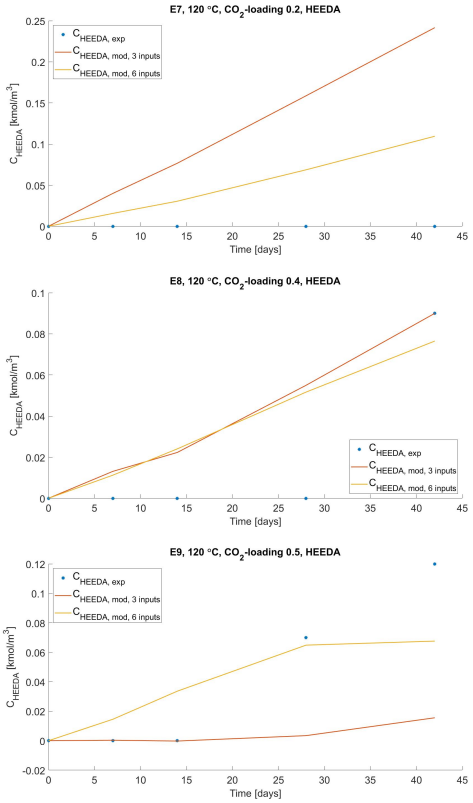


**Figure A.33:** Plotted results for experiment E7, E8 and E9 done at 120°C for HEEDA. The blue dots are the experimental data points, the red line is the ML-model with 3 inputs, and the yellow line is the ML-model with 6 inputs.

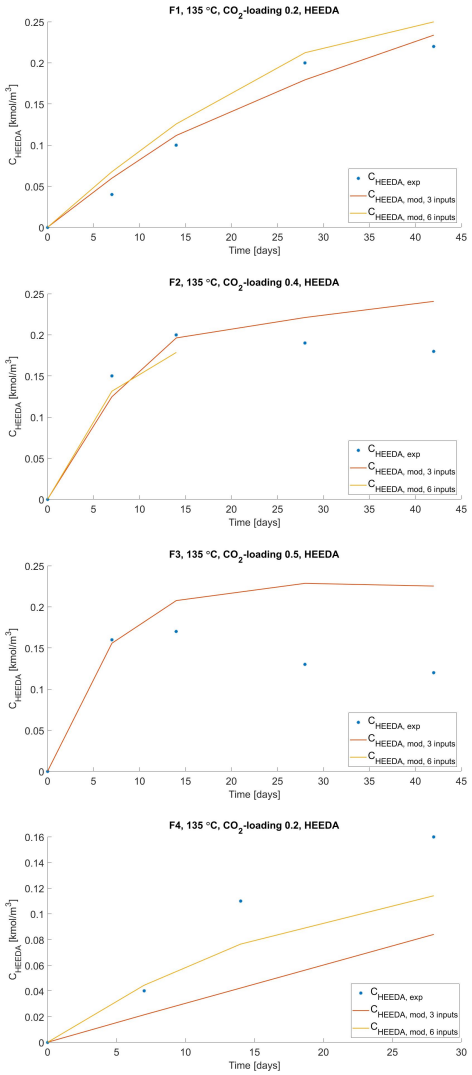


**Figure A.34:** Plotted results for experiment F1, F2, F3 and F4 done at 135°C for HEEDA. The blue dots are the experimental data points, the red line is the ML-model with 3 inputs, and the yellow line is the ML-model with 6 inputs.

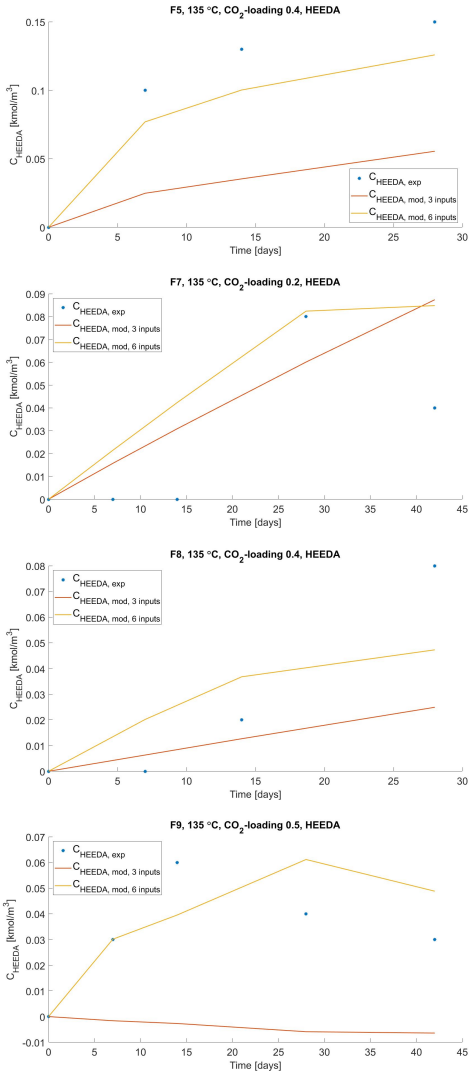


**Figure A.35:** Plotted results for experiment F5, F7, F8 and F9 done at 135°C for HEEDA. The blue dots are the experimental data points, the red line is the ML-model with 3 inputs, and the yellow line is the ML-model with 6 inputs.

## B.3 HEIA

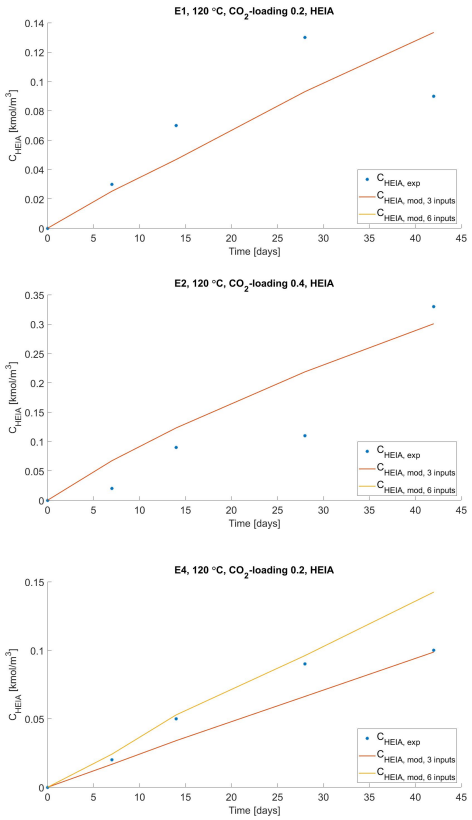


**Figure A.36:** Plotted results for experiment E1, E2, E3 and E4 done at 120°C for HEIA. The blue dots are the experimental data points, the red line is the ML-model with 3 inputs, and the yellow line is the ML-model with 6 inputs.

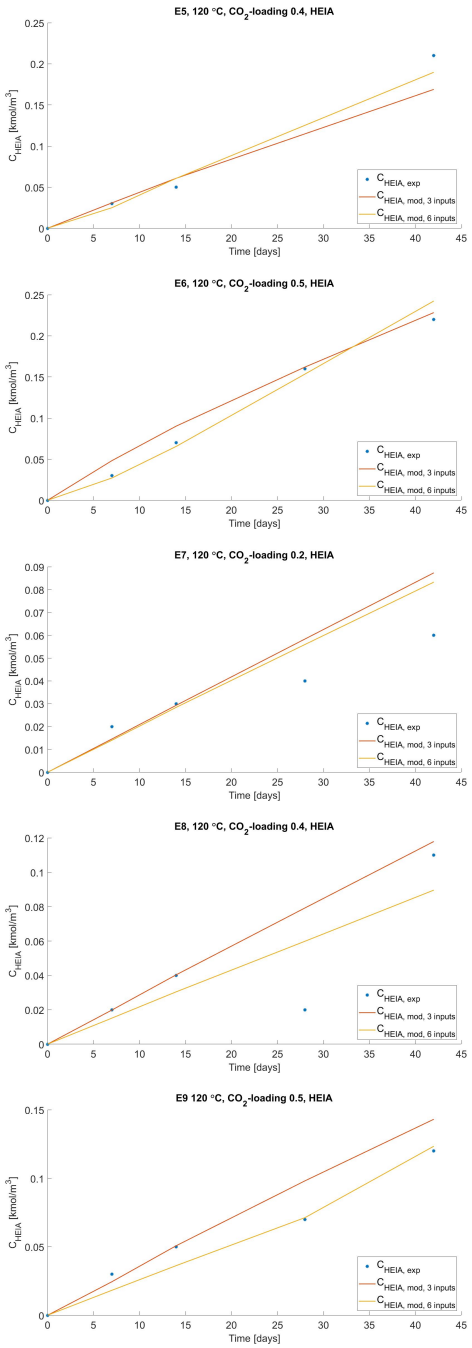


**Figure A.37:** Plotted results for experiment E5, E6, E7, E8 and E9 done at 120°C for HEIA. The blue dots are the experimental data points, the red line is the ML-model with 3 inputs, and the yellow line is the ML-model with 6 inputs.

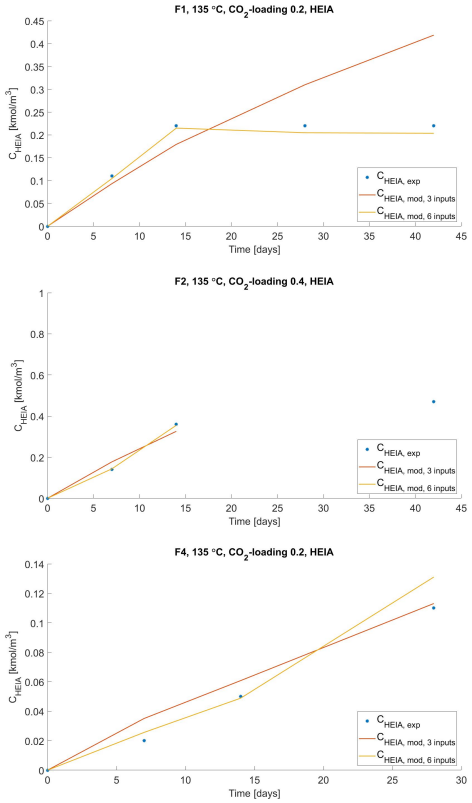


**Figure A.38:** Plotted results for experiment F1, F2, F3 and F4 done at 135°C for HEIA. The blue dots are the experimental data points, the red line is the ML-model with 3 inputs, and the yellow line is the ML-model with 6 inputs.

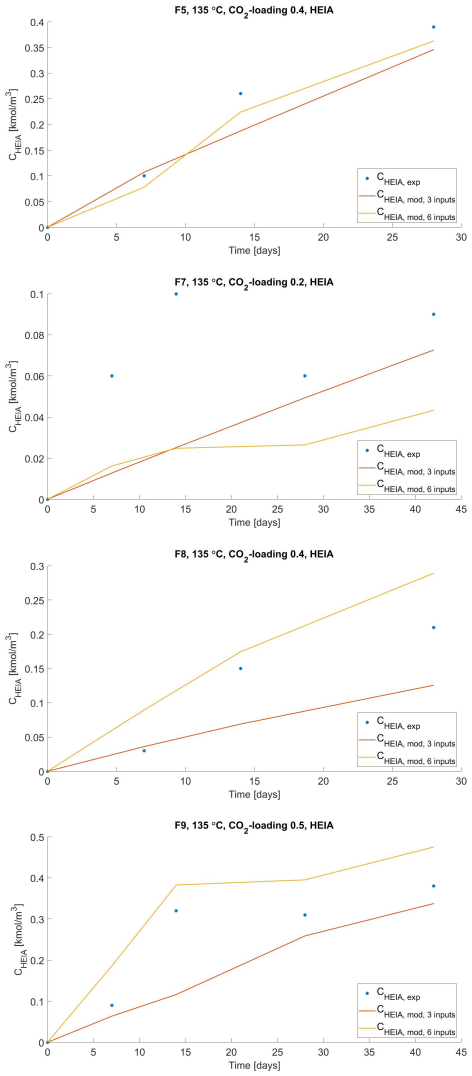


**Figure A.39:** Plotted results for experiment F5, F7, F8 and F9 done at 135°C for HEIA. The blue dots are the experimental data points, the red line is the ML-model with 3 inputs, and the yellow line is the ML-model with 6 inputs.

## B.4 TriHEIA

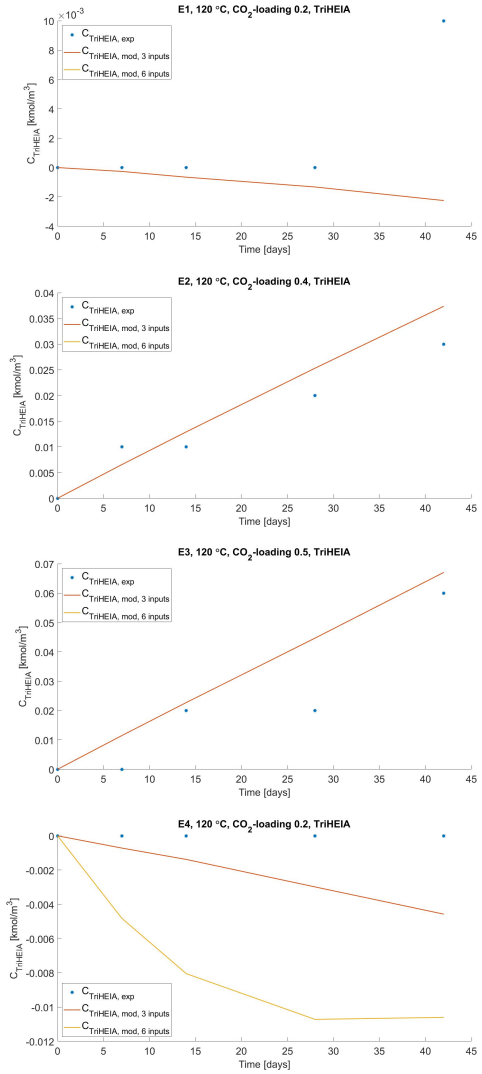


**Figure A.40:** Plotted results for experiment E1, E2, E3 and E4 done at 120°C for TriHEIA. The blue dots are the experimental data points, the red line is the ML-model with 3 inputs, and the yellow line is the ML-model with 6 inputs.

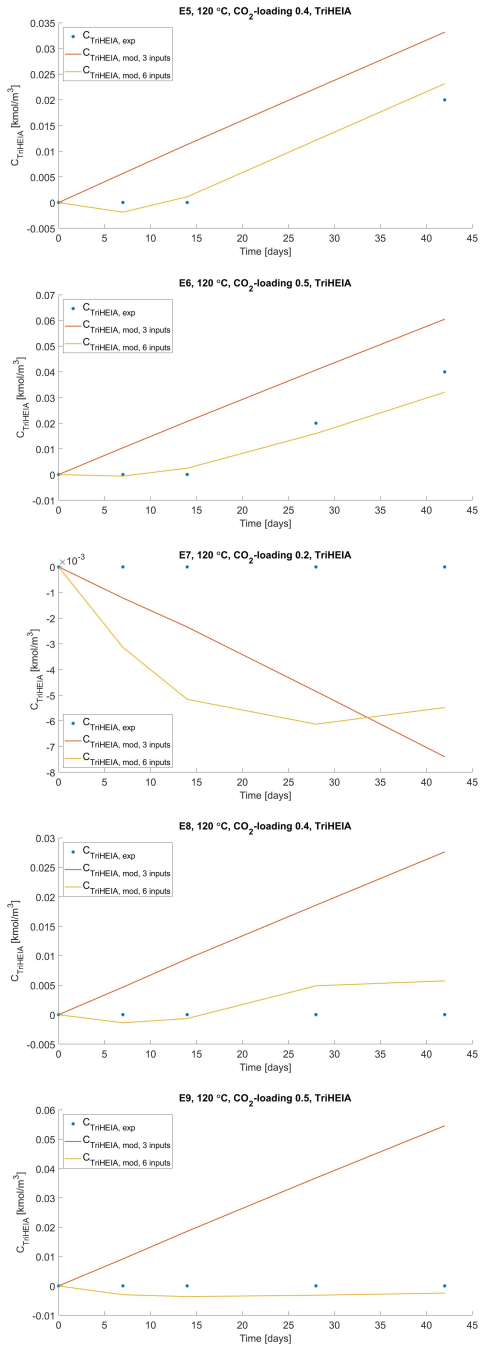


**Figure A.41:** Plotted results for experiment E5, E6, E7, E8 and E9 done at 120°C for TriHEIA. The blue dots are the experimental data points, the red line is the ML-model with 3 inputs, and the yellow line is the ML-model with 6 inputs.

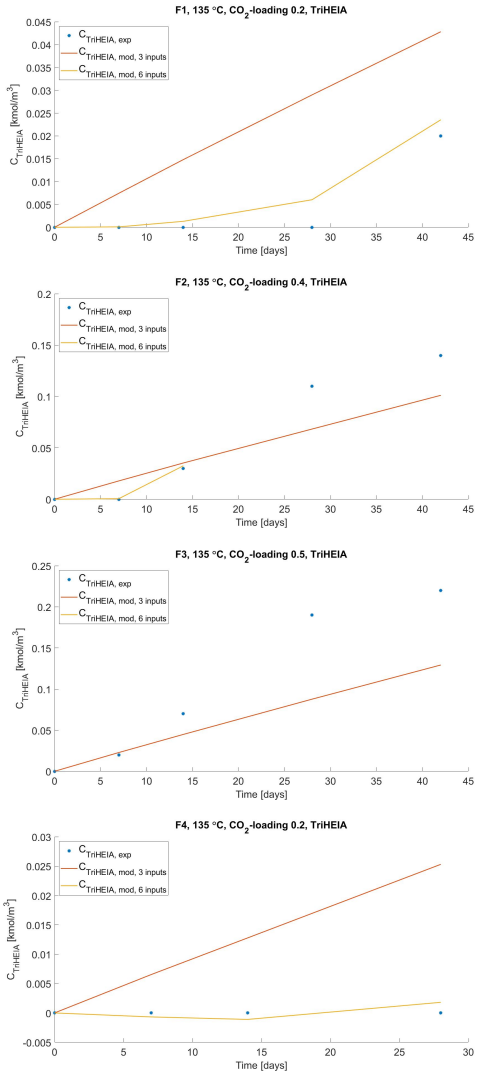


**Figure A.42:** Plotted results for experiment F1, F2, F3 and F4 done at 135°C for TriHEIA. The blue dots are the experimental data points, the red line is the ML-model with 3 inputs, and the yellow line is the ML-model with 6 inputs.

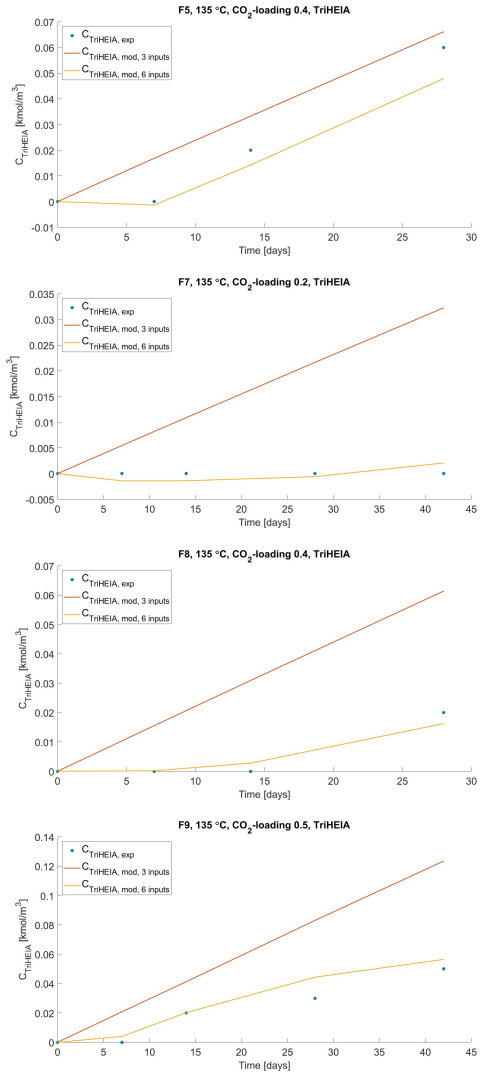


**Figure A.43:** Plotted results for experiment F5, F7, F8 and F9 done at 135°C for TriHEIA. The blue dots are the experimental data points, the red line is the ML-model with 3 inputs, and the yellow line is the ML-model with 6 inputs.

# B Tables with AAD and AARD

## A Oxidative degradation

**Table B.1:** AAD for MEA. (1) AAD between the experimental values and the model with 3 inputs and average rate. (2) AAD between experimental values and the model with 10 inputs. (3) AAD between the experimental values and the model with 3 inputs with simultaneous rate.

| Experiment | AAD (1) | AAD (2) | AAD (3) |
|---|---|---|---|
| A1 | 0.419 | 0.149 | - |
| A2-I | 0.077 | 0.038 | - |
| A2-II | 0.065 | 0.072 | - |
| A3 | 0.065 | 0.066 | - |
| A4 | 0.043 | 0.069 | 0.057 |
| B1 | 1.307 | 0.132 | - |
| B2-II | 0.078 | 0.115 | 0.095 |
| B3 | 0.312 | 0.299 | 0.159 |
| B4 | 0.255 | 0.113 | 0.071 |
| C1 | 0.422 | 0.161 | - |
| C2 | 0.349 | 0.158 | 0.252 |
| C3 | 0.741 | 0.223 | - |
| C4 | 0.571 | 0.048 | - |

**Table B.2:** AARD for MEA. (1) AARDD between the experimental values and the model with 3 inputs and average rate. (2) AARD between the experimental values and the model with 10 inputs. (3) AARD between the experimental values and the model with 3 inputs with simultaneous rate.

| Experiment | AARD (1) [%] | AARD (2) [%] | AARD (3) [%] |
|---|---|---|---|
| A1 | 7.350 | 2.610 | - |
| A2-I | 1.538 | 0.761 | - |
| A2-II | 1.322 | 1.480 | - |
| A3 | 1.313 | 1.344 | - |
| A4 | 0.892 | 1.436 | 1.175 |
| B1 | 24.34 | 2.471 | - |
| B2-II | 1.640 | 2.414 | 1.989 |
| B3 | 5.938 | 5.688 | 3.014 |
| B4 | 5.325 | 2.359 | 1.480 |
| C1 | 7.977 | 3.053 | - |
| C2 | 7.059 | 3.188 | 5.095 |
| C3 | 13.65 | 4.108 | - |
| C4 | 12.16 | 1.031 | - |

**Table B.3:** AAD for formate. (1) AAD between the experimental values and the model with 3 inputs and average rate. (2) AAD between the experimental values and the model with 10 inputs. (3) AAD between the experimental values and the model with 3 inputs with simultaneous rate.

| Experiment | AAD (1) | AAD (2) | AAD (3) |
|---|---|---|---|
| A1 | 0.030 | 0.003 | 0.030 |
| A2-I | 0.135 | 0.004 | - |
| A2-II | 0.014 | 0.001 | 0.014 |
| A3 | 0.007 | 0.005 | 0.007 |
| A4 | 0.006 | 0.006 | 0.006 |
| B1 | 0.049 | 0.008 | 0.049 |
| B2-II | 0.006 | 0.012 | 0.006 |
| B3 | 0.051 | 0.097 | 0.051 |
| B4 | 0.052 | 0.001 | 0.051 |
| C1 | 0.040 | 0.018 | 0.041 |
| C2 | 0.007 | 0.007 | 0.080 |
| C3 | 0.068 | 0.001 | 0.673 |
| C4 | 0.158 | 0.145 | 0.158 |

**Table B.4:** AARD for formate. (1) AARDD between the experimental values and the model with 3 inputs and average rate. (2) AARD between the experimental values and the model with 10 inputs. (3) AARD between the experimental values and the model with 3 inputs with simultaneous rate.

| Experiment | AARD (1) [%] | AARD (2) [%] | AARD (3) [%] |
|---|---|---|---|
| A1 | 84.41 | 9.257 | 85.86 |
| A2-I | 54.68 | 17.70 | - |
| A2-II | 61.14 | 6.208 | 61.93 |
| A3 | 13.97 | 10.84 | 14.46 |
| A4 | 8.737 | 9.030 | 9.328 |
| B1 | 78.66 | 12.52 | 78.92 |
| B2-II | 7.472 | 15.70 | 7.742 |
| B3 | 20.84 | 39.56 | 20.72 |
| B4 | 22.68 | 0.443 | 22.37 |
| C1 | 29.70 | 13.56 | 30.34 |
| C2 | 25.47 | 2.331 | 25.16 |
| C3 | 32.41 | 0.470 | 31.95 |
| C4 | 26.93 | 24.75 | 26.95 |

**Table B.5:** AAD for oxalic acid. (1) AAD between the experimental values and the model with 3 inputs and average rate. (2) AAD between the experimental values and the model with 11 inputs. (3) AAD between the experimental values and the model with 3 inputs with simultaneous rate.

| Experiment | AAD (1) | AAD (2) | AAD (3) |
|---|---|---|---|
| A1 | 0.0025 | 0.0003 | - |
| A2-II | 0.0014 | 0.0002 | - |
| A3 | 0.0004 | 0.0003 | - |
| A4 | 0.0003 | 0.0001 | - |
| B1 | 0.0004 | 0.0008 | - |
| B2-II | 0.0003 | 0.0009 | 0.0003 |
| B3 | 0.0030 | 0.0013 | 0.0029 |
| B4 | 0.0026 | 0.0005 | 0.0010 |
| C1 | 0.0055 | 0.0017 | 0.0039 |
| C2 | 0.0022 | 0.0021 | 0.0020 |
| C3 | 0.0040 | 0.0004 | 0.0018 |
| C4 | 0.0012 | 0.0015 | 0.0010 |

**Table B.6:** AARD for oxalic acid. (1) AARDD between the experimental values and the model with 3 inputs and average rate. (2) AARD between the experimental values and the model with 11 inputs. (3) AARD between the experimental values and the model with 3 inputs with simultaneous rate.

| Experiment | AARD (1) [%] | AARD (2) [%] | AARD (3) [%] |
|---|---|---|---|
| A1 | 78.16 | 10.11 | - |
| A2-II | 153.1 | 27.49 | - |
| A3 | 17.04 | 12.51 | - |
| A4 | 9.022 | 3.669 | - |
| B1 | 6.697 | 14.84 | - |
| B2-II | 5.172 | 18.56 | 6.222 |
| B3 | 13.87 | 6.179 | 13.70 |
| B4 | 16.02 | 2.819 | 6.189 |
| C1 | 53.37 | 16.72 | 38.22 |
| C2 | 6.397 | 6.273 | 5.881 |
| C3 | 7.989 | 0.893 | 3.626 |
| C4 | 2.514 | 3.119 | 2.057 |

**Table B.7:** AAD for HEGly. (1) AAD between the experimental values and the model with 3 inputs and average rate. (2) AAD between the experimental values and the model with 10 inputs. (3) AAD between the experimental values and the model with 3 inputs with simultaneous rate.

| Experiment | AAD (1) | AAD (2) | AAD (3) |
|---|---|---|---|
| A1 | 0.0013 | 0.0020 | 0.0015 |
| A2-I | 0.0009 | 0.0005 | 0.0010 |
| A2-II | 0.0004 | 0.0002 | 0.0005 |
| A3 | 0.0008 | 0.0005 | 0.0010 |
| A4 | 0.0004 | 0.0003 | 0.0004 |
| B1 | 0.0031 | 0.0015 | 0.0030 |
| B2-II | 0.0038 | 0.0005 | 0.0031 |
| B3 | 0.0030 | 0.0015 | 0.0020 |
| B4 | 0.0017 | 0.0007 | 0.0008 |
| C1 | 0.0105 | 0.0030 | 0.0050 |
| C2 | 0.0055 | 0.0009 | 0.0015 |
| C3 | 0.0064 | 0.0011 | 0.0038 |
| C4 | 0.0032 | 0.0004 | 0.0007 |

**Table B.8:** AARD for HEGly. (1) AARDD between the experimental values and the model with 3 inputs and average rate. (2) AARD between the experimental values and the model with 10 inputs. (3) AARD between the experimental values and the model with 3 inputs with simultaneous rate.

| Experiment | AARD (1) [%] | AARD (2) [%] | AARD (3) [%] |
|---|---|---|---|
| A1 | 8.705 | 13.00 | 10.02 |
| A2-I | 12.26 | 7.391 | 13.39 |
| A2-II | 5.796 | 3.268 | 6.661 |
| A3 | 11.06 | 6.904 | 12.29 |
| A4 | 5.636 | 5.182 | 5.520 |
| B1 | 9.139 | 4.421 | 8.873 |
| B2-II | 22.99 | 2.844 | 19.16 |
| B3 | 26.32 | 13.21 | 17.95 |
| B4 | 25.58 | 9.898 | 11.96 |
| C1 | 15.32 | 4.354 | 7.019 |
| C2 | 35.63 | 5.989 | 9.494 |
| C3 | 38.09 | 6.633 | 22.59 |
| C4 | 19.34 | 2.233 | 4.128 |

**Table B.9:** AAD for HEPO. (1) AAD between the experimental values and the model with 3 inputs and average rate. (2) AAD between the experimental values and the model with 10 inputs. (3) AAD between the experimental values and the model with 3 inputs with simultaneous rate.

| Experiment | AAD (1) | AAD (2) | AAD (3) |
|---|---|---|---|
| A1 | 0.037 | 0.010 | 0.050 |
| A2-I | 0.006 | 0.004 | 0.001 |
| A2-II | 0.013 | 0.005 | 0.007 |
| A3 | 0.009 | 0.008 | 0.002 |
| A4 | 0.011 | 0.005 | 0.005 |
| B1 | 0.015 | 0.013 | 0.013 |
| B2-II | 0.018 | 0.008 | 0.009 |
| B3 | 0.075 | 0.007 | 0.054 |
| B4 | 0.014 | 0.009 | 0.023 |
| C1 | 0.141 | 0.007 | 0.122 |
| C2 | 0.178 | 0.004 | 0.147 |
| C3 | 0.107 | 0.048 | 0.081 |
| C4 | 0.059 | 0.001 | 0.017 |

**Table B.10:** AARD for HEPO. (1) AARDD between the experimental values and the model with 3 inputs and average rate. (2) AARD between the experimental values and the model with 10 inputs. (3) AARD between the experimental values and the model with 3 inputs with simultaneous rate.

| Experiment | AARD (1) [%] | AARD (2) [%] | AARD (3) [%] |
|---|---|---|---|
| A1 | 22.6 | 6.31 | 30.7 |
| A2-I | 10.3 | 8.00 | 1.25 |
| A2-II | 21.0 | 8.69 | 11.9 |
| A3 | 11.5 | 9.51 | 2.63 |
| A4 | 14.3 | 6.33 | 6.63 |
| B1 | 5.08 | 4.39 | 4.43 |
| B2-II | 8.25 | 3.76 | 4.29 |
| B3 | 19.9 | 1.84 | 14.4 |
| B4 | 5.94 | 3.61 | 9.49 |
| C1 | 41.4 | 2.12 | 35.9 |
| C2 | 30.7 | 0.64 | 25.3 |
| C3 | 18.7 | 8.25 | 14.0 |
| C4 | 9.87 | 0.15 | 2.76 |

**Table B.11:** AAD for HEF. (1) AAD between the experimental values and the model with 3 inputs and average rate. (2) AAD between the experimental values and the model with 10 inputs. (3) AAD between the experimental values and the model with 3 inputs with simultaneous rate.

| Experiment | AAD (1) | AAD (2) | AAD (3) |
|---|---|---|---|
| A1 | 0.011 | 0.008 | 0.009 |
| A2-I | 0.003 | 0.006 | 0.004 |
| A2-II | 0.009 | 0.004 | 0.007 |
| A3 | 0.008 | 0.003 | 0.007 |
| A4 | 0.008 | 0.003 | 0.008 |
| B1 | 0.007 | 0.005 | 0.006 |
| B2-II | 0.005 | 0.002 | 0.002 |
| B3 | 0.024 | 0.003 | 0.009 |
| B4 | 0.023 | 0.002 | 0.005 |
| C1 | 0.004 | 0.010 | 0.006 |
| C2 | 0.010 | 0.005 | 0.009 |
| C3 | 0.023 | 0.003 | 0.020 |
| C4 | 0.052 | 0.022 | 0.034 |

**Table B.12:** AARD for HEF. (1) AARDD between the experimental values and the model with 3 inputs and average rate. (2) AARD between the experimental values and the model with 10 inputs. (3) AARD between the experimental values and the model with 3 inputs with simultaneous rate.

| Experiment | AARD (1) [%] | AARD (2) [%] | AARD (3) [%] |
|---|---|---|---|
| A1 | 31.61 | 25.28 | 26.48 |
| A2-I | 13.08 | 28.42 | 16.26 |
| A2-II | 22.49 | 9.982 | 18.10 |
| A3 | 10.49 | 4.218 | 8.450 |
| A4 | 9.811 | 3.160 | 9.321 |
| B1 | 25.60 | 16.24 | 23.05 |
| B2-II | 10.94 | 5.119 | 4.341 |
| B3 | 20.63 | 2.764 | 8.217 |
| B4 | 20.05 | 1.479 | 4.281 |
| C1 | 8.845 | 25.57 | 14.23 |
| C2 | 24.72 | 11.75 | 22.27 |
| C3 | 22.14 | 2.545 | 18.74 |
| C4 | 32.86 | 13.69 | 21.74 |

**Table B.13:** AAD for HEA. (1) AAD between the experimental values and the model with 3 inputs and average rate. (2) AAD between the experimental values and the model with 10 inputs. (3) AAD between the experimental values and the model with 3 inputs with simultaneous rate.

| Experiment | AAD (1) | AAD (2) | AAD (3) |
|---|---|---|---|
| A1 | 0.008 | 0.011 | 0.008 |
| A2-I | 0.016 | 0.017 | 0.016 |
| A2-II | 0.016 | 0.024 | 0.016 |
| A3 | 0.012 | 0.008 | 0.013 |
| A4 | 0.009 | 0.010 | 0.010 |
| B1 | 0.031 | 0.031 | 0.033 |
| B2-II | 0.025 | 0.013 | 0.021 |
| B3 | 0.064 | 0.013 | 0.059 |
| B4 | 0.016 | 0.025 | 0.032 |
| C1 | 0.053 | 0.083 | 0.032 |
| C2 | 0.098 | 0.050 | 0.077 |
| C3 | 0.032 | 0.023 | 0.066 |
| C4 | 0.016 | 0.018 | 0.074 |

**Table B.14:** AARD for HEA. (1) AARDD between the experimental values and the model with 3 inputs and average rate. (2) AARD between the experimental values and the model with 10 inputs. (3) AARD between the experimental values and the model with 3 inputs with simultaneous rate.

| Experiment | AARD (1) [%] | AARD (2) [%] | AARD (3) [%] |
|---|---|---|---|
| A1 | 5.05 | 7.08 | 5.18 |
| A2-I | 25.8 | 27.0 | 25.9 |
| A2-II | 23.2 | 34.1 | 23.4 |
| A3 | 12.3 | 8.55 | 12.6 |
| A4 | 5.77 | 6.76 | 6.61 |
| B1 | 10.4 | 10.4 | 11.0 |
| B2-II | 11.1 | 5.83 | 9.04 |
| B3 | 8.69 | 1.82 | 7.99 |
| B4 | 3.57 | 5.51 | 6.98 |
| C1 | 13.2 | 21.1 | 7.94 |
| C2 | 11.3 | 5.78 | 8.83 |
| C3 | 2.28 | 1.68 | 4.74 |
| C4 | 12.0 | 1.37 | 5.63 |

**Table B.15:** AAD for BHEOX. (1) AAD between the experimental values and the model with 3 inputs and average rate. (2) AAD between the experimental values and the model with 10 inputs. (3) AAD between the experimental values and the model with 3 inputs with simultaneous rate.

| Experiment | AAD (1) | AAD (2) | AAD (3) |
|---|---|---|---|
| A1 | 0.0010 | 0.0010 | 0.0010 |
| A2-I | 0.0001 | 0.0000 | 0.0001 |
| A2-II | 0.0002 | 0.0002 | 0.0002 |
| A3 | 0.0012 | 0.0002 | 0.0011 |
| A4 | 0.0005 | 0.0004 | 0.0006 |
| B1 | 0.0011 | 0.0003 | - |
| B2-II | 0.0008 | 0.0003 | 0.0008 |
| B3 | 0.0020 | 0.0012 | 0.0020 |
| B4 | 0.0020 | 0.0004 | 0.0002 |
| C1 | 0.0012 | 0.0002 | 0.0017 |
| C2 | 0.0013 | 0.0007 | 0.0011 |
| C3 | 0.0028 | 0.0013 | 0.0031 |
| C4 | 0.0044 | 0.0007 | 0.0056 |

**Table B.16:** AARD for BHEOX. (1) AARDD between the experimental values and the model with 3 inputs and average rate. (2) AARD between the experimental values and the model with 10 inputs. (3) AARD between the experimental values and the model with 3 inputs with simultaneous rate.

| Experiment | AARD (1) [%] | AARD (2) [%] | AARD (3) [%] |
|---|---|---|---|
| A1 | 62.97 | 65.15 | 64.15 |
| A2-I | 8.386 | 1.121 | 7.144 |
| A2-II | 11.40 | 11.39 | 10.28 |
| A3 | 34.19 | 6.884 | 32.29 |
| A4 | 10.97 | 7.645 | 13.02 |
| B1 | 181.9 | 47.37 | - |
| B2-II | 47.56 | 18.93 | 44.44 |
| B3 | 42.64 | 25.93 | 42.61 |
| B4 | 29.78 | 6.599 | 2.974 |
| C1 | 166.1 | 20.18 | 234.7 |
| C2 | 63.16 | 34.63 | 53.78 |
| C3 | 73.57 | 33.82 | 81.93 |
| C4 | 79.23 | 11.70 | 100.3 |

**Table B.17:** AAD for HEI. (1) AAD between the experimental values and the model with 3 inputs and average rate. (2) AAD between the experimental values and the model with 10 inputs. (3) AAD between the experimental values and the model with 3 inputs with simultaneous rate.

| Experiment | AAD (1) | AAD (2) | AAD (3) |
|---|---|---|---|
| A1 | 0.0013 | 0.0023 | 0.0009 |
| A2-I | 0.0004 | 0.0007 | 0.0006 |
| A2-II | 0.0003 | 0.0004 | 0.0004 |
| A3 | 0.0012 | 0.0007 | 0.0011 |
| A4 | 0.0004 | 0.0003 | 0.0004 |
| B1 | 0.0014 | 0.0045 | 0.0011 |
| B2-II | 0.0025 | 0.0018 | 0.0016 |
| B3 | 0.0030 | 0.0010 | 0.0021 |
| B4 | 0.0067 | 0.0006 | 0.0018 |
| C1 | 0.0028 | 0.0012 | 0.0018 |
| C2 | 0.0049 | 0.0056 | 0.0027 |
| C3 | 0.0065 | 0.0011 | 0.0015 |
| C4 | 0.0278 | 0.0004 | 0.0088 |

**Table B.18:** AARD for HEI. (1) AARDD between the experimental values and the model with 3 inputs and average rate. (2) AARD between the experimental values and the model with 10 inputs. (3) AARD between the experimental values and the model with 3 inputs with simultaneous rate.

| Experiment | AARD (1) [%] | AARD (2) [%] | AARD (3) [%] |
|---|---|---|---|
| A1 | 49.91 | 91.54 | 37.24 |
| A2-I | 19.59 | 30.42 | 25.74 |
| A2-II | 16.83 | 24.55 | 22.61 |
| A3 | 27.47 | 15.49 | 23.93 |
| A4 | 4.887 | 3.798 | 4.754 |
| B1 | 17.31 | 57.14 | 13.44 |
| B2-II | 15.48 | 11.35 | 9.824 |
| B3 | 10.41 | 3.438 | 7.412 |
| B4 | 12.45 | 1.110 | 3.404 |
| C1 | 12.16 | 5.084 | 7.948 |
| C2 | 21.33 | 2.427 | 11.90 |
| C3 | 14.47 | 2.587 | 3.284 |
| C4 | 24.21 | 0.368 | 7.677 |

# B Thermal degradation

**Table B.19:** AAD for MEA. (1) AAD between the experimental values and the ML model with 3 inputs. (2) AAD between the experimental values and the model with 6 inputs.

| Experiment | AAD (1) | AAD 6 (2) |
|---|---|---|
| E1 | 0.38 | - |
| E2 | 0.18 | - |
| E3 | 0.57 | - |
| E4 | 0.39 | 0.10 |
| E5 | 0.20 | 0.14 |
| E6 | 0.09 | 0.17 |
| E7 | 0.47 | 0.17 |
| E8 | 0.29 | 0.18 |
| E9 | 0.20 | 0.21 |
| F1 | 0.24 | 0.36 |
| F2 | 0.18 | - |
| F3 | 0.10 | - |
| F4 | 0.13 | 0.10 |
| F5 | 0.12 | 0.12 |
| F6 | 0.11 | 0.09 |
| F7 | 0.17 | 0.06 |
| F8 | 0.04 | 0.06 |
| F9 | 0.37 | 0.23 |

**Table B.20:** AARD for MEA. (1) AARD between the experimental values and the ML model with 3 inputs. (2) AARD between the experimental values and the model with 6 inputs.

| Experiment | AARD (1) [%] | AARD (2) [%] |
|---|---|---|
| E1 | 5.7 | - |
| E2 | 2.7 | - |
| E3 | 8.7 | - |
| E4 | 7.7 | 2.0 |
| E5 | 4.1 | 2.8 |
| E6 | 1.9 | 3.4 |
| E7 | 14.4 | 5.1 |
| E8 | 9.1 | 5.7 |
| E9 | 6.3 | 6.7 |
| F1 | 3.7 | 5.4 |
| F2 | 2.8 | - |
| F3 | 1.6 | - |
| F4 | 2.7 | 2.1 |
| F5 | 2.4 | 2.4 |
| F6 | 2.1 | 1.8 |
| F7 | 6.0 | 2.0 |
| F8 | 1.3 | 2.1 |
| F9 | 12.0 | 7.5 |

**Table B.21:** AAD for HEIA. (1) AAD between the experimental values and the ML model with 3 inputs. (2) AAD between the experimental values and the model with 6 inputs.

| Experiment | AAD (1) | AAD (2) |
|---|---|---|
| E1 | 0.02 | - |
| E2 | 0.04 | - |
| E4 | 0.01 | 0.01 |
| E5 | 0.01 | 0.01 |
| E6 | 0.01 | 0.01 |
| E7 | 0.01 | 0.01 |
| E8 | 0.01 | 0.01 |
| E9 | 0.01 | 0.01 |
| F1 | 0.07 | 0.01 |
| F4 | 0.01 | 0.01 |
| F5 | 0.03 | 0.02 |
| F6 | 0.04 | 0.01 |
| F7 | 0.03 | 0.04 |
| F8 | 0.04 | 0.04 |
| F9 | 0.06 | 0.07 |

**Table B.22:** AARD for HEIA. (1) AARD between the experimental values and the ML model with 3 inputs. (2) AARD between the experimental values and the model with 6 inputs.

| Experiment | AARD (1)[%] | AARD (2)[%] |
|---|---|---|
| E1 | 16.6 | - |
| E2 | 13.3 | - |
| E4 | 8.82 | 11.1 |
| E5 | 6.28 | 4.28 |
| E6 | 4.45 | 3.29 |
| E7 | 17.3 | 15.6 |
| E8 | 12.3 | 13.6 |
| E9 | 9.60 | 5.03 |
| F1 | 31.4 | 3.82 |
| F4 | 6.58 | 6.32 |
| F5 | 7.93 | 5.44 |
| F6 | 8.61 | 2.74 |
| F7 | 30.0 | 39.8 |
| F8 | 20.4 | 19.4 |
| F9 | 17.0 | 17.9 |

**Table B.23:** AAD for HEEDA. (1) AAD between the experimental values and the ML model with 3 inputs. (2) AAD between the experimental values and the model with 6 inputs.

| Experiment | AARD (1) | AAD (2) |
|---|---|---|
| E4 | 0.03 | 0.01 |
| E5 | 0.01 | 0.01 |
| E6 | 0.01 | 0.01 |
| E7 | 0.10 | 0.04 |
| E8 | 0.02 | 0.02 |
| E9 | 0.03 | 0.02 |
| F1 | 0.01 | 0.02 |
| F2 | 0.02 | - |
| F3 | 0.05 | - |
| F4 | 0.04 | 0.02 |
| F5 | 0.07 | 0.02 |
| F6 | 0.04 | 0.02 |
| F7 | 0.02 | 0.02 |
| F8 | 0.02 | 0.02 |
| F9 | 0.04 | 0.01 |

**Table B.24:** AARD for HEEDA. (1) AARD between the experimental values and the ML model with 3 inputs. (2) AARD between the experimental values and the model with 6 inputs.

| Experiment | AARD (1) [%] | AARD (2) [%] |
|---|---|---|
| E4 | 81.2 | 16.8 |
| E5 | 7.04 | 9.30 |
| E6 | 7.69 | 7.17 |
| E7 | - | - |
| E8 | 20.1 | 22.3 |
| E9 | 28.6 | 17.6 |
| F1 | 5.99 | 8.69 |
| F2 | 12.1 | - |
| F3 | 29.9 | - |
| F4 | 25.4 | 13.1 |
| F5 | 44.1 | 12.8 |
| F6 | 33.6 | 19.7 |
| F7 | 28.5 | 27.8 |
| F8 | 21.5 | 21.8 |
| F9 | 58.9 | 20.2 |

**Table B.25:** AAD for TriHEIA. (1) AAD between the experimental values and the ML model with 3 inputs. (2) AAD between the experimental values and the model with 6 inputs.

| Experiment | AAD (1) | AAD (2) |
|---|---|---|
| E1 | 0.00 | - |
| E2 | 0.00 | - |
| E3 | 0.01 | - |
| E4 | 0.00 | 0.01 |
| E5 | 0.01 | 0.00 |
| E6 | 0.01 | 0.00 |
| E7 | 0.00 | 0.00 |
| E8 | 0.01 | 0.00 |
| E9 | 0.00 | 0.01 |
| F1 | 0.01 | 0.00 |
| F2 | 0.02 | - |
| F3 | 0.04 | - |
| F4 | 0.01 | 0.00 |
| F5 | 0.01 | 0.00 |
| F6 | 0.01 | 0.00 |
| F7 | 0.01 | 0.00 |
| F8 | 0.02 | 0.00 |
| F9 | 0.03 | 0.01 |

**Table B.26:** AARD for TriHEIA. (1) AARD between the experimental values and the ML model with 3 inputs. (2) AARD between the experimental values and the model with 6 inputs.

| Experiment | AARD (1) [%] | AARD (2) [%] |
|---|---|---|
| E1 | 29.0 | - |
| E2 | 12.7 | - |
| E3 | 15.3 | - |
| E4 | - | - |
| E5 | 37.7 | 7.68 |
| E6 | 36.2 | 7.50 |
| E7 | - | - |
| E8 | - | - |
| E9 | - | - |
| F1 | 74.1 | 11.0 |
| F2 | 14.8 | - |
| F3 | 20.1 | - |
| F4 | - | - |
| F5 | 15.1 | 7.99 |
| F6 | 9.76 | 1.36 |
| F7 | - | - |
| F8 | 110 | 8.37 |
| F9 | 67.4 | 10.0 |

# C MATLAB code

In this chapter, some example code from the modelling in MATLAB is given.

## A MATLAB code oxidative degradation

### A.1 Example: HEPO 3 input model data file

```
clear
clc
close all

DOT = [

5.560000000 6 328.15
5.711823131 6 328.15
5.465229927 6 328.15
5.341912612 6 328.15
5.052484218 6 328.15
4.963055823 6 328.15
4.631034815 6 328.15
4.712075773 6 328.15

4.95        21  328.15
4.948427315 21  328.15
4.925410918 21  328.15
4.830016762 21  328.15
4.774658871 21  328.15
4.716091961 21  328.15
4.576204533 21  328.15
4.472071886 21  328.15

4.875       21  328.15
4.737944046 21  328.15
4.692972306 21  328.15
4.626608838 21  328.15
4.548468095 21  328.15
4.448673133 21  328.15

4.87        49  328.15
4.56647853  49  328.15
4.539215368 49  328.15
```

```
4.479785934 49  328.15
4.313389169 49  328.15
4.263836337 49  328.15

4.817       98  328.15
4.55720619  98  328.15
4.311055911 98  328.15
4.167074428 98  328.15
3.991948363 98  328.15
3.859212836 98  328.15

5.37        6 338.15
4.911035228 6 338.15
4.863074058 6 338.15
4.716951419 6 338.15
4.974640781 6 338.15
4.690677151 6 338.15
4.446093649 6 338.15
4.492912239 6 338.15

4.775       21  338.15
4.651566177 21  338.15
4.498363888 21  338.15
4.334036235 21  338.15
4.249692067 21  338.15
4.142513473 21  338.15
3.955865155 21  338.15
3.753967639 21  338.15

5.26        49  338.15
4.506904135 49  338.15
4.470774185 49  338.15
3.980779552 49  338.15
3.555425284 49  338.15
3.337613545 49  338.15
2.651222746 49  338.15

4.798       98  338.15
4.405681764 98  338.15
3.896320554 98  338.15
3.606477896 98  338.15
3.373334889 98  338.15
3.022642215 98  338.15
2.714667974 98  338.15
```

```
2.387096959 98  338.15

5.27        6 348.15
5.2879338 6 348.15
4.974793126 6 348.15
4.769646356 6 348.15
4.97394122  6 348.15
4.870772163 6 348.15
4.526150579 6 348.15
4.238312461 6 348.15
4.069101956 6 348.15
4.139477397 6 348.15
3.968698224 6 348.15

4.944       21  348.15
4.690061157 21  348.15
4.196898229 21  348.15
3.836553249 21  348.15
3.499202912 21  348.15
3.0930167 21  348.15
2.824493483 21  348.15
2.362609886 21  348.15

5.06        49  348.15
5.428108647 49  348.15
4.165642573 49  348.15
3.434605249 49  348.15
3.129162546 49  348.15
3.139614905 49  348.15
2.045924558 49  348.15

4.62        98  348.15
4.69620739  98  348.15
3.041796127 98  348.15
2.276859458 98  348.15
1.896128731 98  348.15
1.704424298 98  348.15
1.601117644 98  348.15
1.693475041 98  348.15

];
```

```
123
124 rHEPO = [
125
126 0
127 5.4500E-04
128 1.3625E-03
129 3.1143E-03
130 2.6471E-03
131 7.4743E-03
132 9.1871E-03
133 6.0729E-03
134
135
136 0.0000E+00
137 1.3015E-03
138 1.6010E-03
139 2.5832E-03
140 3.2332E-03
141 3.9625E-03
142 5.4721E-03
143 8.8939E-03
144
145
146 0.0000E+00
147 6.2460E-03
148 3.9194E-03
149 4.0720E-03
150 5.9992E-03
151 7.2398E-03
152
153
154 0.0000E+00
155 6.2479E-03
156 4.8167E-03
157 6.1967E-03
158 7.8763E-03
159 4.9998E-03
160
161
162 0.0000E+00
163 6.9940E-03
164 4.3770E-03
165 6.8378E-03
166 4.1261E-03
```

```
6.1547E-03


0.0000E+00
2.1800E-03
5.4500E-03
9.8100E-03
9.1871E-03
9.4986E-03
9.8100E-03
1.1367E-02


0.0000E+00
7.0850E-03
1.0426E-02
1.6350E-02
1.5260E-02
1.4533E-02
1.5805E-02
1.3824E-02


4.3600E-03
1.4715E-02
2.7523E-02
2.8703E-02
1.7985E-02
1.0744E-02
-8.0971E-03


0.0000E+00
1.8530E-02
1.4217E-02
2.6569E-02
2.2176E-02
1.5260E-02
4.5195E-03
2.6585E-04


3.6333E-03
5.1905E-03
```

```
8.5879E-03
1.0173E-02
7.5826E-03
1.2403E-02
1.1160E-02
1.2535E-02
1.2068E-02
1.6627E-02
1.7258E-02


1.2974E-02
5.4801E-02
7.4791E-02
5.8104E-02
4.5633E-02
2.5921E-02
1.4741E-03
-4.6728E-03


1.5260E-02
5.8315E-02
5.7225E-02
-1.4533E-03
5.4773E-02
-3.3634E-02
-3.1143E-04


2.4222E-02
7.0071E-02
5.6103E-02
2.5006E-02
1.3625E-02
2.1800E-02
2.5693E-02
9.2650E-03

];
```

## A.2 Example: HEPO 10 input model data file

```
clear
clc
close all


Input = [


5.560000000 6 328.15  0.000000000 0.001167320 2.675430E-05
   0.0000000000  0.0000671596  0.0000000000  0.0000000000
5.711823131 6 328.15  0.000000000 0.002559941 1.248930E-04
   0.0000000000  0.0001175670  0.0000000000  0.0000000000
5.465229927 6 328.15  0.000680503 0.005370319 2.856530E-04
   0.0000000000  0.0006050160  0.0109000000  0.0010900000
5.341912612 6 328.15  0.003139448 0.010990578 6.256630E-04
   0.0007168170  0.0023474270  0.0185300000  0.0065400000
5.052484218 6 328.15  0.009611549 0.018399819 1.200369E-03
   0.0010491140  0.0065098750  0.0468700000  0.0283400000
4.963055823 6 328.15  0.014842849 0.026519892 1.598068E-03
   0.0015486010  0.0095921610  0.0850200000  0.0468700000
4.631034815 6 328.15  0.025515765 0.028028314 2.078502E-03
   0.0012141410  0.0125694890  0.1122700000  0.0991900000
4.712075773 6 328.15  0.035207176 0.033447441 2.524977E-03
   0.0014406820  0.0152543180  0.1613200000  0.1635000000

4.95        21  328.15  0.000000000 0.001851997 0.000178362
   0.0000340580  0.0000839496  0.0000000000  0.0000000000
5.020220179 21  328.15  0.000000000 0.00178473  0.000160533
   0.0000283829  0.0000755579  0.0011554000  0.0000000000
4.948427315 21  328.15  0.000000000 0.005171952 0.000384133
   0.0001990110  0.0004456920  0.0024198000  0.0000000000
4.925410918 21  328.15  0.000000000 0.009195184 0.000672327
   0.0005078140  0.0015442440  0.0069869000  0.0027250000
4.830016762 21  328.15  0.000000000 0.011668854 0.000827321
   0.0007555360  0.0028527350  0.0128838000  0.0057770000
4.774658871 21  328.15  0.000000000 0.014033799 0.001226909
   0.0010163460  0.0039148910  0.0197290000  0.0107910000
4.716091961 21  328.15  0.000000000 0.016564843 0.001504684
   0.0012404260  0.0053328910  0.0309996000  0.0201650000
4.576204533 21  328.15  0.021625775 0.018791558 0.001803706
   0.0014205660  0.0063456700  0.0449407000  0.0322640000
```

```
26 4.472071886 21  328.15  0.024610715 0.021589855 0.002227916
       0.0015989620  0.0071806080  0.0626968000  0.0539550000
27
28 4.875 21  328.15  0.000000000 0.000325503 5.35E-05  0.0000000000
       0.0000000000  0.0015478000  0.0000000000
29 4.884367008 21  328.15  0.000000000 0.00467921  0.000303861
       0.0002104710  0.0003112740  0.0037060000  0.0000000000
30 4.784768453 21  328.15  0.001464546 0.011321236 0.000717463
       0.0004509530  0.0009033140  0.0081750000  0.0000000000
31 4.737944046 21  328.15  0.003355889 0.016008308 0.000765136
       0.0006417010  0.0018302860  0.0134070000  0.0000000000
32 4.692972306 21  328.15  0.005187114 0.022311813 0.001192687
       0.0010581940  0.0029003620  0.0240890000  0.0125350000
33 4.626608838 21  328.15  0.009688289 0.027709017 0.001299333
       0.0012492030  0.0043706960  0.0366567000  0.0243070000
34 4.548468095 21  328.15  0.014359781 0.031770166 0.001443485
       0.0012967470  0.0057104280  0.0489083000  0.0362970000
35 4.448673133 21  328.15  0.022750730 0.038750445 0.001832231
       0.0015061050  0.0070636630  0.0703486000  0.0615850000
36
37 4.87  49  328.15  0.000000000 0.000538763 0 0.0000000000
       0.0000000000  0.0000000000  0.0000000000
38 4.914460858 49  328.15  0.000000000 0.008852726 0.000499868
       0.0005170160  0.0001596490  0.0039948500  0.0000000000
39 4.632419663 49  328.15  0.004658231 0.024365776 0.001189298
       0.0011838520  0.0009595980  0.0104727200  0.0000000000
40 4.56647853  49  328.15  0.006273717 0.034143841 0.001593174
       0.0016634930  0.0018030270  0.0158235300  0.0000000000
41 4.539215368 49  328.15  0.014272319 0.050486006 0.002423489
       0.0024509230  0.0037599550  0.0330052000  0.0187436400
42 4.479785934 49  328.15  0.021596268 0.058413341 0.002888367
       0.0027662380  0.0049211750  0.0483883700  0.0331937700
43 4.313389169 49  328.15  0.036498834 0.069041742 0.003955089
       0.0030576570  0.0065281280  0.0742159200  0.0579803700
44 4.263836337 49  328.15  0.049114278 0.078088735 0.004517778
       0.0035209550  0.0072612140  0.0994614100  0.0816093900
45
46 4.817 98  328.15  0.000000000 0.001459149 0 0.0000000000
       0.0000923445  0.0181724800  0.0000000000
47 4.709764828 98  328.15  0.001652208 0.013356282 0.000794347
       0.0006248960  0.0004032800  0.0185387200  0.0000000000
48 4.579582871 98  328.15  0.006131649 0.028350565 0.002189999
       0.0016101240  0.0014472770  0.0261719900  0.0000000000
49 4.55720619  98  328.15  0.008912293 0.033451455 0.002746423
```

```
    0.0020441770  0.0019537200  0.0363482300  0.0000000000
50 4.311055911 98  328.15  0.019774405 0.051583293 0.004619679
    0.0033686160  0.0037913700  0.0669587000  0.0244301700
51 4.167074428 98  328.15  0.029152302 0.055753351 0.00504187
    0.0035180250  0.0040777550  0.0680487000  0.0351753900
52 3.991948363 98  328.15  0.047633520 0.075498269 0.007266176
    0.0046535750  0.0062289120  0.1196351300  0.0625736300
53 3.859212836 98  328.15  0.065180119 0.08330043  0.008224628
    0.0048782680  0.0067467300  0.1508309300  0.0762128000
54
55 5.37  6 338.15  0.000000000 0.000987732 2.68E-05  0.0000000000
    0.0000419748  0.0000000000  0.0000000000
56 4.911035228 6 338.15  0.000000000 0.003962987 0.00042816
    0.0000000000  0.0005122000  0.0119900000  0.0000000000
57 4.863074058 6 338.15  0.001991993 0.007603608 0.001481343
    0.0000000000  0.0025200800  0.0218000000  0.0043600000
58 4.716951419 6 338.15  0.007074489 0.014669234 0.00335816
    0.0000000000  0.0092901160  0.0566800000  0.0261600000
59 4.974640781 6 338.15  0.014167669 0.020139413 0.005330886
    0.0000000000  0.0212766710  0.1318900000  0.0948300000
60 4.690677151 6 338.15  0.026593320 0.020687649 0.006413643
    0.0000000000  0.0294787090  0.1667700000  0.1591400000
61 4.446093649 6 338.15  0.032193193 0.025956834 0.007741769
    0.0000000000  0.0330433870  0.2354400000  0.2256300000
62 4.492912239 6 338.15  0.062638069 0.028075417 0.007833983
    0.0006175680  0.0339629310  0.2964800000  0.2943000000
63
64 4.775 21  338.15  0.000000000 0.000112242 0 0.0000000000
    0.0000000000  0.0000000000  0.0000000000
65 4.651566177 21  338.15  0.002340968 0.006600521 0.001843104
    0.0001473490  0.0010393130  0.0130800000  0.0000000000
66 4.498363888 21  338.15  0.008552750 0.015929131 0.005848906
    0.0010224990  0.0038766140  0.0414200000  0.0141700000
67 4.334036235 21  338.15  0.015387731 0.024773839 0.009116822
    0.0014183400  0.0070920160  0.0708500000  0.0381500000
68 4.249692067 21  338.15  0.037208405 0.029849656 0.011069013
    0.0014146880  0.0090912710  0.0904700000  0.0643100000
69 4.142513473 21  338.15  0.037809127 0.035913554 0.013455512
    0.0016983480  0.0122200100  0.1318900000  0.1100900000
70 3.955865155 21  338.15  0.054237290 0.040410995 0.014778864
    0.0016789690  0.0145121150  0.1744000000  0.1536900000
71 3.753967639 21  338.15  0.079352092 0.046067145 0.016157756
    0.0013697710  0.0163208270  0.2278100000  0.2169100000
72
```

```
73 5.26  49  338.15  0.000000000 0.000729575 4.46E-05  0.0000170290
      0.0000419748  0.0054500000  0.0000000000
74 4.506904135 49  338.15  0.006615347 0.026706538 0.003270701
      0.0014918510  0.0014261630  0.0207100000  0.0043600000
75 4.470774185 49  338.15  0.026190101 0.052578019 0.008962048
      0.0031438780  0.0052779300  0.0784800000  0.0337900000
76 3.980779552 49  338.15  0.073265974 0.082179843 0.016144102
      0.0041803040  0.0101425040  0.2147300000  0.1438800000
77 3.555425284 49  338.15  0.000000000 0.096411945 0.020592286
      0.0046621050  0.0113220920  0.3433500000  0.2299900000
78 3.337613545 49  338.15  0.193603882 0.108328919 0.024509937
      0.0044580750  0.0113822460  0.4915900000  0.3019300000
79 2.651222746 49  338.15  0.245713982 0.115392159 0.028917644
      0.0041958820  0.0108057640  0.7335700000  0.3771400000
80
81 4.798 98  338.15  0.000000000 0.000123466 0 0.0000000000
      0.0000000000  0.0000000000  0.0000000000
82 4.405681764 98  338.15  0.004653673 0.023913146 0.005704446
      0.0018295870  0.0011979450  0.0163500000  0.0000000000
83 3.896320554 98  338.15  0.028780374 0.058827431 0.019158696
      0.0038674840  0.0037603760  0.0773900000  0.0370600000
84 3.606477896 98  338.15  0.055686743 0.076957314 0.027256169
      0.0051977960  0.0061696820  0.1438800000  0.0697600000
85 3.373334889 98  338.15  0.082330280 0.086042401 0.035489743
      0.0046138850  0.0055762320  0.1951100000  0.1122700000
86 3.022642215 98  338.15  0.136031584 0.101637866 0.044142745
      0.0053419660  0.0064319290  0.2779500000  0.1765800000
87 2.714667974 98  338.15  0.190521427 0.110543766 0.049440438
      0.0050832180  0.0066625530  0.3640600000  0.2223600000
88 2.387096959 98  338.15  0.228195067 0.11359935  0.053636501
      0.0048147350  0.0068384530  0.4599800000  0.2408900000
89
90 5.27  6 348.15  0.000000000 0.001762204 0.000160526 0.0000567634
      0.0000419748  0.0032700000  0.0000000000
91 5.2879338 6 348.15  0.001727214 0.004698776 0.001250412 0.0001193820
      0.0016983290  0.0109000000  0.0032700000
92 4.974793126 6 348.15  0.007389358 0.009204843 0.005297005
      0.0002453050  0.0102678330  0.0348800000  0.0141700000
93 4.769646356 6 348.15  0.017186234 0.015289402 0.010796278
      0.0003785790  0.0279438440  0.0763000000  0.0425100000
94 4.97394122  6 348.15  0.024549150 0.017317112 0.012638919
      0.0003680160  0.0366279330  0.0915600000  0.0577700000
95 4.870772163 6 348.15  0.027835989 0.019368704 0.013838528
      0.0003751830  0.0425886800  0.1079100000  0.0752100000
```

```
96  4.526150579 6 348.15  0.040684708 0.022304952 0.01656503
        0.0004929610  0.0542248230  0.1613200000  0.1111800000
97  4.238312461 6 348.15  0.058853583 0.02856616  0.018999795
        0.0005722550  0.0619548780  0.2147300000  0.1580500000
98  4.069101956 6 348.15  0.080063623 0.031285096 0.02005575
        0.0006171110  0.0645127190  0.2637800000  0.2081900000
99  4.139477397 6 348.15  0.098401549 0.03574572  0.021491243
        0.0006671280  0.0675194400  0.3215500000  0.2419800000
100 3.968698224 6 348.15  0.134400736 0.040338486 0.023118009
        0.0007449620  0.0682646830  0.3978500000  0.3400800000
101
102 4.944 21  348.15  0.000000000 0.000325503 0 0.0000000000
        0.0000000000  0.0000000000  0.0000000000
103 4.690061157 21  348.15  0.013281985 0.014537159 0.003434418
        0.0008883610  0.0028045260  0.0372322200  0.0123802200
104 4.196898229 21  348.15  0.043611634 0.027905986 0.010699939
        0.0018113740  0.0114955820  0.1676975900  0.1198117100
105 3.836553249 21  348.15  0.084608760 0.032382334 0.014696422
        0.0020773510  0.0147639920  0.3057537200  0.2689749400
106 3.499202912 21  348.15  0.131368185 0.034062035 0.016939144
        0.0020153040  0.0154780480  0.4164355900  0.3822771700
107 3.0930167 21  348.15  0.193529959 0.037686142 0.020461174
        0.0020589730  0.0141670720  0.6028288600  0.5209208100
108 2.824493483 21  348.15  0.231152006 0.039631362 0.022839995
        0.0020314080  0.0137465540  0.7213609100  0.5739863700
109 2.362609886 21  348.15  0.317002761 0.038941214 0.022911482
        0.0017821280  0.0104450210  0.8719389600  0.5813068100
110
111 5.06  49  348.15  0.000000000 0.000561211 3.37E-05  0.0000113527
        0.0000167899  0.0000000000  0.0000000000
112 5.428108647 49  348.15  0.009434389 0.024168562 0.005419413
        0.0013391490  0.0041540550  0.0425100000  0.0152600000
113 4.165642573 49  348.15  0.039496290 0.050893527 0.016975721
        0.0024609550  0.0132921000  0.1863900000  0.1318900000
114 3.434605249 49  348.15  0.117476598 0.077818173 0.028731141
        0.0032332850  0.0167908450  0.5112100000  0.3607900000
115 3.129162546 49  348.15  0.210658429 0.095263758 0.035233162
        0.0038294940  0.0129668570  0.7117700000  0.3564300000
116 3.139614905 49  348.15  0.000000000 0.093712041 0.042779156
        0.0032875170  0.0158475720  1.0322300000  0.5755200000
117 2.045924558 49  348.15  0.000000000 0.105605064 0.045181318
        0.0030540700  0.0108002800  1.3875700000  0.3400800000
118
119 4.62  98  348.15  0.000937345 0.001784652 0.000224485 0.0000624397
```

```
    0.0000839496   0.0043600000   0.0000000000
4.69620739   98   348.15   0.022051269 0.074199559 0.034610012
    0.0036129080   0.0048735330   0.0817500000   0.0218000000
3.041796127 98   348.15   0.172964598 0.146832164 0.084022431
    0.0055591680   0.0110850240   0.3477100000   0.1689500000
2.276859458 98   348.15   0.000000000 0.157442729 0.103384565
    0.0044980790   0.0117188830   0.6649000000   0.3597000000
1.896128731 98   348.15   0.482465869 0.154192835 0.103471215
    0.0037811600   0.0127843360   0.7848000000   0.4022100000
1.704424298 98   348.15   0.000000000 0.145383293 0.104696881
    0.0036843310   0.0129858550   0.9232300000   0.4294600000
1.601117644 98   348.15   0.000000000 0.141684896 0.106773968
    0.0030743750   0.0135823620   1.0801900000   0.4926800000
1.693475041 98   348.15   0.587886570 0.140393582 0.114854416
    0.0028949970   0.0163160820   1.3123600000   0.6005900000



];

Output = [


0.0000000000
0.0005450000
0.0013625000
0.0031142857
0.0026471429
0.0074742857
0.0091871429
0.0060728571

0.0000000000
0.0000000000
0.0013015236
0.0016010072
0.0025832045
0.0032331942
0.0039624681
0.0054721360
0.0088938779

0.0000000000
0.0000000000
```

```
0.0000000000
0.0062459515
0.0039194273
0.0040719986
0.0059992408
0.0072397679

0.0000000000
0.0000000000
0.0000000000
0.0062478800
0.0048167100
0.0061966500
0.0078763400
0.0049998300

0.0000000000
0.0000000000
0.0000000000
0.0069940366
0.0043770500
0.0068377649
0.0041260800
0.0061546622

0.0000000000
0.0021800000
0.0054500000
0.0098100000
0.0091871429
0.0094985714
0.0098100000
0.0113671429

0.0000000000
0.0070850000
0.0104260870
0.0163500000
0.0152600000
0.0145333333
0.0158050000
0.0138243902

0.0043600000
```

```
0.0147150000
0.0275225000
0.0287033333
0.0179850000
0.0107442857
-0.0080971429

0.0000000000
0.0185300000
0.0142173913
0.0265687500
0.0221758621
0.0152600000
0.0045195122
0.0002658537

0.0036333333
0.0051904762
0.0085878788
0.0101733333
0.0075826087
0.0124034483
0.0111595238
0.0125350000
0.0120678571
0.0166271186
0.0172583333

0.0129744498
0.0548008009
0.0747910299
0.0581037077
0.0456334804
0.0259210434
0.0014741120
-0.0046728307

0.0152600000
0.0583150000
0.0572250000
-0.0014533333
0.0547725000
-0.0336342857
-0.0003114286
```

```
244
245 0.0242222222
246 0.0700714286
247 0.0561029412
248 0.0250058824
249 0.0136250000
250 0.0218000000
251 0.0256928571
252 0.0092650000
253
254 ];
```

### A.3 Example: HEPO machine learning model

```
1  function [y1] = myNeuralNetworkFunction(x1)
2  %MYNEURALNETWORKFUNCTION neural network simulation function.
3  %
4  % Auto-generated by MATLAB, 21-Apr-2021 09:25:18.
5  %
6  % [y1] = myNeuralNetworkFunction(x1) takes these arguments:
7  %   x = Qx10 matrix, input #1
8  % and returns:
9  %   y = Qx1 matrix, output #1
10 % where Q is the number of samples.
11
12 %#ok<*RPMT0>
13
14 % ===== NEURAL NETWORK CONSTANTS =====
15
16 % Input 1
17 x1_step1.xoffset = [1.601117644;6;328.15;0;0.000112242;0;0;0;0;0];
18 x1_step1.gain =
       [0.486534490569793;0.0217391304347826;0.1;3.40201682103403;
19 12.7120943825719;17.4133487388069;359.766065713431;29.2977263221159;
20 1.44136872374006;3.33005877553739];
21 x1_step1.ymin = -1;
22
23 % Layer 1
24 b1 =
       [-0.47872977914236120034;1.2786511101914832533;-1.4971016117307271998];

25 IW1_1 = [0.94312394416852174395 -0.11206548441644094416
       0.93660825264448477334 1.1552573135201360532
```

```
    0.38025026570939007842 0.43469722227676665938
    0.003592139700887845 8608 -0.66351598580508719394
    0.64149606969172934257
    -0.69253155682261591242;-0.70454721456875890606
    -0.81997983357239812019 -3.079652332314779084
    -2.9685322158861500164 -1.352191162043323347
    1.8328410582875043211 -2.2127753394987017543
    -0.38577084088525881445 -1.8441903839229920603
    0.040932223018159220873;1.185659753415429174
    -0.13202324897596046105 0.83415606577463041749
    1.4506475481156042573 -0.027705190520301407192
    1.5835386691143724658 -0.643797560743477714 77
    -0.46884830722346726439 0.761423739037676905 46
    -2.0915975087964815415];

% Layer 2
b2 = -2.084601385894188752;
LW2_1 = [2.7470944772556880054 1.0168490111870966963
    -3.4723638174334068296];

% Output 1
y1_step1.ymin = -1;
y1_step1.gain = 18.4458766749488;
y1_step1.xoffset = -0.0336342857;

% ======= SIMULATION ========

% Dimensions
Q = size(x1,1); % samples

% Input 1
x1 = x1';
xp1 = mapminmax_apply(x1,x1_step1);

% Layer 1
a1 = tansig_apply(repmat(b1,1,Q) + IW1_1*xp1);

% Layer 2
a2 = repmat(b2,1,Q) + LW2_1*a1;

% Output 1
y1 = mapminmax_reverse(a2,y1_step1);
y1 = y1';
end
```

```
55
56 % ====== MODULE FUNCTIONS ========
57
58 % Map Minimum and Maximum Input Processing Function
59 function y = mapminmax_apply(x,settings)
60 y = bsxfun(@minus,x,settings.xoffset);
61 y = bsxfun(@times,y,settings.gain);
62 y = bsxfun(@plus,y,settings.ymin);
63 end
64
65 % Sigmoid Symmetric Transfer Function
66 function a = tansig_apply(n,~)
67 a = 2 ./ (1 + exp(-2*n)) - 1;
68 end
69
70 % Map Minimum and Maximum Output Reverse-Processing Function
71 function x = mapminmax_reverse(y,settings)
72 x = bsxfun(@minus,y,settings.ymin);
73 x = bsxfun(@rdivide,x,settings.gain);
74 x = bsxfun(@plus,x,settings.xoffset);
75 end
```

## A.4 Example: Obtaining modelled rates 3-input model

```
1 clear
2 clc
3 close all
4 %% Experiment #1, A1
5
6 %Inputs [Time [days], O2-concentration [%], Temperature [K] ]
7 X1 = [
8 5.560000000 6 328.15
9 5.711823131 6 328.15
10 5.465229927 6 328.15
11 5.341912612 6 328.15
12 5.052484218 6 328.15
13 4.963055823 6 328.15
14 4.631034815 6 328.15
15 4.712075773 6 328.15
16
17 ];
18
19 %Output: rHEF [kg/kmol]?
```

```
Y1 = [
0
5.4500E-04
1.3625E-03
3.1143E-03
2.6471E-03
7.4743E-03
9.1871E-03
6.0729E-03

];


%% Experiment #2, A2-I

 X2 = [
4.95          21   328.15
5.020220179   21   328.15
4.948427315   21   328.15
4.925410918   21   328.15
4.830016762   21   328.15
4.774658871   21   328.15
4.716091961   21   328.15
4.576204533   21   328.15
4.472071886   21   328.15


];

Y2 = [
0
0
1.3015E-03
1.6010E-03
2.5832E-03
3.2332E-03
3.9625E-03
5.4721E-03
8.8939E-03


];


```

```
%% Experiment #3, A2-II

X3 = [
4.875        21   328.15
4.884367008  21   328.15
4.784768453  21   328.15
4.737944046  21   328.15
4.692972306  21   328.15
4.626608838  21   328.15
4.548468095  21   328.15
4.448673133  21   328.15


];

Y3 = [
0
0
0
6.2460E-03
3.9194E-03
4.0720E-03
5.9992E-03
7.2398E-03

];

%% Experiment #4, A2-III


%% Experiment #5, A3

X5 = [
4.87         49   328.15
4.914460858  49   328.15
4.632419663  49   328.15
4.56647853   49   328.15
4.539215368  49   328.15
4.479785934  49   328.15
4.313389169  49   328.15
4.263836337  49   328.15
];

Y5 = [
```

```
0
0
0
6.2479E-03
4.8167E-03
6.1967E-03
7.8763E-03
4.9998E-03




];

%% Experiment #6, A4

X6 = [
4.817        98   328.15
4.709764828  98   328.15
4.579582871  98   328.15
4.55720619   98   328.15
4.311055911  98   328.15
4.167074428  98   328.15
3.991948363  98   328.15
3.859212836  98   328.15


];

Y6 = [
0
0
0
6.9940E-03
4.3770E-03
6.8378E-03
4.1261E-03
6.1547E-03


];

%% Experiment #7, B1
```

```
X7 = [
5.37          6 338.15
4.911035228 6 338.15
4.863074058 6 338.15
4.716951419 6 338.15
4.974640781 6 338.15
4.690677151 6 338.15
4.446093649 6 338.15
4.492912239 6 338.15

];

Y7 = [
0
2.1800E-03
5.4500E-03
9.8100E-03
9.1871E-03
9.4986E-03
9.8100E-03
1.1367E-02



];

%% Experiment #8, B2-I

%% Experiment #9, B2-II

X9 = [
4.775         21  338.15
4.651566177 21  338.15
4.498363888 21  338.15
4.334036235 21  338.15
4.249692067 21  338.15
4.142513473 21  338.15
3.955865155 21  338.15
3.753967639 21  338.15


];

Y9 = [
```

```
0
7.0850E-03
1.0426E-02
1.6350E-02
1.5260E-02
1.4533E-02
1.5805E-02
1.3824E-02


];

%% Experiment 10, B3

X10 = [
5.26          49   338.15
4.506904135   49   338.15
4.470774185   49   338.15
3.980779552   49   338.15
3.555425284   49   338.15
3.337613545   49   338.15
2.651222746   49   338.15


];

Y10 = [
4.3600E-03
1.4715E-02
2.7523E-02
2.8703E-02
1.7985E-02
1.0744E-02
-8.0971E-03




];

%% Experiment #11, B4

X11 = [
4.798         98   338.15
```

```
4.405681764 98  338.15
3.896320554 98  338.15
3.606477896 98  338.15
3.373334889 98  338.15
3.022642215 98  338.15
2.714667974 98  338.15
2.387096959 98  338.15

];

Y11 = [
0
1.8530E-02
1.4217E-02
2.6569E-02
2.2176E-02
1.5260E-02
4.5195E-03
2.6585E-04

];

%% Experiment #12, C1

X12 = [
5.27        6 348.15
5.2879338 6 348.15
4.974793126 6 348.15
4.769646356 6 348.15
4.97394122  6 348.15
4.870772163 6 348.15
4.526150579 6 348.15
4.238312461 6 348.15
4.069101956 6 348.15
4.139477397 6 348.15
3.968698224 6 348.15

];

Y12 = [
3.6333E-03
5.1905E-03
8.5879E-03
1.0173E-02
```

```
7.5826E-03
1.2403E-02
1.1160E-02
1.2535E-02
1.2068E-02
1.6627E-02
1.7258E-02


];

%% Experiment #13, C2

X13 = [
4.944        21   348.15
4.690061157  21   348.15
4.196898229  21   348.15
3.836553249  21   348.15
3.499202912  21   348.15
3.0930167  21   348.15
2.824493483  21   348.15
2.362609886  21   348.15


];

Y13 = [
1.2974E-02
5.4801E-02
7.4791E-02
5.8104E-02
4.5633E-02
2.5921E-02
1.4741E-03
-4.6728E-03


];

%% Experiment #14, C3

X14 = [
5.06         49   348.15
5.428108647  49   348.15
```

```
4.165642573 49  348.15
3.434605249 49  348.15
3.129162546 49  348.15
3.139614905 49  348.15
2.045924558 49  348.15


];

Y14 = [
1.5260E-02
5.8315E-02
5.7225E-02
-1.4533E-03
5.4773E-02
-3.3634E-02
-3.1143E-04




];

%% Experiment #15, C4

X15 = [
4.62        98  348.15
4.69620739  98  348.15
3.041796127 98  348.15
2.276859458 98  348.15
1.896128731 98  348.15
1.704424298 98  348.15
1.601117644 98  348.15
1.693475041 98  348.15

];

Y15 = [
2.4222E-02
7.0071E-02
5.6103E-02
2.5006E-02
1.3625E-02
2.1800E-02
```

```
2.5693E-02
9.2650E-03

];

Yc = [

HEPO_ML(X1)
HEPO_ML(X2)
HEPO_ML(X3)
HEPO_ML(X5)
HEPO_ML(X6)
HEPO_ML(X7)
HEPO_ML(X9)
HEPO_ML(X10)
HEPO_ML(X11)
HEPO_ML(X12)
HEPO_ML(X13)
HEPO_ML(X14)
HEPO_ML(X15)


];
```

## A.5 Example: Oxidative degradation time measurements

```
A1 = [

0
1
3
7
14
21
28
35
%42

];

A2I = [

0.00
0.03
1.03
3.12
5.03
6.97
9.87
12.92
16.88
%21.03

];

A2II = [

0
1.1181
2.9653
4.9375
6.9444
9.9479
12.8924
17.1076
%20.9167

```

```
42
43 ];
44
45 A3 = [
46
47 0
48 1
49 3
50 4
51 7
52 10
53 14
54 17
55 %21
56
57 ];
58
59 A4 = [
60
61 0
62 1.0278
63 2.9757
64 4.0174
65 7.5104
66 9.9653
67 13.9722
68 17.2778
69 %21.1944
70
71 ];
72
73 B1 = [
74
75 0
76 1
77 3
78 7
79 14
80 21
81 28
82 35
83 %42
84
85 ];
```

```
86
87  B2II = [
88
89  0
90  1
91  3
92  5.3
93  6.9
94  9.9
95  12.9
96  16.9
97  %21
98
99
100 ];
101
102 B3 = [
103
104 0
105 1
106 3
107 7
108 10
109 14
110 21
111 %28
112
113 ];
114
115 B4 = [
116
117 0
118 0.9
119 2.9
120 5.2
121 6.8
122 9.7
123 12.7
124 16.8
125 %20.9
126
127 ];
128
129 C1 = [
```

```
130
131 0
132 0.9
133 3
134 6.3
135 7.8
136 10.1
137 13
138 17.2
139 21.2
140 24
141 29.9
142 %35.9
143
144 ];
145
146 C2 = [
147
148 0
149 0.9542
150 2.9146
151 4.909
152 6.859
153 9.8972
154 11.9444
155 16.9104
156 %19.909
157
158
159 ];
160
161 C3 = [
162
163 0
164 1
165 3
166 7
167 10
168 14
169 21
170 %28
171
172 ];
173
```

```
C4 = [

0
0.9
3
6.4
8.1
10.1
13
17.2
%21.2


];
```

## A.6 Example: Plotting 3-input model

```
clear
clc
close all
TIME


A1HEPO = [
0.0000000000   0.0000000000
0.0000000000   0.0004716359
0.0010900000   0.0014149078
0.0065400000   0.0033014516
0.0283400000   0.0066029031
0.0468700000   0.0099043547
0.0991900000   0.0132058063
0.1635000000   0.0165072579


];

A2IHEPO = [

0.0000000000   0.0000000000
0.0000000000   0.0000813013
0.0000000000   0.0031608962
0.0027250000   0.0096086439
0.0057770000   0.0154792755
```

```
0.0107910000   0.0214567691
0.0201650000   0.0303854385
0.0322640000   0.0397886734
0.0539550000   0.0519958794




];

A2IIHEPO = [

0.0000000000   0.0000000000
0.0000000000   0.0047597572
0.0000000000   0.0126232967
0.0000000000   0.0210189618
0.0125350000   0.0295623449
0.0243070000   0.0423482592
0.0362970000   0.0548830102
0.0615850000   0.0728271373


];

A3HEPO = [

0.0000000000   0.0000000000
0.0000000000   0.0046974149
0.0000000000   0.0140922447
0.0000000000   0.0187896597
0.0187436400   0.0328819044
0.0331937700   0.0469741491
0.0579803700   0.0657638088
0.0816093900   0.0798560536

];

A4HEPO = [

0.0000000000   0.0000000000
0.0000000000   0.0051775459
0.0000000000   0.0149900986
0.0000000000   0.0202376658
0.0244301700   0.0378336648
```

```
71  0.0351753900   0.0502002317
72  0.0625736300   0.0703850037
73  0.0762128000   0.0870369746
74
75
76  ];
77
78  B1HEPO = [
79
80  0.0000000000   0.0000000000
81  0.0000000000   0.0073584875
82  0.0043600000   0.0220754625
83  0.0261600000   0.0515094126
84  0.0948300000   0.1030188252
85  0.1591400000   0.1545282378
86  0.2256300000   0.2060376504
87  0.2943000000   0.2575470631
88
89
90
91
92  ];
93
94  B2IIHEPO = [
95
96  0.0000000000   0.0000000000
97  0.0000000000   0.0132478325
98  0.0141700000   0.0397434975
99  0.0381500000   0.0702135123
100 0.0643100000   0.0914100443
101 0.1100900000   0.1311535418
102 0.1536900000   0.1708970393
103 0.2169100000   0.2238883693
104
105
106
107 ];
108
109 B3HEPO = [
110
111 0.0000000000   0.0000000000
112 0.0043600000   0.0103306534
113 0.0337900000   0.0309919601
114 0.1438800000   0.0723145737
```

```
115 0.2299900000   0.1033065338
116 0.3019300000   0.1446291473
117 0.3771400000   0.2169437210
118
119 ];
120
121 B4HEPO = [
122
123 0.0000000000   0.0000000000
124 0.0000000000   0.0129557024
125 0.0370600000   0.0417461523
126 0.0697600000   0.0748551697
127 0.1122700000   0.0978875296
128 0.1765800000   0.1396336819
129 0.2223600000   0.1828193567
130 0.2408900000   0.2418397789
131
132
133
134
135 ];
136
137 C1HEPO = [
138
139 0.0000000000   0.0000000000
140 0.0032700000   0.0188858549
141 0.0141700000   0.0629528497
142 0.0425100000   0.1322009844
143 0.0577700000   0.1636774092
144 0.0752100000   0.2119412606
145 0.1111800000   0.2727956820
146 0.1580500000   0.3609296716
147 0.2081900000   0.4448668045
148 0.2419800000   0.5036227976
149 0.3400800000   0.6274300686
150
151
152
153 ];
154
155 C2HEPO = [
156
157 0.0000000000   0.0000000000
158 0.0123802200   0.0183351820
```

```
0.1198117100   0.0560047385
0.2689749400   0.0943276131
0.3822771700   0.1317973310
0.5209208100   0.1901770732
0.5739863700   0.2295145125
0.5813068100   0.3249373942


];

C3HEPO = [
0.0000000000   0.0000000000
0.0152600000   0.0264356179
0.1318900000   0.0793068538
0.3607900000   0.1850493256
0.3564300000   0.2643561794
0.5755200000   0.3700986512
0.3400800000   0.5551479767


];

C4HEPO = [

0.0000000000   0.0000000000
0.0218000000   0.0309656578
0.1689500000   0.1032188594
0.3597000000   0.2202002334
0.4022100000   0.2786909204
0.4294600000   0.3475034933
0.4926800000   0.4472817241
0.6005900000   0.5917881273


];

a = figure();

subplot(2,3,1)
hold on
plot(A1, A1HEPO(:,1), '*')
plot(A1, A1HEPO(:,2), '-')
xlabel('Time [days]')
ylabel('C_{HEPO} [kmol/kg]')
```

```
203 legend({'C_{HEPO, exp}', 'C_{HEPO, mod}'},'Location','southeast')
204 title('A1, 55 \circC, 6 % O_2, HEPO')
205
206 subplot(2,3,2)
207 hold on
208 plot(A2I, A2IHEPO(:,1), '*')
209 plot(A2I, A2IHEPO(:,2), '-')
210 xlabel('Time [days]')
211 ylabel('C_{HEPO} [kmol/kg]')
212 legend({'C_{HEPO, exp}', 'C_{HEPO, mod}'},'Location','southeast')
213 title('A2-I, 55 \circC, 21 % O_2, HEPO')
214
215 subplot(2,3,3)
216 hold on
217 plot(A2II, A2IIHEPO(:,1), '*')
218 plot(A2II, A2IIHEPO(:,2), '-')
219 xlabel('Time [days]')
220 ylabel('C_{HEPO} [kmol/kg]')
221 legend({'C_{HEPO, exp}', 'C_{HEPO, mod}'},'Location','southeast')
222 title('A2-II, 55 \circC, 21 % O_2, HEPO')
223
224 subplot(2,3,4)
225 hold on
226 plot(A3, A3HEPO(:,1), '*')
227 plot(A3, A3HEPO(:,2), '-')
228 xlabel('Time [days]')
229 ylabel('C_{HEPO} [kmol/kg]')
230 legend({'C_{HEPO, exp}', 'C_{HEPO, mod}'},'Location','southeast')
231 title('A3, 55 \circC, 49 % O_2, HEPO')
232
233 subplot(2,3,5)
234 hold on
235 plot(A4, A4HEPO(:,1), '*')
236 plot(A4, A4HEPO(:,2), '-')
237 xlabel('Time [days]')
238 ylabel('C_{HEPO} [kmol/kg]')
239 legend({'C_{HEPO, exp}', 'C_{HEPO, mod}'},'Location','southeast')
240 title('A4, 55 \circC, 98 % O_2, HEPO')
241
242 b = figure();
243
244
245 subplot(2,2,1)
246 hold on
```

```
247 plot(B1, B1HEPO(:,1), '*')
248 plot(B1, B1HEPO(:,2), '-')
249 xlabel('Time [days]')
250 ylabel('C_{HEPO} [kmol/kg]')
251 legend({'C_{HEPO, exp}', 'C_{HEPO, mod}'},'Location','southeast')
252 title('B1, 65 \circC, 6 % O_2, HEPO')
253
254 subplot(2,2,2)
255 hold on
256 plot(B2II, B2IIHEPO(:,1), '*')
257 plot(B2II, B2IIHEPO(:,2), '-')
258 xlabel('Time [days]')
259 ylabel('C_{HEPO} [kmol/kg]')
260 legend({'C_{HEPO, exp}', 'C_{HEPO, mod}'},'Location','southeast')
261 title('B2-II, 65 \circC, 21 % O_2, HEPO')
262
263 subplot(2,2,3)
264 hold on
265 plot(B3, B3HEPO(:,1), '*')
266 plot(B3, B3HEPO(:,2), '-')
267 xlabel('Time [days]')
268 ylabel('C_{HEPO} [kmol/kg]')
269 legend({'C_{HEPO, exp}', 'C_{HEPO, mod}'},'Location','southeast')
270 title('B3, 65 \circC, 49 % O_2, HEPO')
271
272 subplot(2,2,4)
273 hold on
274 plot(B4, B4HEPO(:,1), '*')
275 plot(B4, B4HEPO(:,2), '-')
276 xlabel('Time [days]')
277 ylabel('C_{HEPO} [kmol/kg]')
278 legend({'C_{HEPO, exp}', 'C_{HEPO, mod}'},'Location','southeast')
279 title('B4, 65 \circC, 98 % O_2, HEPO')
280
281 c = figure();
282
283
284 subplot(2,2,1)
285 hold on
286 plot(C1, C1HEPO(:,1), '*')
287 plot(C1, C1HEPO(:,2), '-')
288 xlabel('Time [days]')
289 ylabel('C_{HEPO} [kmol/kg]')
290 legend({'C_{HEPO, exp}', 'C_{HEPO, mod}'},'Location','southeast')
```

```
291 title('C1, 75 \circC, 6 % O_2, HEPO')
292
293 subplot(2,2,2)
294 hold on
295 plot(C2, C2HEPO(:,1), '*')
296 plot(C2, C2HEPO(:,2), '-')
297 xlabel('Time [days]')
298 ylabel('C_{HEPO} [kmol/kg]')
299 legend({'C_{HEPO, exp}', 'C_{HEPO, mod}'},'Location','southeast')
300 title('C2, 75 \circC, 21 % O_2, HEPO')
301
302 subplot(2,2,3)
303 hold on
304 plot(C3, C3HEPO(:,1), '*')
305 plot(C3, C3HEPO(:,2), '-')
306 xlabel('Time [days]')
307 ylabel('C_{HEPO} [kmol/kg]')
308 legend({'C_{HEPO, exp}', 'C_{HEPO, mod}'},'Location','southeast')
309 title('C3, 75 \circC, 49 % O_2, HEPO')
310
311 subplot(2,2,4)
312 hold on
313 plot(C4, C4HEPO(:,1), '*')
314 plot(C4, C4HEPO(:,2), '-')
315 xlabel('Time [days]')
316 ylabel('C_{HEPO} [kmol/kg]')
317 legend({'C_{HEPO, exp}', 'C_{HEPO, mod}'},'Location','southeast')
318 title('C4, 65 \circC, 98 % O_2, HEPO')
```

# B MATLAB code thermal degradation

```
clear
clc
close all

DOT = [

393 6.58  0.2
%393  6.12  0.2
393 6.33  0.2
%393  5.86  0.2
393 6.24  0.2

393 6.58  0.4
393 6.22  0.4
393 5.9 0.4
393 5.58  0.4
393 5.14  0.4

393 6.58  0.5
393 6.19  0.5
%393  5.76  0.5
393 6.1 0.5
393 4.18  0.5

%393  4.9 0.2
393 5.11  0.2
%393  4.57  0.2
393 4.6 0.2
%393  4.39  0.2

393 4.9 0.4
393 4.82  0.4
393 4.5 0.4
%393  4.25  0.4

393 4.9 0.5
393 4.6 0.5
393 4.22  0.5
393 4 0.5
```

```
393 3.68  0.5

%393  2.88  0.2
393 3.24  0.2
393 2.72  0.2
393 2.63  0.2
%393  2.59  0.2

%393  2.88  0.4
393 3.17  0.4
393 2.66  0.4
393 2.58  0.4
%393  2.48  0.4

%393  2.88  0.5
393 3.22  0.5
393 2.69  0.5
393 2.33  0.5
%393  2.31  0.5

408 6.58  0.2
408 6.42  0.2
408 5.92  0.2
408 5.61  0.2
408 5.18  0.2

408 6.58  0.4
408 5.8 0.4
408 4.43  0.4
408 4.26  0.4
408 3.27  0.4

408 6.58  0.5
408 5 0.5
408 4.09  0.5
408 2.95  0.5
408 2.48  0.5

408 4.9 0.2
408 4.41  0.2
408 4.27  0.2

408 4.31  0.4
408 4.28  0.4
```

```
84  408  3.42   0.4
85
86  408  4.9      0.5
87  408  4.05   0.5
88  408  3.46   0.5
89  408  2.69   0.5
90  408  2.42   0.5
91
92  408  2.88   0.2
93  408  2.79   0.2
94  408  2.71   0.2
95  408  2.58   0.2
96  408  2.54   0.2
97
98
99  408  2.88   0.4
100 408  2.72   0.4
101 408  2.43   0.4
102 408  2.24   0.4
103
104 408  2.88   0.5
105 %408   2.54   0.5
106 408  3.09   0.5
107 408  2.01   0.5
108 408  1.93   0.5
109
110
111
112 ];
113
114 rMEA = [
115
116  -0.065714286
117 %0.03
118  -0.033571429
119 %0.027142857
120  -0.032857143
121
122
123  -0.051428571
124  -0.045714286
125  -0.022857143
126  -0.031428571
127  -0.019285714
```

```
128
129
130 -0.055714286
131 -0.061428571
132 %0.024285714
133 -0.137142857
134 -0.016428571
135
136
137 %0.03
138 -0.077142857
139 %0.002142857
140 -0.015
141 %0.000714286
142
143
144 -0.011428571
145 -0.045714286
146 -0.008928571
147 %0.004285714
148
149
150 -0.042857143
151 -0.054285714
152 -0.015714286
153 -0.022857143
154 -0.012857143
155
156
157 %0.051428571
158 -0.074285714
159 -0.006428571
160 -0.002857143
161 %0.002142857
162
163
164 %0.041428571
165 -0.072857143
166 -0.005714286
167 -0.007142857
168 %0.025
169
170
171 %0.048571429
```

```
-0.075714286
-0.025714286
-0.001428571
%0.005714286

-0.022857143
-0.071428571
-0.022142857
-0.030714286
-0.034285714


-0.111428571
-0.195714286
-0.012142857
-0.070714286
-0.037142857


-0.225714286
-0.13
-0.081428571
-0.033571429
-0.045


-0.074285714
-0.01
-0.0275


-0.004285714
-0.061428571
-0.0375


-0.121428571
-0.084285714
-0.055
-0.019285714
-0.049285714


-0.012857143
```

```
-0.011428571
-0.009285714
-0.002857143
-0.015714286


-0.022857143
-0.041428571
-0.013571429
-0.078214286


-0.048571429
%0.078571429
-0.077142857
-0.005714286
-0.031428571


];
```

## B.2 Example: MEA 6 input model data file with all inputs and outputs

```
clear
clc
close all

Input = [

393 6.58  0.2 6.58  NaN 0       0
393 6.12  0.2 6.12  NaN 0.03  0
393 6.33  0.2 6.33  NaN 0.07  0
393 5.86  0.2 5.86  NaN 0.13  0
393 6.24  0.2 6.24  NaN 0.09  0.01
%393  5.78  0.2 5.78  NaN 0.15  0.01

393 6.58  0.4 6.58  NaN 0       0
393 6.22  0.4 6.22  NaN 0.02  0.01
393 5.9     0.4 5.9     NaN 0.09  0.01
393 5.58  0.4 5.58  NaN 0.11  0.02
393 5.14  0.4 5.14  NaN 0.33  0.03
%393  4.87  0.4 4.87  NaN 0.41  0.05
```

```
20
21 393 6.58  0.5 6.58  NaN NaN     0
22 393 6.19  0.5 6.19  NaN NaN     0
23 393 5.76  0.5 5.76  NaN NaN     0.02
24 393 6.1     0.5 6.1     NaN NaN     0.02
25 393 4.18  0.5 4.18  NaN NaN     0.06
26 %393  3.95  0.5 3.95  NaN NaN     0.09
27
28 393 4.9     0.2 4.9     0       0       0
29 393 5.11  0.2 5.11  0       0.02  0
30 393 4.57  0.2 4.57  0       0.05  0
31 393 4.6     0.2 4.6     0       0.09  0
32 393 4.39  0.2 4.39  0.04  0.1     0
33 %393  4.4     0.2 4.4     0.08  0.13  0
34
35 393 4.9     0.4 4.9     0       0       0
36 393 4.82  0.4 4.82  0.04  0.03  0
37 393 4.5     0.4 4.5     0.05  0.05  0
38 393 4.25  0.4 4.25  0.1     0.21  0.02
39 %393  4.31  0.4 4.31  0.12  0.35  0.03
40
41 393 4.9     0.5 4.9     0       0       0
42 393 4.6     0.5 4.6     0.05  0.03  0
43 393 4.22  0.5 4.22  0.08  0.07  0
44 393 4       0.5 4       0.09  0.16  0.02
45 393 3.68  0.5 3.68  0.12  0.22  0.04
46 %393  3.5     0.5 3.5     0.12  0.3     0.06
47
48 393 2.88  0.2 2.88  0       0       0
49 393 3.24  0.2 3.24  0       0.02  0
50 393 2.72  0.2 2.72  0       0.03  0
51 393 2.63  0.2 2.63  0       0.04  0
52 393 2.59  0.2 2.59  0       0.06  0
53 %393  2.62  0.2 2.62  0.17  0.03  0
54
55 393 2.88  0.4 2.88  0       0       0
56 393 3.17  0.4 3.17  0       0.02  0
57 393 2.66  0.4 2.66  0       0.04  0
58 393 2.58  0.4 2.58  0       0.02  0
59 393 2.48  0.4 2.48  0.09  0.11  0
60 %393  2.83  0.4 2.83  0.07  0.2     0.02
61
62 393 2.88  0.5 2.88  0       0       0
63 393 3.22  0.5 3.22  0       0.03  0
```

```
393  2.69   0.5  2.69   0        0.05   0
393  2.33   0.5  2.33   0.07   0.07   0
393  2.31   0.5  2.31   0.12   0.12   0
%393   2.39   0.5  2.39   0.12   0.17   0

408  6.58   0.2  6.58   0        0        0
408  6.42   0.2  6.42   0.04   0.11   0
408  5.92   0.2  5.92   0.1      0.22   0
408  5.61   0.2  5.61   0.2      0.22   0
408  5.18   0.2  5.18   0.22   0.22   0.02
%408   4.7      0.2  4.7      0.26   0.28   0.05

408  6.58   0.4  6.58   0        0        0
408  5.8      0.4  5.8      0.15   0.14   0
408  4.43   0.4  4.43   0.2      0.36   0.03
408  4.26   0.4  4.26   0.19   NaN      0.11
408  3.27   0.4  3.27   0.18     0.47   0.14
%408   2.75   0.4  2.75   0.16   NaN      0.25

408  6.58   0.5  6.58   0        0 0
408  5        0.5  5        0.16   NaN 0.02
408  4.09   0.5  4.09   0.17   NaN 0.07
408  2.95   0.5  2.95   0.13   NaN 0.19
408  2.48   0.5  2.48   0.12   NaN 0.22
%408   1.85   0.5  1.85   0.09   NaN 0.3

408  4.9      0.2  4.9      0        0        0
408  4.38   0.2  4.38   0.04   0.02   0
408  4.41   0.2  4.41   0.11   0.05   0
408  4.27   0.2  4.27   0.16   0.11   0
%408   3.5      0.2  3.5      0.18   0.19   0.03

408  4.9      0.4  4.9      0        0        0
408  4.31   0.4  4.31   0.1      0.1      0
408  4.28   0.4  4.28   0.13   0.26   0.02
408  3.42   0.4  3.42   0.15   0.39   0.06
%408   2.37   0.4  2.37   0.13   0.61   0.13

408  4.9      0.5  4.9      0        0        0
408  4.05   0.5  4.05   0.11   0.15   0
408  3.46   0.5  3.46   0.12   0.32   0.04
408  2.69   0.5  2.69   0.09   0.49   0.1
408  2.42   0.5  2.42   0.09   0.45   0.17
%408   1.73   0.5  1.73   0.08   0.5      0.19
```

```
108
109 408  2.88   0.2  2.88   0        0        0
110 408  2.79   0.2  2.79   0        0.06   0
111 408  2.71   0.2  2.71   0        0.1      0
112 408  2.58   0.2  2.58   0.08   0.06   0
113 408  2.54   0.2  2.54   0.04   0.09   0
114 %408   2.32   0.2  2.32   0.06   0.12   0.02
115
116 408  2.88   0.4  2.88   0        0        0
117 408  2.72   0.4  2.72   0        0.03   0
118 408  2.43   0.4  2.43   0.02   0.15   0
119 408  2.24   0.4  2.24   0.08   0.21   0.02
120 %408   0.05   0.4  0.05   0        0.36   0
121
122 408  2.88   0.5  2.88   0        0        0
123 408  2.54   0.5  2.54   0.03   0.09   0
124 408  3.09   0.5  3.09   0.06   0.32   0.02
125 408  2.01   0.5  2.01   0.04   0.31   0.03
126 408  1.93   0.5  1.93   0.03   0.38   0.05
127 %408   1.49   0.5  1.49   0.05   0.37   0.07
128
129 ];
130
131 Output_MEA = [
132
133 -0.065714286
134 0.03
135 -0.033571429
136 0.027142857
137 -0.032857143
138
139
140 -0.051428571
141 -0.045714286
142 -0.022857143
143 -0.031428571
144 -0.019285714
145
146
147 -0.055714286
148 -0.061428571
149 0.024285714
150 -0.137142857
151 -0.016428571
```

```
152
153
154 0.03
155 -0.077142857
156 0.002142857
157 -0.015
158 0.000714286
159
160
161 -0.011428571
162 -0.045714286
163 -0.008928571
164 0.004285714
165
166
167 -0.042857143
168 -0.054285714
169 -0.015714286
170 -0.022857143
171 -0.012857143
172
173
174 0.051428571
175 -0.074285714
176 -0.006428571
177 -0.002857143
178 0.002142857
179
180
181 0.041428571
182 -0.072857143
183 -0.005714286
184 -0.007142857
185 0.025
186
187
188 0.048571429
189 -0.075714286
190 -0.025714286
191 -0.001428571
192 0.005714286
193
194
195 -0.022857143
```

```
196 -0.071428571
197 -0.022142857
198 -0.030714286
199 -0.034285714
200
201
202 -0.111428571
203 -0.195714286
204 -0.012142857
205 -0.070714286
206 -0.037142857
207
208
209 -0.225714286
210 -0.13
211 -0.081428571
212 -0.033571429
213 -0.045
214
215
216 -0.074285714
217 0.004285714
218 -0.01
219 -0.0275
220
221
222 -0.084285714
223 -0.004285714
224 -0.061428571
225 -0.0375
226
227
228 -0.121428571
229 -0.084285714
230 -0.055
231 -0.019285714
232 -0.049285714
233
234
235 -0.012857143
236 -0.011428571
237 -0.009285714
238 -0.002857143
239 -0.015714286
```

```
240
241
242 -0.022857143
243 -0.041428571
244 -0.013571429
245 -0.078214286
246
247
248 -0.048571429
249 0.078571429
250 -0.077142857
251 -0.005714286
252 -0.031428571
253
254
255
256 ];
257
258
259 Output_HEEDA = [
260
261 NaN
262 NaN
263 NaN
264 NaN
265 NaN
266
267 NaN
268 NaN
269 NaN
270 NaN
271 NaN
272
273 NaN
274 NaN
275 NaN
276 NaN
277 NaN
278
279 0
280 0
281 0
282 0.002857143
283 0.002857143
```

```
284
285 0.005714286
286 0.001428571
287 0.001785714
288 0.001428571
289
290 0.007142857
291 0.004285714
292 0.000714286
293 0.002142857
294 0
295
296 0
297 0
298 0
299 0
300 0.012142857
301
302 0
303 0
304 0
305 0.006428571
306 -0.001428571
307
308 0
309 0
310 0.005
311 0.003571429
312 0
313
314 0.005714286
315 0.008571429
316 0.007142857
317 0.001428571
318 0.002857143
319
320 0.021428571
321 0.007142857
322 -0.000714286
323 -0.000714286
324 -0.001428571
325
326 0.022857143
327 0.001428571
```

```
-0.002857143
-0.000714286
-0.002142857

0.005714286
0.01
0.003571429
0.000714286

0.014285714
0.004285714
0.001428571
-0.000714286

0.015714286
0.001428571
-0.002142857
0
-0.000714286

0
0
0.005714286
-0.002857143
0.001428571

0
0.002857143
0.004285714
-0.002857143

0.004285714
0.004285714
-0.001428571
-0.000714286
0.001428571


];


Output_HEIA = [

0.004285714
```

```
0.005714286
0.004285714
-0.002857143
0.004285714

0.002857143
0.01
0.001428571
0.015714286
0.005714286

NaN
NaN
NaN
NaN
NaN

0.002857143
0.004285714
0.002857143
0.000714286
0.002142857

0.004285714
0.002857143
0.005714286
0.01

0.004285714
0.005714286
0.006428571
0.004285714
0.005714286

0.002857143
0.001428571
0.000714286
0.001428571
-0.002142857

0.002857143
0.002857143
-0.001428571
0.006428571
```

```
0.006428571

0.004285714
0.002857143
0.001428571
0.003571429
0.003571429

0.015714286
0.015714286
0
0
0.004285714

0.02
0.031428571
NaN
NaN
NaN

NaN
NaN
NaN
NaN
NaN

0.002857143
0.004285714
0.004285714
0.002857143

0.014285714
0.022857143
0.009285714
0.007857143

0.021428571
0.024285714
0.012142857
-0.002857143
0.003571429

0.008571429
0.005714286
```

```
-0.002857143
0.002142857
0.002142857

0.004285714
0.017142857
0.004285714
0.005357143

0.012857143
0.032857143
-0.000714286
0.005
-0.000714286


];

Output_TriHEIA = [

0
0
0
0.000714286
0

0.001428571
0
0.000714286
0.000714286
0.001428571

0
0.002857143
0
0.002857143
0.002142857

0
0
0
0
0

```

```
0
0
0.000714286
0.000714286

0
0
0.001428571
0.001428571
0.001428571

0
0
0
0
0

0
0
0
0
0.001428571

0
0
0
0
0

0
0
0
0.001428571
0.002142857

0
0.004285714
0.005714286
0.002142857
0.007857143

0.002857143
0.007142857
0.008571429
```

```
548 0.002142857
549 0.005714286
550
551 0
552 0
553 0
554 0.001071429
555
556 0
557 0.002857143
558 0.002857143
559 0.0025
560
561 0
562 0.005714286
563 0.004285714
564 0.005
565 0.001428571
566
567 0
568 0
569 0
570 0
571 0.001428571
572
573 0
574 0
575 0.001428571
576 -0.000714286
577
578 0
579 0.002857143
580 0.000714286
581 0.001428571
582 0.001428571
583
584
585
586 ];
```

### B.3 Example: MEA machine learning model

```
function [y1] = myNeuralNetworkFunction(x1)
%MYNEURALNETWORKFUNCTION neural network simulation function.
%
% Auto-generated by MATLAB, 14-Apr-2021 13:37:58.
%
% [y1] = myNeuralNetworkFunction(x1) takes these arguments:
%   x = Qx3 matrix, input #1
% and returns:
%   y = Qx1 matrix, output #1
% where Q is the number of samples.

%#ok<*RPMT0>

% ===== NEURAL NETWORK CONSTANTS =====

% Input 1
x1_step1.xoffset = [393;1.93;0.2];
x1_step1.gain =
    [0.133333333333333;0.43010752688172;6.66666666666667];
x1_step1.ymin = -1;

% Layer 1
b1 =
    [-1.5746388810380491652;0.021319806190481817992;-0.020786658904295585854];

IW1_1 = [0.51181388799705329617 0.88690316085691345283
    0.729024021949272627 02;0.12431852575192366139
    -0.032181772504924176237
    0.13507381922287772791;-0.1237962766908106832
    0.032913040483900299349 -0.1346362178511378016];

% Layer 2
b2 = -0.30807497583435677901;
LW2_1 = [-1.1547236028974714461 0.21763249586769245481
    -0.21695040679872487632];

% Output 1
y1_step1.ymin = -1;
y1_step1.gain = 8.91719742383058;
y1_step1.xoffset = -0.225714286;

```

```
% ====== SIMULATION ==========

% Dimensions
Q = size(x1,1); % samples

% Input 1
x1 = x1';
xp1 = mapminmax_apply(x1,x1_step1);

% Layer 1
a1 = tansig_apply(repmat(b1,1,Q) + IW1_1*xp1);

% Layer 2
a2 = repmat(b2,1,Q) + LW2_1*a1;

% Output 1
y1 = mapminmax_reverse(a2,y1_step1);
y1 = y1';
end

% ====== MODULE FUNCTIONS ==========

% Map Minimum and Maximum Input Processing Function
function y = mapminmax_apply(x,settings)
y = bsxfun(@minus,x,settings.xoffset);
y = bsxfun(@times,y,settings.gain);
y = bsxfun(@plus,y,settings.ymin);
end

% Sigmoid Symmetric Transfer Function
function a = tansig_apply(n,~)
a = 2 ./ (1 + exp(-2*n)) - 1;
end

% Map Minimum and Maximum Output Reverse-Processing Function
function x = mapminmax_reverse(y,settings)
x = bsxfun(@minus,y,settings.ymin);
x = bsxfun(@rdivide,x,settings.gain);
x = bsxfun(@plus,x,settings.xoffset);
end
```

### B.4 Example: Thermal degradation time measurements

```
clear
clc
close all

TE1 = [

0
7
14
28
42

];

TE2 = [

0
7
14
28
42

];

TE3 = [

0
7
14
28
42

];

TE4 = [

0
7
14
28
42
```

```
42
43 ];
44
45 TE5 = [
46
47 0
48 7
49 14
50 42
51
52
53 ];
54
55 TE6 = [
56
57 0
58 7
59 14
60 28
61 42
62
63 ];
64
65 TE7 = [
66
67 0
68 7
69 14
70 28
71 42
72
73 ];
74
75 TE8 = [
76
77 0
78 7
79 14
80 28
81 42
82
83 ];
84
85 TE9 = [
```

```
86
87 0
88 7
89 14
90 28
91 42
92
93 ];
94
95 TF1 = [
96
97 0
98 7
99 14
100 28
101 42
102
103 ];
104
105 TF2 = [
106
107 0
108 7
109 14
110 28
111 42
112
113 ];
114
115 TF3 = [
116
117 0
118 7
119 14
120 28
121 42
122
123 ];
124
125 TF4 = [
126
127 0
128 7
129 14
```

```
28


];

TF5 = [

0
7
14
28


];

TF6 = [

0
7
14
28
42

];

TF7 = [

0
7
14
28
42

];

TF8 = [

0
7
14
28

];

```

```
TF9 = [

0
7
14
28
42

];
```

### B.5 Example: MEA all plots

```
clear
clc
close all
THERMAL_TIME
set(groot,'defaultLineLineWidth',1.5)

E1_MEA = [

6.58   6.58000000000000          NaN
6.12   6.32204413541079          NaN
6.33   6.07707514441802          NaN
5.86   5.57619058091935          NaN
6.24   5.09801931107691          NaN

];

E2_MEA = [

6.58   6.58000000000000          NaN
6.22   6.18559155445716          NaN
5.9      5.84324777271713          NaN
5.58   5.23441267993921          NaN
5.14   4.68797130426874          NaN


];

E3_MEA = [

6.58   6.58000000000000          NaN
6.19   5.94051797054882          NaN
```

```
5.76   5.40443449133772          NaN
6.1      4.52486957379720          NaN
4.18   3.49611022224730          NaN


];

E4_MEA = [

4.9      4.90000000000000   4.90000000000000
5.11   4.67649471407249   4.80723428252824
4.57   4.45022190942435   4.70490356923068
4.6      4.01086561950235   4.56114697744983
4.39   3.57085979685593   4.42265975947287


];

E5_MEA = [

4.9      4.90000000000000   4.90000000000000
4.82   4.67540906123845   4.66951855276596
4.5      4.45526678842533   4.46580084023358
4.25   3.63738307488669   3.88034300379937


];

E6_MEA = [

4.9      4.90000000000000   4.90000000000000
4.6      4.60023747267246   4.49596766314742
4.22   4.33527562923556   4.16467568838407
4        3.87697366706872   3.69689137793502
3.68   3.45294779708397   3.31295891335673

];

E7_MEA = [

2.88   2.88000000000000   2.88000000000000
3.24   2.67393240901055   2.85672646120665
2.72   2.46550949324481   2.82645111877345
2.63   2.05535443589185   2.79250474939521
```

```
2.59   1.64628704830735   2.76430194262755


];

E8_MEA = [

2.88   2.88000000000000   2.88000000000000
3.17   2.72061891964655   2.84739912154367
2.66   2.55599258751855   2.80016288836989
2.58   2.24416593767766   2.76670703440018
2.48   1.93467240134749   2.73639533530704


];

E9_MEA = [

2.88   2.88000000000000   2.88000000000000
3.22   2.72594167323439   2.80753429791252
2.69   2.55844862117512   2.70469436348007
2.33   2.26301421161241   2.60754032847966
2.31   1.98787801077467   2.67862289030410


];

F1_MEA = [

6.58   6.58000000000000   6.58000000000000
6.42   6.18702716254070   6.10856294981150
5.92   5.82041179169698   5.67624756030738
5.61   5.22435799969755   5.03817065938236
5.18   4.69502930546699   4.52735323726988


];

F2_MEA = [

6.58   6.58000000000000   6.58000000000000
5.8      5.53573764260373   5.56676534573707
4.43   4.76109975395887   4.73554349398986
4.26   3.96872448871623   NaN
```

```
3.27   3.24492012237961   3.06178197261633


];

F3_MEA = [

6.58   6.58000000000000   6.58000000000000
5        5.17008173688541          NaN
4.09   4.26796404266877          NaN
2.95   3.06568105880457          NaN
2.48   2.42487440577308          NaN


];

F4_MEA = [

4.9      4.90000000000000   4.90000000000000
4.38   4.69125808400730   4.68124062587235
4.41   4.51003328670225   4.52132915491829
4.27   4.14488399032678   4.26665642021020


];

F5_MEA = [

4.9      4.90000000000000   4.90000000000000
4.31   4.39391281665650   4.39253637308310
4.28   4.02222187017508   4.01999361833809
3.42   3.29064500283009   3.28968517917833


];

F6_MEA = [

4.9      4.90000000000000   4.90000000000000
4.05   4.03273798583193   4.12638924272244
3.46   3.44356801399938   3.59273497603730
2.69   2.58356341111304   2.79414101129343
2.42   2.03499094323044   2.28416922077770

```

```
164
165 ];
166
167 F7_MEA = [
168
169 2.88   2.88000000000000   2.88000000000000
170 2.79   2.74221500427992   2.77244804738971
171 2.71   2.60600805555225   2.67224245747956
172 2.58   2.33627346581151   2.48263217518174
173 2.54   2.07065752021148   2.41139839015401
174
175
176 ];
177
178 F8_MEA = [
179
180 2.88   2.88000000000000   2.88000000000000
181 2.72   2.70461576344569   2.70808554773775
182 2.43   2.54246944408620   2.55423090042582
183 2.24   2.25978439727425   2.34214994344376
184
185 ];
186
187 F9_MEA = [
188
189 2.88   2.88000000000000   2.88000000000000
190 2.54   2.57263639632440   2.60774051495939
191 3.09   2.32216481565399   2.40855536716565
192 2.01   1.62635372590170   1.87356587912771
193 1.93   1.26440243863403   1.65582517046464
194
195 ];
196
197
198 AD_E1_3 = mean(abs(E1_MEA(:,1)-E1_MEA(:,2)))
199 AD_E1_6 = mean(abs(E1_MEA(:,1)-E1_MEA(:,3)))
200
201 AD_E2_3 = mean(abs(E2_MEA(:,1)-E2_MEA(:,2)))
202 AD_E2_6 = mean(abs(E2_MEA(:,1)-E2_MEA(:,3)))
203
204 AD_E3_3 = mean(abs(E3_MEA(:,1)-E3_MEA(:,2)))
205 AD_E3_6 = mean(abs(E3_MEA(:,1)-E3_MEA(:,3)))
206
207 AD_E4_3 = mean(abs(E4_MEA(:,1)-E4_MEA(:,2)))
```

```
208 AD_E4_6 = mean(abs(E4_MEA(:,1)-E4_MEA(:,3)))
209
210 AD_E5_3 = mean(abs(E5_MEA(:,1)-E5_MEA(:,2)))
211 AD_E5_6 = mean(abs(E5_MEA(:,1)-E5_MEA(:,3)))
212
213 AD_E6_3 = mean(abs(E6_MEA(:,1)-E6_MEA(:,2)))
214 AD_E6_6 = mean(abs(E6_MEA(:,1)-E6_MEA(:,3)))
215
216 AD_E7_3 = mean(abs(E7_MEA(:,1)-E7_MEA(:,2)))
217 AD_E7_6 = mean(abs(E7_MEA(:,1)-E7_MEA(:,3)))
218
219 AD_E8_3 = mean(abs(E8_MEA(:,1)-E8_MEA(:,2)))
220 AD_E8_6 = mean(abs(E8_MEA(:,1)-E8_MEA(:,3)))
221
222 AD_E9_3 = mean(abs(E9_MEA(:,1)-E9_MEA(:,2)))
223 AD_E9_6 = mean(abs(E9_MEA(:,1)-E9_MEA(:,3)))
224
225 AD_F1_3 = mean(abs(F1_MEA(:,1)-F1_MEA(:,2)))
226 AD_F1_6 = mean(abs(F1_MEA(:,1)-F1_MEA(:,3)))
227
228 AD_F2_3 = mean(abs(F2_MEA(:,1)-F2_MEA(:,2)))
229 AD_F2_6 = mean(abs(F2_MEA(:,1)-F2_MEA(:,3)))
230
231 AD_F3_3 = mean(abs(F3_MEA(:,1)-F3_MEA(:,2)))
232 AD_F3_6 = mean(abs(F3_MEA(:,1)-F3_MEA(:,3)))
233
234 AD_F4_3 = mean(abs(F4_MEA(:,1)-F4_MEA(:,2)))
235 AD_F4_6 = mean(abs(F4_MEA(:,1)-F4_MEA(:,3)))
236
237 AD_F5_3 = mean(abs(F5_MEA(:,1)-F5_MEA(:,2)))
238 AD_F5_6 = mean(abs(F5_MEA(:,1)-F5_MEA(:,3)))
239
240 AD_F6_3 = mean(abs(F6_MEA(:,1)-F6_MEA(:,2)))
241 AD_F6_6 = mean(abs(F6_MEA(:,1)-F6_MEA(:,3)))
242
243 AD_F7_3 = mean(abs(F7_MEA(:,1)-F7_MEA(:,2)))
244 AD_F7_6 = mean(abs(F7_MEA(:,1)-F7_MEA(:,3)))
245
246 AD_F8_3 = mean(abs(F8_MEA(:,1)-F8_MEA(:,2)))
247 AD_F8_6 = mean(abs(F8_MEA(:,1)-F8_MEA(:,3)))
248
249 AD_F9_3 = mean(abs(F9_MEA(:,1)-F9_MEA(:,2)))
250 AD_F9_6 = mean(abs(F9_MEA(:,1)-F9_MEA(:,3)))
251
```

```
252
253 AARD_E1_3 = mean(abs((E1_MEA(:,1)-E1_MEA(:,2))/E1_MEA(:,1)))*100
254 AARD_E1_6 = mean(abs((E1_MEA(:,1)-E1_MEA(:,3))/E1_MEA(:,1)))*100
255
256 AARD_E2_3 = mean(abs((E2_MEA(:,1)-E2_MEA(:,2))/E2_MEA(:,1)))*100
257 AARD_E2_6 = mean(abs((E2_MEA(:,1)-E2_MEA(:,3))/E2_MEA(:,1)))*100
258
259 AARD_E3_3 = mean(abs((E3_MEA(:,1)-E3_MEA(:,2))/E3_MEA(:,1)))*100
260 AARD_E3_6 = mean(abs((E3_MEA(:,1)-E3_MEA(:,3))/E3_MEA(:,1)))*100
261
262 AARD_E4_3 = mean(abs((E4_MEA(:,1)-E4_MEA(:,2))/E4_MEA(:,1)))*100
263 AARD_E4_6 = mean(abs((E4_MEA(:,1)-E4_MEA(:,3))/E4_MEA(:,1)))*100
264
265 AARD_E5_3 = mean(abs((E5_MEA(:,1)-E5_MEA(:,2))/E5_MEA(:,1)))*100
266 AARD_E5_6 = mean(abs((E5_MEA(:,1)-E5_MEA(:,3))/E5_MEA(:,1)))*100
267
268 AARD_E6_3 = mean(abs((E6_MEA(:,1)-E6_MEA(:,2))/E6_MEA(:,1)))*100
269 AARD_E6_6 = mean(abs((E6_MEA(:,1)-E6_MEA(:,3))/E6_MEA(:,1)))*100
270
271 AARD_E7_3 = mean(abs((E7_MEA(:,1)-E7_MEA(:,2))/E7_MEA(:,1)))*100
272 AARD_E7_6 = mean(abs((E7_MEA(:,1)-E7_MEA(:,3))/E7_MEA(:,1)))*100
273
274 AARD_E8_3 = mean(abs((E8_MEA(:,1)-E8_MEA(:,2))/E8_MEA(:,1)))*100
275 AARD_E8_6 = mean(abs((E8_MEA(:,1)-E8_MEA(:,3))/E8_MEA(:,1)))*100
276
277 AARD_E9_3 = mean(abs((E9_MEA(:,1)-E9_MEA(:,2))/E9_MEA(:,1)))*100
278 AARD_E9_6 = mean(abs((E9_MEA(:,1)-E9_MEA(:,3))/E9_MEA(:,1)))*100
279
280 AARD_F1_3 = mean(abs((F1_MEA(:,1)-F1_MEA(:,2))/F1_MEA(:,1)))*100
281 AARD_F1_6 = mean(abs((F1_MEA(:,1)-F1_MEA(:,3))/F1_MEA(:,1)))*100
282
283 AARD_F2_3 = mean(abs((F2_MEA(:,1)-F2_MEA(:,2))/F2_MEA(:,1)))*100
284 AARD_F2_6 = mean(abs((F2_MEA(:,1)-F2_MEA(:,3))/F2_MEA(:,1)))*100
285
286 AARD_F3_3 = mean(abs((F3_MEA(:,1)-F3_MEA(:,2))/F3_MEA(:,1)))*100
287 AARD_F3_6 = mean(abs((F3_MEA(:,1)-F3_MEA(:,3))/F3_MEA(:,1)))*100
288
289 AARD_F4_3 = mean(abs((F4_MEA(:,1)-F4_MEA(:,2))/F4_MEA(:,1)))*100
290 AARD_F4_6 = mean(abs((F4_MEA(:,1)-F4_MEA(:,3))/F4_MEA(:,1)))*100
291
292 AARD_F5_3 = mean(abs((F5_MEA(:,1)-F5_MEA(:,2))/F5_MEA(:,1)))*100
293 AARD_F5_6 = mean(abs((F5_MEA(:,1)-F5_MEA(:,3))/F5_MEA(:,1)))*100
294
295 AARD_F6_3 = mean(abs((F6_MEA(:,1)-F6_MEA(:,2))/F6_MEA(:,1)))*100
```

```
296 AARD_F6_6 = mean(abs((F6_MEA(:,1)-F6_MEA(:,3))/F6_MEA(:,1)))*100
297
298 AARD_F7_3 = mean(abs((F7_MEA(:,1)-F7_MEA(:,2))/F7_MEA(:,1)))*100
299 AARD_F7_6 = mean(abs((F7_MEA(:,1)-F7_MEA(:,3))/F7_MEA(:,1)))*100
300
301 AARD_F8_3 = mean(abs((F8_MEA(:,1)-F8_MEA(:,2))/F8_MEA(:,1)))*100
302 AARD_F8_6 = mean(abs((F8_MEA(:,1)-F8_MEA(:,3))/F8_MEA(:,1)))*100
303
304 AARD_F9_3 = mean(abs((F9_MEA(:,1)-F9_MEA(:,2))/F9_MEA(:,1)))*100
305 AARD_F9_6 = mean(abs((F9_MEA(:,1)-F9_MEA(:,3))/F9_MEA(:,1)))*100
306
307
308 a = figure();
309
310 hold on
311 plot(TE1, E1_MEA(:,1), '*');
312 plot(TE1, E1_MEA(:,2), '-');
313 plot(TE1, E1_MEA(:,3), '-');
314 xlabel('Time [days]');
315 ylabel('C_{MEA} [kmol/m^3]');
316 legend('C_{MEA, exp}', 'C_{MEA, mod, 3 inputs}', 'C_{MEA, mod, 6
    inputs}','Location','southwest');
317 title('E1, 120 \circC, CO_2-loading 0.2, MEA');
318 set(findall(gcf,'-property','FontSize'),'FontSize',18);
319
320 b = figure();
321
322 hold on
323 plot(TE2, E2_MEA(:,1), '*');
324 plot(TE2, E2_MEA(:,2), '-');
325 plot(TE2, E2_MEA(:,3), '-');
326 xlabel('Time [days]');
327 ylabel('C_{MEA} [kmol/m^3]');
328 legend('C_{MEA, exp}', 'C_{MEA, mod, 3 inputs}', 'C_{MEA, mod, 6
    inputs}','Location','southwest');
329 title('E2, 120 \circC, CO_2-loading 0.4, MEA');
330 set(findall(gcf,'-property','FontSize'),'FontSize',18);
331
332 c = figure();
333
334 hold on
335 plot(TE3, E3_MEA(:,1), '*');
336 plot(TE3, E3_MEA(:,2), '-');
337 plot(TE3, E3_MEA(:,3), '-');
```

```
338 xlabel('Time [days]');
339 ylabel('C_{MEA} [kmol/m^3]');
340 legend('C_{MEA, exp}', 'C_{MEA, mod, 3 inputs}', 'C_{MEA, mod, 6
    inputs}','Location','southwest');
341 title('E3, 120 \circC, CO_2-loading 0.5, MEA');
342 set(findall(gcf,'-property','FontSize'),'FontSize',18);
343
344 d = figure();
345
346 hold on
347 plot(TE4, E4_MEA(:,1), '*');
348 plot(TE4, E4_MEA(:,2), '-');
349 plot(TE4, E4_MEA(:,3), '-');
350 xlabel('Time [days]');
351 ylabel('C_{MEA} [kmol/m^3]');
352 legend('C_{MEA, exp}', 'C_{MEA, mod, 3 inputs}', 'C_{MEA, mod, 6
    inputs}','Location','southwest');
353 title('E4, 120 \circC, CO_2-loading 0.2, MEA');
354 set(findall(gcf,'-property','FontSize'),'FontSize',18);
355
356 e = figure();
357
358 hold on
359 plot(TE5, E5_MEA(:,1), '*');
360 plot(TE5, E5_MEA(:,2), '-');
361 plot(TE5, E5_MEA(:,3), '-');
362 xlabel('Time [days]');
363 ylabel('C_{MEA} [kmol/m^3]');
364 legend('C_{MEA, exp}', 'C_{MEA, mod, 3 inputs}', 'C_{MEA, mod, 6
    inputs}','Location','southwest');
365 title('E5, 120 \circC, CO_2-loading 0.4, MEA');
366 set(findall(gcf,'-property','FontSize'),'FontSize',18);
367
368 f = figure();
369
370 hold on
371 plot(TE6, E6_MEA(:,1), '*');
372 plot(TE6, E6_MEA(:,2), '-');
373 plot(TE6, E6_MEA(:,3), '-');
374 xlabel('Time [days]');
375 ylabel('C_{MEA} [kmol/m^3]');
376 legend('C_{MEA, exp}', 'C_{MEA, mod, 3 inputs}', 'C_{MEA, mod, 6
    inputs}','Location','southwest');
377 title('E6, 120 \circC, CO_2-loading 0.5, MEA');
```

```
set(findall(gcf,'-property','FontSize'),'FontSize',18);

g = figure();

hold on
plot(TE7, E7_MEA(:,1), '*');
plot(TE7, E7_MEA(:,2), '-');
plot(TE7, E7_MEA(:,3), '-');
xlabel('Time [days]');
ylabel('C_{MEA} [kmol/m^3]');
legend('C_{MEA, exp}', 'C_{MEA, mod, 3 inputs}', 'C_{MEA, mod, 6 inputs}','Location','southwest');
title('E7, 120 \circC, CO_2-loading 0.2, MEA');
set(findall(gcf,'-property','FontSize'),'FontSize',18);

h = figure();

hold on
plot(TE8, E8_MEA(:,1), '*');
plot(TE8, E8_MEA(:,2), '-');
plot(TE8, E8_MEA(:,3), '-');
xlabel('Time [days]');
ylabel('C_{MEA} [kmol/m^3]');
legend('C_{MEA, exp}', 'C_{MEA, mod, 3 inputs}', 'C_{MEA, mod, 6 inputs}','Location','southwest');
title('E8, 120 \circC, CO_2-loading 0.4, MEA');
set(findall(gcf,'-property','FontSize'),'FontSize',18);

i= figure();

hold on
plot(TE9, E9_MEA(:,1), '*');
plot(TE9, E9_MEA(:,2), '-');
plot(TE9, E9_MEA(:,3), '-');
xlabel('Time [days]');
ylabel('C_{MEA} [kmol/m^3]');
legend('C_{MEA, exp}', 'C_{MEA, mod, 3 inputs}', 'C_{MEA, mod, 6 inputs}','Location','southwest');
title('E9, 120 \circC, CO_2-loading 0.5, MEA');
set(findall(gcf,'-property','FontSize'),'FontSize',18);

j = figure();

hold on
```

```
419 plot(TF1, F1_MEA(:,1), '*');
420 plot(TF1, F1_MEA(:,2), '-');
421 plot(TF1, F1_MEA(:,3), '-');
422 xlabel('Time [days]');
423 ylabel('C_{MEA} [kmol/m^3]');
424 legend('C_{MEA, exp}', 'C_{MEA, mod, 3 inputs}', 'C_{MEA, mod, 6
    inputs}','Location','southwest');
425 title('F1, 135 \circC, CO_2-loading 0.2, MEA');
426 set(findall(gcf,'-property','FontSize'),'FontSize',18);
427
428 k = figure();
429
430 hold on
431 plot(TF2, F2_MEA(:,1), '*');
432 plot(TF2, F2_MEA(:,2), '-');
433 plot(TF2, F2_MEA(:,3), '-');
434 xlabel('Time [days]');
435 ylabel('C_{MEA} [kmol/m^3]');
436 legend('C_{MEA, exp}', 'C_{MEA, mod, 3 inputs}', 'C_{MEA, mod, 6
    inputs}','Location','southwest');
437 title('F2, 135 \circC, CO_2-loading 0.4, MEA');
438 set(findall(gcf,'-property','FontSize'),'FontSize',18);
439
440 l = figure();
441
442 hold on
443 plot(TF3, F3_MEA(:,1), '*');
444 plot(TF3, F3_MEA(:,2), '-');
445 plot(TF3, F3_MEA(:,3), '-');
446 xlabel('Time [days]');
447 ylabel('C_{MEA} [kmol/m^3]');
448 legend('C_{MEA, exp}', 'C_{MEA, mod, 3 inputs}', 'C_{MEA, mod, 6
    inputs}','Location','southwest');
449 title('F3, 135 \circC, CO_2-loading 0.5, MEA');
450 set(findall(gcf,'-property','FontSize'),'FontSize',18);
451
452
453 m = figure();
454
455 hold on
456 plot(TF4, F4_MEA(:,1), '*');
457 plot(TF4, F4_MEA(:,2), '-');
458 plot(TF4, F4_MEA(:,3), '-');
459 xlabel('Time [days]');
```

```
460 ylabel('C_{MEA} [kmol/m^3]');
461 legend('C_{MEA, exp}', 'C_{MEA, mod, 3 inputs}', 'C_{MEA, mod, 6
    inputs}','Location','southwest');
462 title('F4, 135 \circC, CO_2-loading 0.2, MEA');
463 set(findall(gcf,'-property','FontSize'),'FontSize',18);
464
465
466 n = figure();
467
468 hold on
469 plot(TF5, F5_MEA(:,1), '*');
470 plot(TF5, F5_MEA(:,2), '-');
471 plot(TF5, F5_MEA(:,3), '-');
472 xlabel('Time [days]');
473 ylabel('C_{MEA} [kmol/m^3]');
474 legend('C_{MEA, exp}', 'C_{MEA, mod, 3 inputs}', 'C_{MEA, mod, 6
    inputs}','Location','southwest');
475 title('F5, 135 \circC, CO_2-loading 0.4, MEA');
476 set(findall(gcf,'-property','FontSize'),'FontSize',18);
477
478
479 o = figure();
480
481 hold on
482 plot(TF6, F6_MEA(:,1), '*');
483 plot(TF6, F6_MEA(:,2), '-');
484 plot(TF6, F6_MEA(:,3), '-');
485 xlabel('Time [days]');
486 ylabel('C_{MEA} [kmol/m^3]');
487 legend('C_{MEA, exp}', 'C_{MEA, mod, 3 inputs}', 'C_{MEA, mod, 6
    inputs}','Location','southwest');
488 title('F6, 135 \circC, CO_2-loading 0.5, MEA');
489 set(findall(gcf,'-property','FontSize'),'FontSize',18);
490
491
492 p = figure();
493
494 hold on
495 plot(TF7, F7_MEA(:,1), '*');
496 plot(TF7, F7_MEA(:,2), '-');
497 plot(TF7, F7_MEA(:,3), '-');
498 xlabel('Time [days]');
499 ylabel('C_{MEA} [kmol/m^3]');
500 legend('C_{MEA, exp}', 'C_{MEA, mod, 3 inputs}', 'C_{MEA, mod, 6
```

```
    inputs}','Location','southwest');
501 title('F7, 135 \circC, CO_2-loading 0.2, MEA');
502 set(findall(gcf,'-property','FontSize'),'FontSize',18);
503
504 q = figure();
505
506 hold on
507 plot(TF8, F8_MEA(:,1), '*');
508 plot(TF8, F8_MEA(:,2), '-');
509 plot(TF8, F8_MEA(:,3), '-');
510 xlabel('Time [days]');
511 ylabel('C_{MEA} [kmol/m^3]');
512 legend('C_{MEA, exp}', 'C_{MEA, mod, 3 inputs}', 'C_{MEA, mod, 6
    inputs}','Location','southwest');
513 title('F8, 135 \circC, CO_2-loading 0.4, MEA');
514 set(findall(gcf,'-property','FontSize'),'FontSize',18);
515
516 r = figure();
517
518 hold on
519 plot(TF9, F9_MEA(:,1), '*');
520 plot(TF9, F9_MEA(:,2), '-');
521 plot(TF9, F9_MEA(:,3), '-');
522 xlabel('Time [days]');
523 ylabel('C_{MEA} [kmol/m^3]');
524 legend('C_{MEA, exp}', 'C_{MEA, mod, 3 inputs}', 'C_{MEA, mod, 6
    inputs}','Location','southwest');
525 title('F9, 135 \circC, CO_2-loading 0.5, MEA');
526 set(findall(gcf,'-property','FontSize'),'FontSize',18);
```

Ingvild Emilie Solnes

# Machine Learning Modelling of the Oxidative and Thermal Degradation of Monoethanolamine (MEA)

NTNU
Kunnskap for en bedre verden